

A Biomechanical Investigation of Collagen, Platelet-rich Plasma, and
Mesenchymal Stromal Cells on the Achilles Tendon in a Rat Model

by

Brittany L. Austin

Submitted in Partial Fulfillment of the Requirements

for the Degree of

Master of Science in Engineering

in the

Mechanical Engineering

Program

YOUNGSTOWN STATE UNIVERSITY

May, 2019

A Biomechanical Investigation of Collagen, Platelet-rich Plasma, and Mesenchymal
Stromal Cells on the Achilles Tendon in a Rat Model

Brittany L. Austin

I hereby release this thesis to the public. I understand that this thesis will be made available from the OhioLINK ETD Center and the Maag Library Circulation Desk for public access. I also authorize the University or other individuals to make copies of this thesis as needed for scholarly research.

Signature:

Brittany L. Austin, Student

Date

Approvals:

Dr. Hazel Marie, Thesis Advisor

Date

Dr. Diana Fagan, Committee Member

Date

Dr. Virgil Solomon, Committee Member

Date

Dr. Jason Walker, Committee Member

Date

Dr. Salvatore A. Sanders, Dean of Graduate Studies

Date

ABSTRACT

It is estimated that about 18 out of 100,000 people rupture their Achilles tendon every year. A review of 4000 Achilles tendon ruptures found that 75% were related to sports activities. Currently, the methods for fixing Achilles tendon ruptures are in need of improvement. Due to the prevalence of Achilles tendon injuries in sports and the fact that tendons have poor wound healing, there has been an abundance of studies on treatments for Achilles tendon injuries. Many different techniques and therapies using biologics have been researched. One area, however, that has not been well researched is the addition of a combination of mesenchymal stromal cells and platelet-rich plasma as a treatment method for wound healing enhancement. There is also a lack of studies comparing different treatment methods as they progress through time. This study chose the following treatment methods: collagen (CoTa); collagen and platelet-rich plasma (PRP); collagen and mesenchymal stromal cells (MSC); and collagen, platelet-rich plasma, and mesenchymal stromal cells (CPM) to follow through two recovery times: 1 week and 2 weeks. Lewis rats were chosen and a full transection of the right Achilles tendon was performed 6 mm proximal to the calcaneal bone. At 1 or 2 weeks both Achilles tendons of the rats were extracted and tensile tests were performed. Maximum force, engineering stress, strain, modulus of elasticity, total strain energy, and elastic strain energy were determined. Differences in the treatment groups at 1 week recovery were notable, no differences were found between the treatment groups at 2 week recovery, however differences could be seen when compared to the left virgin tissue

controls. Computational modeling led to preliminary finite element models for each treatment group. Validation for each model was achieved by comparison with experimental data. Further development of the finite element analysis would allow for a more accurate model and allow for better comparisons between treatment groups.

IACUC PROTOCOL



**YOUNGSTOWN
STATE
UNIVERSITY**

One University Plaza, Youngstown, Ohio 44555

Office of Research
330.541.2377

November 7, 2018

Dr. Diana Fagan
Department of Biological Sciences
UNIVERSITY

Re: IACUC Protocol, 08-18
Title: An Investigation of collegan, platelet-rich plasma, and bone marrow derived mesenchymal stem cells on the Achilles tendon in a rat model


Dear Dr. Fagan:

The Institutional Animal Care and Use Committee of Youngstown State University has reviewed the aforementioned protocol you submitted for consideration and determined it should be unconditionally approved for the period of August 14, 2018 through its expiration date of August 14, 2021.

This protocol is approved for a period of three years; however, it must be updated yearly via the submission of an Annual Review-Request to Use Animals form. These Annual Review forms must be submitted to the IACUC at least thirty days prior to the protocol's yearly anniversary dates of August 14, 2019 and August 14, 2020. If you do not submit the forms as requested, this protocol will be immediately suspended. You must adhere to the procedures described in your approved request; any modification of your project must first be authorized by the Institutional Animal Care and Use Committee.

Good luck with your research!

Sincerely,


Dr. Gregory Dillon
Interim Associate Vice President for Research
Authorized Institutional Official

GD:dka

C: Dr. Stanley Dannemiller, Consulting Veterinarian, NEOMED
Dawn Amolach, Animal Tech., Biological Sciences

Youngstown State University does not discriminate on the basis of race, color, national origin, sex, sexual orientation, gender identity and/or expression, disability, age, religion or veteran/military status in its programs or activities. Please visit www.yosu.edu/understanding for contact information or persons designated to handle questions about this policy.

www.yosu.edu

ACKNOWLEDGEMENTS

My sincerest appreciation to those who have made this possible.

Thesis Advisor

Dr. Hazel Marie

Thesis Committee

Dr. Diana Fagan, Dr. Virgil Solomon, Dr. Jason Walker

Corporate Partners

Mercy Health Boardman Medical Research Committee grant

Faculty

Anthony Viviano, Dr. Yong Zhang, Dawn Amolsch

Additional Assistance

Dr. Stuart Drew, YSU Machine Shop, Kiraly Tool and Die, Ice., Biological Sciences

Animal Facility

Students

Jared Vanasdale, Kathryn Platt, Thywill Ettey, Errek Pham, Dragon Juzbasich, Alexander

Huber

DEDICATION

First, I'd like to give my love and deepest thanks to my parents, Cindy and Darren, and my fiancée Adam. Your support and unending love and understanding throughout this project has made this possible. I would not be where I am today without you.

Secondly, I give my absolute thanks and unconditional gratitude to the most influential professors of my academic career. Dr. Hazel Marie and Dr. Stefan Moldovan, thank you for your guidance and pushing me to always do my best.

Table of Contents

	Page
ABSTRACT	iii
IACUC PROTOCOL	v
CHAPTER	
1 INTRODUCTION.....	1
1.1 BACKGROUND	1
1.1.1 The Achilles Tendon	6
1.1.2 Mechanical Properties of the Achilles Tendon	9
1.1.3 Rats in Medical Advancement.....	12
1.2 LITERATURE REVIEW	12
1.2.1 Platelet-Rich Plasma.....	13
1.2.2 Mesenchymal Stem Cells.....	14
1.2.3 Mesenchymal Stem Cells & Platelet-Rich Plasma Combination	17
1.2.4 Achilles Tendon Finite Element Modeling.....	20
1.3 SCOPE OF WORK.....	22
1.3.1 Experimental Design	22
1.3.2 Elastography	23
1.3.3 Finite Element Modeling.....	23
1.3.4 Results and Analysis	24
1.3.5 Conclusions and Recommendations	24

2	EXPERIMENTAL METHODS	25
2.1	TEST SPECIMEN AND PROTOCOL	25
2.2	TREATMENT METHODS	25
2.2.1	Collagen Matrix	26
2.2.2	Platelet-Rich Plasma (PRP)	26
2.2.3	Bone Marrow-derived Mesenchymal Stromal Cells (MSC)	27
2.3	STUDY DESIGN	28
2.3.1	Sample Size Determination	29
2.4	ACHILLES TENDON INCISION AND REPAIR	31
2.5	POST PROCEDURE MONITORING	35
2.6	RECOVERY OF ACHILLES TENDON	35
2.7	MECHANICAL TESTING	36
2.8	FINITE ELEMENT ANALYSIS	43
2.8.1	Material Model	44
2.8.2	Boundary Conditions	45
2.8.3	Meshing	46
2.9	ELASTOGRAPHY	47
2.9.1	Elastography of Tendon 45	49
2.9.2	Finite Element Analysis using Elastography	51
2.10	STATISTICAL ANALYSIS	52
2.10.1	Left Tendon vs. Right Tendon	52
2.10.2	Differences between Treatment Methods through Time	53
3	RESULTS AND CONCLUSIONS	55
3.1	DIFFERENCES IN TENDON SIZES	55
3.2	MECHANICAL TESTING RESULTS	58

3.2.1	Location of Failure.....	60
3.2.2	Average Mechanical Properties of Each Treatment Group	62
3.2.3	Mechanical Properties Based on Averaged Stress-Strain Curves	66
3.2.4	Differences Between 1 and 2 Week Recovery.....	74
3.3	STATISTICAL ANALYSIS OF TREATMENT GROUPS	80
3.4	RESULTS COMPARED TO LITERATURE.....	82
3.5	FINITE ELEMNT ANALYSIS RESULTS.....	83
3.5.1	Finite Element Analysis Using Elastography	85
3.5.2	Finite Element Analysis Compared to Literature	86
3.6	ELASTOGRAPHY OF A TENDON.....	87
3.7	FUTURE WORK	89
A.	APPENDIX A	91
B.	APPENDIX B	92
C.	APPENDIX C	95
D.	APPENDIX D	103
	REFERENCES.....	118

LIST OF FIGURES

	Page
Figure 1.1: Placement of the Achilles Tendon (Mazzone & McCue, 2002) ¹	7
Figure 1.2: Force-Relaxation Graph of a Tendon (Maganaris & Narici, 2005) ²	9
Figure 1.3: Creep Graph of a Tendon (Maganaris & Narici, 2005) ³	10
Figure 1.4: Mechanical Hysteresis of a Tendon (Maganaris & Narici, 2005) ⁴	10
Figure 1.5: Stress-Strain Curve of Tendon (Wang, 2006) ⁵	11
Figure 2.1: Minitab Sample Size Determination	30
Figure 2.2: Inhalation Anesthesia	32
Figure 2.3: Nose Cone and Surgery Site.....	32
Figure 2.4: Dry Sterilization Unit.....	33
Figure 2.5: Achilles Tendon Surgery.....	34
Figure 2.6: Post Surgery	35
Figure 2.7: Instron Testing Machine.....	36
Figure 2.8: Upper Grips	37
Figure 2.9: Bottom Grips Open	38
Figure 2.10: Bottom Grips Closed.....	38
Figure 2.11: Tendon Prepped with Sandpaper.....	40
Figure 2.12: Tendon Pinched in Bottom Clamp	40
Figure 2.13: Tendon Before and After Testing (a) Before Tensile Testing (b) After Tensile Testing.....	41

Figure 2.14: Strain-Strain Curve of Control Tendon	43
Figure 2.15: Tendon Geometry Model (Tendon 45 from 1 Week Recovery Collagen....	44
Figure 2.16: Boundary Conditions.....	45
Figure 2.17: Side of Tendon Mesh	47
Figure 2.18: Front of Tendon Mesh.....	47
Figure 2.19: Images of Tendon During Testing and Corresponding Elastography Images	
(a) Tendon Prior to Test, Marked with Six Pints to be traced During Elastography	
(b) Tendon During Test at Frame 420 (c) Tendon at Frame 1000 Near End of Test	
(d) No Displacement Before Testing (e) Elastography Image at Mid Test (f)	
Elastography Image at End of Test.....	50
Figure 2.20: Geometry of Elastography Model	51
Figure 3.1: (a) Left Untreated Tendon (b) Right MSC Treated Tendon 1 Week Recovery	
.....	58
Figure 3.2: Stress-Strain of Tendon 50.....	59
Figure 3.3: Stress-Strain to Failure of Tendon 50.....	59
Figure 3.4: Modulus of Elasticity of Tendon 50.....	60
Figure 3.5: 1 Week Recovery Failure Site (a) Tendon Prior to Testing (b) Tendon Post	
Failure	60
Figure 3.6: Control Tendon Strained to Failure (a) Tendon Prior to Testing (b) Tendon	
Post Failure	61
Figure 3.7: Control Tendon Torn at Bottom (a) Tendon Prior to Testing (b) Tendon Post	
Failure	61

Figure 3.8: 2 Week Recovery Failure Site (a) Tendon Prior to Testing (b) Tendon Post Failure	62
Figure 3.9: Plot of Modulus of Elasticity at 1 Week Recovery	65
Figure 3.10: Plot of Modulus of Elasticity at 2 Week Recovery	65
Figure 3.11: 1 Week Recovery: Stress-Strain to Failure, Original Treated Cross-Section	66
Figure 3.12: 1 Week Recovery: Stress-Strain to Failure, Control Cross-Section.....	67
Figure 3.13: 2 Week Recovery: Stress-Strain to Failure, Original Treated Cross-Section	70
Figure 3.14: 2 Week Recovery: Stress-Strain to Failure, Control Cross-Section.....	71
Figure 3.15: Stress-Strain to Failure Collagen at 1 and 2 Week Recovery and Controls. 74	
Figure 3.16: Stress-Strain to Failure PRP Group at 1 and 2 Week Recovery and Controls	76
Figure 3.17: Stress-Strain to Failure MSC Group at 1 and 2 Week Recovery and Controls	77
Figure 3.18: Stress-Strain to Failure CPM Group at 1 and 2 Week Recovery and Controls	79
Figure 3.19: Deformed Model (a) Undeformed Tendon Model (b) Deformed Tendon Model	83
Figure 3.20: Deformed Elastography Model (a) Undeformed Model (b) Deformed Model	85
Figure 3.21: Mechanical vs Optical Strain	87
Figure 3.22: Optical Strain at Points.....	88

Figure 3.23: Optical Strain at Points vs Time..... 89

LIST OF TABLES

	Page
Table 1.1: Treatment Types and Times	23
Table 2.1: Number of Rats per Group per Time Period	31
Table 2.2: Elements in FEA Models.....	46
Table 2.3: Modulus of Elasticity at Each Point in Elastography	52
Table 2.4: Statistical Analysis of Left vs Right Tendon.....	53
Table 3.1: Average Cross Sectional Areas at 1 Week Recovery	56
Table 3.2: Average Cross-Sectional Area of 2 Week Recovery.....	57
Table 3.3: Average Mechanical Properties at 1 Week Recovery	63
Table 3.4: Average Mechanical Properties at 2 Weeks Recovery.....	63
Table 3.5: Average Mechanical Properties of Treated Tendons 1 Week Recovery from Average Stress-Strain Curves	68
Table 3.6: Average Mechanical Properties of Control Tendons 1 Week Recovery from Average Stress-Strain Curves	69
Table 3.7: Percent Difference between Treatments and Controls and Treatments and Collagen 1 Week Recovery	69
Table 3.8: Average Mechanical Properties of Treated Tendons 2 Week Recovery from Average Stress-Strain Curves	72
Table 3.9: Average Mechanical Properties of Control Tendons 2 Week Recovery from Average Stress-Strain Curves	73

Table 3.10: Percent Difference between Treatments and Controls and Treatments and Collagen 2 Week Recovery	73
Table 3.11: Percent Difference Between Collagen Group at 1 and 2 Weeks Recovery...	75
Table 3.12: Percent Difference Between PRP Group at 1 and 2 Weeks Recovery	76
Table 3.13 Percent Difference Between MSC Group at 1 and 2 Weeks Recovery	78
Table 3.14: Percent Difference Between CPM Group at 1 and 2 Weeks Recovery	79
Table 3.15: Percent Difference Between Actual and Simulated Force and Modulus of Elasticity at 1 Week Recovery	84
Table 3.16: Percent Difference Between Actual and Simulated Force and Modulus of Elasticity at 2 Week Recovery	84
Table 3.17: Results of FEA of Elastography Model	86

NOMENCLATURE

Symbol	Description	Unit
σ	Engineering stress	kPa
ε	Engineering strain	mm/mm
Φ	Statistical parameter	-
σ^2	Variance	-
F	Force	N
A _{CS}	Cross sectional area	mm
ΔL	Extension	mm
L _i	Overall length	mm
u	Modulus of toughness / strain energy	kPa
ε_{\max}	Strain at failure	mm/mm
E	Modulus of elasticity	kPa
ε_{UTS}	Strain at ultimate tensile strength	mm/mm
F _{max}	Max force	N
u _E	Elastic Strain Energy	kPa

CHAPTER I

INTRODUCTION

There has been an abundance of studies on treatments for tendon injuries, specifically Achilles tendon ruptures. Many different techniques and therapies for wound healing enhancement using biologics have been researched. One area, however, that has not been well researched is the injection of a combination of mesenchymal stem cells and platelet-rich plasma to the wound site. This study aims to compare the addition of bone marrow-derived mesenchymal stromal cells and platelet-rich plasma both as separate treatments and as a combined treatment. The treatment types were compared both to a control group as well as to each other. The goal was to determine whether or not a combined mesenchymal stromal cell and platelet-rich plasma treatment is a significantly better treatment option for the Achilles tendon than using each treatment individually.

1.1 BACKGROUND

The human body is amazing and complex. It consists of trillions of cells that make up every part of a being. These cells form many different aspects of a person, such as muscles, tendons, ligaments, and so on. These fundamental tissues of the human body are made up of four basic cell types and extracellular material. These cell types include: epithelial tissue, muscle tissue, nerve tissue, and connective tissue (Encyclopedia Britannica, 2000).

The first cell type, epithelial tissue, is essentially a sheet of cells that protect the surfaces of the body that interact with the outside world. Other than skin, epithelial tissue also covers the airways, digestive system, reproductive system, and urinary system. They also line and protect the inside and outside of organs (OpenStax College).

The second type, muscle tissue, comes in three different types, skeletal, smooth, and cardiac. This tissue specializes in creating tension, which in turn generates a force, which facilitates body movement. Skeletal muscle tissue is usually attached to the skeletal system by way of tendons. This allows people to control movement and maintain posture. Skeletal muscle tissue can also attach to other muscles or the skin directly. Smooth muscle tissue, on the other hand, is associated with movement in the internal organs. They assist the digestive, urinary, and the reproductive systems. Finally, cardiac muscle tissue is found in the heart and contributes to the contractions of the heart to pump blood throughout the body (Rice University).

The third cell type, nerve tissue, is located in the brain, spinal cord, and nerves. This tissue stimulates muscle contractions and has a part in emotions, memory, and reasoning through electrical nerve impulses (National Cancer Institute).

Lastly, connective tissue provides internal support as well as support of the organs and aids in maintaining the form of the body. All connective tissue is made up of ground substance, a shapeless viscous gel-like substance that is transparent (Encyclopedia

Britannica, 1998a); extracellular fibers, such as collagen, reticular, and elastic fibers (Southern Illinois University, 2015); and stationary and migrating cells. There are a few different types of tissue that are considered connective tissue and each has a slightly different make up of these three components. The types of connective tissue are: bone, ligaments, adipose, or fat, cartilage, and tendons. (Fawcett, 1999).

There are a total of 206 bones in the adult human body (Dowshen, 2015). Bones, as mentioned before, are connective tissue and made up of the three materials listed previously. In addition, bones also contain a mineral called hydroxyapatite. The mineralization of the matrix comprised of these substances is the reason bones are considered hard connective tissue (Fawcett, 1999).

Another type of connective tissue is ligament. Ligaments support organs as well as attach bones together at the joints. They have the same make-up as other connective tissue, although they do not contain much ground substance and are mostly comprised of dense fibrous bundles of collagen fibers. There are two types of ligaments, white ligaments and yellow ligaments. White ligaments are inelastic and are rich in collagen fibers. Yellow ligaments are elastic and rich in elastic fibers (Encyclopedia Britannica, 1998c).

Adipose tissue is mostly composed of fat cells that store fat within their fibers. This tissue can be found in many places, including under the skin, between muscles, around the heart, and in the intestines. There are two different types of adipose tissue,

white and brown tissue. White adipose tissue is the most common form in adults. It provides insulation, stores energy, and forms pads between organs. Brown adipose tissue is commonly found in newborns and the relative amount decreases with age. This particular tissue consumes energy and creates heat (Encyclopedia Britannica, 2009).

The fourth type of connective tissue is cartilage. Cartilage has an abundance of ground substance in its make up, which causes it to have a firm gelatin-like consistency. Due to its composition, cartilage has a strong resistance to compression and has rigidity. There are three different types of cartilage found in the body. They are: hyaline cartilage, elastic cartilage, and fibrocartilage. Hyaline cartilage has little elastin and has randomly oriented fibrils. It is commonly found in the skeletal make up of fetuses as well as on the surface of joints. Unlike hyaline cartilage, elastic cartilage is a substance in which an abundance of elastic fibers is present. These fibers make it more elastic than hyaline cartilage. Elastic cartilage is usually found in the outer ear, the larynx, and the epiglottis. Finally, fibrocartilage has parallel oriented, dense, collagen bundles. It is generally found in articular disks of certain joints, in the space between tendon and bone connections, and in intervertebral disks (Fawcett, 1999).

The final type of connective tissue is tendon. Tendons are an important part of the body because they attach muscle to bone. When a muscle contracts it induces a force; this force is carried by a tendon to the attached bone. Tendons are considered to have the highest tensile strength compared to all soft tissue (Encyclopedia Britannica, 1998b).

They are made up of compact fibrous connective tissue that forms parallel bundles and are inelastic and tough (C, 2017).

Tendons can become injured if they are overworked. There are different common injuries that can occur, which include tendinitis, tendinosis, and a rupture. Tendinitis happens when the tendon becomes inflamed, swollen, and painful. Tendinosis is when the tendon degenerates and fibers of the tendon start to show signs of small tears or the tendon stops the ability to heal (Cleveland Clinic, 2016). A rupture is classified as either a partial or complete tear in the tendon (Ode, 2016).

There are various ways to heal these three different injuries. Typically for tendinitis the treatment is rest and the elimination of the motion that caused the injury. Taking anti-inflammatories is also recommended. Sometimes braces are used as well to help the tendon rest. Tendinosis is dealt with through physical therapy to strengthen the surrounding muscles as well as stretch the tendon. If pain is continuous, then an injection of platelet-rich plasma may be recommended to aid with the healing process (Cleveland Clinic, 2016). A rupture treatment depends on a few different factors such as the tendon in question, the extent of the symptoms, and the size of the tear. Once these factors have been taken into account, the doctor may decide that the ruptured tendon needs surgical treatment, or he or she may just prescribe rest (Ode, 2016).

1.1.1 The Achilles Tendon

One of the tendons in the body that is commonly injured is the calcaneal tendon, also known as the Achilles tendon. The Achilles tendon is named after the Greek figure, Achilles. As the legend goes, Achilles mother, Thetis, wanted to keep her son immortal, to do this she dipped him in the River Styx. To keep Achilles from being swept away, Thetis held on to him by his heels as he was dipped. Because of this, Achilles was only immortal above the heels. While the Greeks were attempting to take over Troy, a warrior named Paris took a poison laden arrow and was able to shoot the immortal Achilles in the heel, killing him. This is how the Achilles tendon got its name (Silverman, 2015).

The Achilles tendon connects the soleus-gastrocnemius complex, or the bottom of the calf muscle, to the calcaneal, or heel bone, at the back of the leg, as shown in Figure 1.1. This tendon facilitates movements such as running, jumping, rising on the toes, and walking up stairs (Health Communities, 1999a). Of course, the Achilles tendon is not the only tendon in the foot that provides for these and more types of foot and leg motion, in fact, there are over 100 tendons, muscles, and ligaments in the foot alone (Health Communities, 1999b). However, the Achilles tendon is the largest and strongest tendon in the body and injury to such an important tendon could cause quite a bit of debilitating situations.

Tendonitis of the Achilles tendon and an Achilles tendon rupture are both common sports injuries. Tendonitis in the Achilles tendon occurs due to too much stress on the feet and usually occurs in those aged 30 to 50. It is generally treated with rest and

followed by physical therapy. It is estimated Achilles tendon ruptures occur in 18 out of 100,000 people every year (Cleveland Clinic, 2017) (Leppilahti, Puranen, & Orava, 1996). This injury, as previously stated, can be treated both surgically and non-surgically. The treatment method is chosen based on certain criteria, such as the patient's age and activity level (Mayo Clinic, 2017).

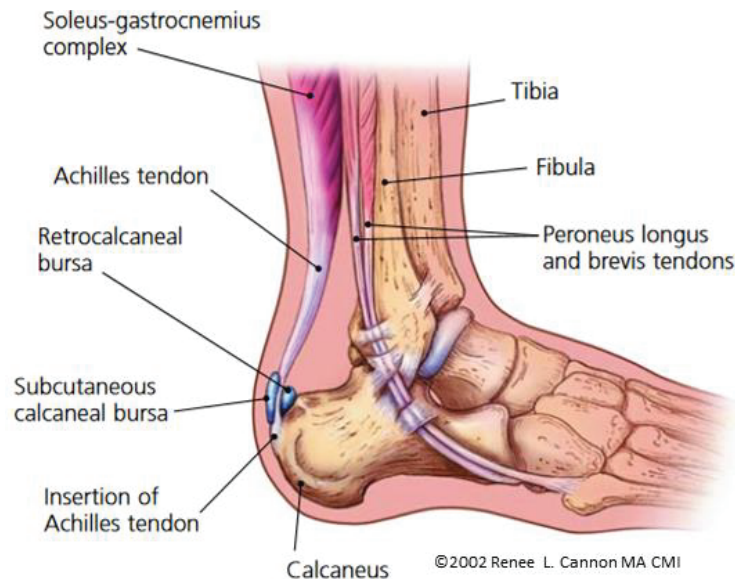


Figure 1.1: Placement of the Achilles Tendon (Mazzone & McCue, 2002)¹

The less invasive method of treatment, the non-surgical method, involves resting the tendon and keeping the ankle from moving using a boot or a cast (Mayo Clinic, 2017). Although the non-surgical method may seem like a safer alternative to surgery, it has a 10-30% chance of re-rupture. There have also been reports of limited plantar flexion as well as a decrease in endurance compared with the surgical method (Strauss, Ishak, Jazrawi, Sherman, & Rosen, 2007) (Cetti, Christensen, Ejsted, Jensen, &

¹ From "Common Conditions of the Achilles Tendon," by M. Mazzone & T. McCue, 2002, *American Family Physician*, 65, p. 1806. Copyright 2002 by Renee Cannon. Reprinted with permission.

Jorgensen, 1993) (Jacobs, Martens, Audekercke, Mulier, & Mulier, 1978) (Cretnik, Kosanovic, & Smrolj, 2004).

For the surgical option, there have been two different methods tested, open procedures and percutaneous. A decrease in re-rupture has been observed for both methods compared to the non-surgical method, but there has been no significant difference found between the two operating methods. The operative method, however, is not without its downfalls. The open procedure can have complications such as infection and poor wound healing. The percutaneous method also has some complications, such as complete and partial re-ruptures, sural neuritis, and superficial wound infection, though the infection rate has been shown to be lower in the percutaneous method (Cretnik, Kosanovic, & Smrolj, 2004).

Regardless of which treatment method is chosen, as the Achilles tendon is healing, scar tissue forms and can cause the tendon to become weaker than it was before injury. This can increase the risk of re-rupture as well as cause other complications. Because of this, research is being done to investigate different opportunities to better the treatment of Achilles tendons as well as other tendons in the body. Therapy using the addition of biologics to the wound site is a common method currently being researched to improve the healing of Achilles tendons. These include research into platelet-rich plasma, bone marrow aspirate, bone morphogenetic proteins, stem cells, bioscaffolds, growth factors, and various combinations of these techniques (Shapiro, Grande, & Drakos, 2015).

1.1.2 Mechanical Properties of the Achilles Tendon

Tendons do not exhibit purely elastic behavior. This is because the tendon's fibers contain viscous properties. Due to the viscous nature of tendons, during certain loading conditions they experience force-relaxation, creep, and mechanical hysteresis (Butler, Grood, Noyes, & Zernicke, 1978).

First, force-relaxation, as plotted in Figure 1.2, explains that the force required to induce a certain elongation decreases over time. This decrease in force follows a curvilinear path until a steady-state is reached (Maganaris & Narici, 2005). This is documented by applying a constant displacement to the tissue and measuring the force required to keep it at that displacement with a load cell.

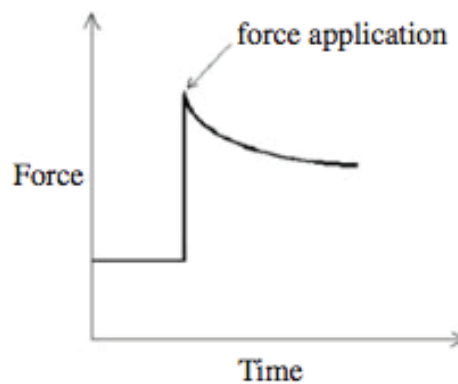


Figure 1.2: Force-Relaxation Graph of a Tendon (Maganaris & Narici, 2005)²

Secondly, creep, shown in Figure 1.3, is when a constant load is applied to a part and the deformation of the part continues to increase over time, despite the constant load. The path of the increasing creep follows a curvilinear line until reaching steady-state, much like force-relaxation (Maganaris & Narici, 2005).

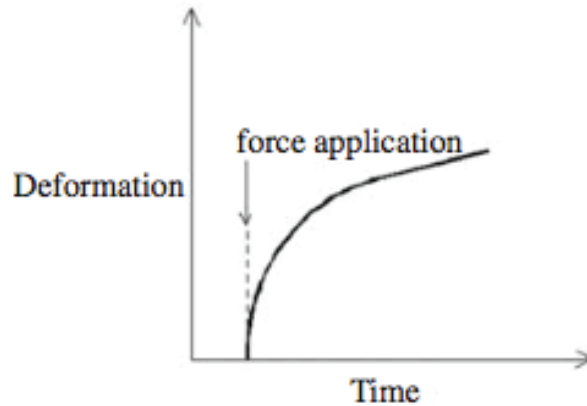


Figure 1.3: Creep Graph of a Tendon (Maganaris & Narici, 2005)³

Finally, mechanical hysteresis is seen in the load-deformation plots when a specimen is loaded and then unloaded. In Figure 1.4, it can be seen that a smaller amount of deformation occurs with stretching than it does when unstretching, creating a different force-deformation path. This creates a loop, known as a hysteresis loop. The area inside the loop represents the energy lost during the unloading phase due to heat because of the viscous components (Maganaris & Narici, 2005).

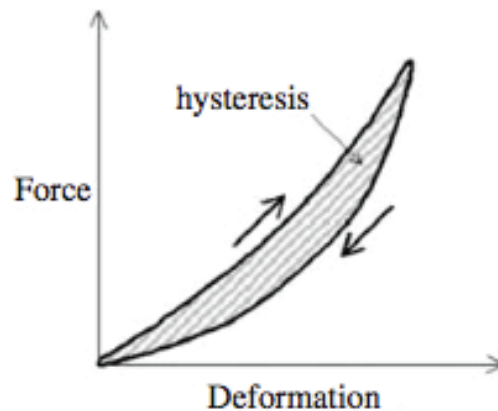


Figure 1.4: Mechanical Hysteresis of a Tendon (Maganaris & Narici, 2005)⁴

^{2,3,4} From “Mechanical Properties of Tendons,” by C. Maganaris and M. Narici, 2005, *Tendon Injuries*, 2, p. 15. Copyright 2005 by Springer Nature. Reprinted with permission.

Because of these material characteristics, tendons are considered visco-elastic material and their stress-strain curves measured to failure are not the same as that of an elastic material. Figure 1.5 shows a typical stress-strain curve of a tendon. Notice during the initial 2% of strain, the graph is slightly concave; this area is considered to be the toe region. This is because before any load is applied to the tendon, the fibers are crimped. The first 2% of strain is when these fibers are being stretched out and the force required to do so is minimal. During the linear portion of the graph, roughly 2% - 4% of strain, the fibers have lost their crimp pattern. This is the region where the linear relationship between the force and deflection occurs and so the Modulus of Elasticity can be found. Beyond 4% strain, the tendon fibers start to develop microscopic tears. At around 8% - 10% strain macroscopic tears begin to form, and beyond that tendon rupture occurs (Butler, Grood, Noyes, & Zernicke, 1978).

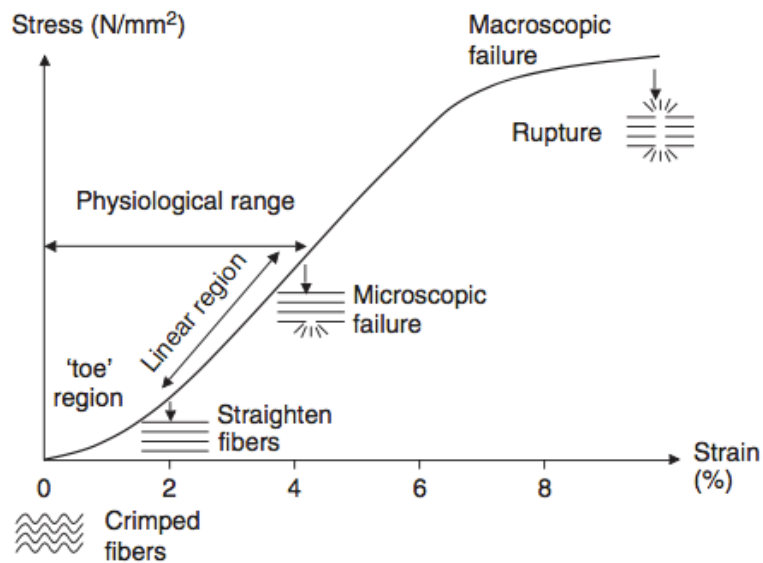


Figure 1.5: Stress-Strain Curve of Tendon (Wang, 2006)⁵

⁵ From "Mechanobiology of tendon," by J. Wang, 2006, *Journal of Biomechanics*, 39, p. 1567. Copyright 2005 by Elsevier. Reprinted with permission

1.1.3 Rats in Medical Advancement

Rats have been an important part of medical advancement since the beginning. Rats and mice combined are approximately 95% of all laboratory animals. Since they have a similar physiological and genetic make up to humans, they are easy to use to study human diseases through genetic engineering. There are a multitude of areas where rats have been used to further knowledge in the medical field. Some of these areas include but are not limited to: cancer, Alzheimer's disease, cardiovascular disease, diabetes, and infectious disease. They have contributed to the development of countless drugs to combat against all of the previously listed conditions and more. They have, for example, aided in the availability of antibiotics such as penicillin, amoxicillin, and many other drugs used today (National Association for Biomedical Research). Modern medicine would not be where it is today without the help of the common lab rat.

Other than for their similar genetic make up to human, rats are often chosen for certain studies because, through generations of breeding, they are considered genetically identical to each other. This allows certain pieces, such as stem cells and organs to be removed from one rat and placed in another without fear of rejection or interference, which keeps the results of studies more uniform (Melina, 2010).

1.2 LITERATURE REVIEW

Sections 1.2.1, 1.2.2, and 1.2.3 give insight into research that has been done with platelet-rich plasma and mesenchymal stem cells to improve healing in various tissue

models. There have been investigations into platelet-rich plasma and mesenchymal stem cells as separate treatments as well as combined treatments.

1.2.1 Platelet-Rich Plasma

Platelet-rich plasma (PRP) is a concentration of a cell fragment in the blood called platelets and is created from a person's blood. Platelets and plasma are essential for healing because platelets are imperative to blood clotting, and the factors found in platelets and plasma are vital for cell recruitment, multiplication, and specialization. PRP is produced by taking a sample of a patient's blood and centrifuging it. A centrifuge is able to separate all the different components of blood, which allows the PRP to be collected and treated. PRP treatments can be used to assist in the healing of bone or soft tissue and has actually been used by some professional athletes (Kohen, Warren, & Rodeo, 2010). These treatments can be given one of two ways. The first is an injection of PRP given right at the site of interest. The second way is for PRP to be applied during surgery to encourage healing of the tissue in, for example, a complete tendon rupture. To apply PRP during surgery, it must be absorbed into a matrix to allow it to be stitched into the tissue (American Academy of Orthopaedic Surgeons, 2011).

Aspenburg and Virchenko (2004) researched whether platelet concentrate (PC) increased healing of the Achilles tendon in a rat model. Six hours after surgery platelet concentrate was injected percutaneously into the surgical site. Rats were sacrificed at 8, 11, 14, 21, and 28 days. On days 21 and 28 the maximum stress of the PC group was greater than that of the control group by 31% and 23%, respectively. The stiffness of the

tendons was affected by PC the greatest at 11 days, being 41% of the unoperated tendons. The effect of the PC on stiffness was nonexistent at 28 days. The use of PRP to assist in the healing of not only tendons, like the Achilles, but in other areas as well is promising.

1.2.2 Mesenchymal Stem Cells

Stem cells are very interesting and critical to all living beings. They act as a repair system to replenish cells that have begun to wear out or become injured, such as in the gut. Stem cells do this by dividing, practically without limit, as long as the person or animal is living and healthy. Stem cells are classified by two characteristics. Firstly, they are unspecialized and able to divide as a way of renewing themselves. Secondly, they have the potential, under certain circumstances, to change into a tissue or organ specific cell with certain functions. There are three major subdivisions of stem cells, which include: embryonic stem cells (ESCs), adult stem cells (ASCs), and induced pluripotent stem cells (iPSCs) (Department of Health and Human Services, 2016).

The first type of stem cells, the embryonic stem cells, are found in the embryo and are pluripotent, meaning they have the potential to differentiate into any cell type. They are used for research purposes only from in vitro fertilization clinics, never from eggs fertilized in a woman's body. These stem cells are donated with informed consent by the donor (Department of Health and Human Services, 2016).

The second type of stem cells is adult stem cells. These stem cells basically have unlimited cell division capabilities, however, once they are removed from the body, this

ability becomes limited. This makes it difficult to culture stem cells for research into treatment of injuries and diseases. Along with being able to multiply without limit, ASCs are considered to be unspecialized cells and are found among specialized cells in tissues and organs. ASCs can also differentiate into some or all of the major cell types in the tissue or organ. Some of the tissues and organs ASCs have been found in include: bone marrow, peripheral blood, blood vessels, skeletal muscle, skin, teeth, gut, liver, ovarian epithelium, and testis. ASCs have even been found in the brain and heart, where they were not expected to be originally. Researchers discovered ASCs in the bone marrow in the 1950s. They found two different types, hematopoietic stem cells and bone marrow stromal stem cells, or, mesenchymal stem cells (Department of Health and Human Services, 2016). Hematopoietic stem cells, also known as blood stem cells, are found in the bone marrow and also in the peripheral blood. These cells can differentiate into red and white blood cells, as well as into platelets (National Cancer Institute). The second type, mesenchymal stem cells (MSCs) can be found in many places other than in bone marrow, such as: adipose, muscle, umbilical cord, and gingiva. These stem cells aid in the repairing of muscle, bone, cartilage, and fat (Balaji, Keswani, & Crombleholme, 2012).

The final type of stem cell is the induced pluripotent stem cells. These are adult stem cells that have been genetically manipulated to act more like embryonic stem cells (Department of Health and Human Services, 2016). A big difference between ASCs and ESCs is that ESCs are pluripotent. ASCs are multipotent, meaning they can differentiate into different types of cells, but are more limited than pluripotent stem cells (New York

State Stem Cell Science). The reason to manipulate ASCs is to unlock the ability for them to differentiate as pluripotent, which iPSCs have the capability to do. Currently the method used to cause this transformation uses viruses. However, these viruses have sometimes been found to cause cancer in mice. Researchers are still looking for a method to start the transformation without the use of viruses (Department of Health and Human Services, 2016).

Since MSCs are self-renewing and aid in tissue repair, this makes them ideal candidates to promote healing in areas that are known to have poor wound healing characteristics, such as the Achilles tendon, or with chronic diseases such as diabetes. MSCs have the potential to increase wound healing as well as increase the integrity of the healing tissue (Balaji, Keswani, & Crombleholme, 2012). For instance, in a study by Chong et al. (2007), a rabbit model was used to compare the healing capabilities of MSCs versus a controlled group in Achilles tendons by way of an injection at and around the wound site. Tendons were harvested at 1, 3, 6, and 12 weeks. The results showed that the treatment group had a 32% increase in the modulus of repair at 3 weeks. The modulus of repair is considered to be the modulus of elasticity, however, since the modulus of elasticity remains constant within the same material, the researchers called it the modulus of repair. No significant difference was found between groups at 6 and 12 weeks and the control groups. This indicates positive results for MSCs to aid in wound healing at earlier time periods.

Young et al. (1998) also conducted a study with a rabbit model and used bone marrow-derived mesenchymal stem cells suspended in a collagen gel to study the healing effects on the Achilles tendon. The researcher condensed the MSCs in collagen gel on a pretensioned suture and evaluated the tendons biomechanical and histological properties at 4, 8, and 12 weeks. The results showed that the Achilles tendons with the MSCs had greatly increased structural and material properties compared to the control tendons. The treated group in this study required, on average, 60-90% of the energy needed to create failure of a normal Achilles tendon, compared to 30-40% of energy in the control group. This was the case for all time periods. The maximum stress of the treated group at 12 weeks was 37.3% that of a normal tendon, versus 19.2% for the control group. The treated cross-sectional areas were also significantly greater than the controls. At 4, 8, and 12 weeks the averaged measured cross-sectional areas ($\text{mm}^2 \pm \text{SD}$) of the treated group, respectively were found to be: 15.1 ± 6.8 , 10.4 ± 3.7 , and 7.4 ± 2.8 . To compare, the following is the recorded averaged cross-sectional areas of the control group at the same respective time periods: 8.4 ± 1.9 , 6.3 ± 1.9 , and 5.4 ± 2.6 . The researchers noted that the treated tendons have a larger cross-sectional area at every time interval. Their results indicate a positive sign that MSCs can be used to promote healing in areas that generally have poor wound healing capabilities.

1.2.3 Mesenchymal Stem Cells & Platelet-Rich Plasma Combination

Both MSCs and PRP are known to aid in healing. They have been shown separately to improve the healing process in tendons, specifically in the Achilles tendon. It is an obvious next step to study whether or not the combination of these two would

speed up the healing process even more than one alone. That was one of the questions this study aimed to answer. In fact, this study not only compared the healing capabilities of MSCs and PRP, but also the capabilities of them as a combined treatment. There are some studies that compare MSCs and PRP separately, however there has been little research done on a combined treatment of MSCs and PRP in the Achilles tendon.

There is one study, however, performed by Heffner et al. (2012) that used rats to compare the healing capabilities of a combined MSC and PRP with CollaTape (CoTa), which is a collagen scaffold, PRP with CoTa, and a control group, in the abdominal wall fascia. Samples were extracted at 4 and 8 weeks. The tensile strength and modulus of toughness of the fascia in each group at each time period was found through biomechanical testing. The results showed that the PRP and CoTa group had a 101% increase in tensile strength at 4 weeks and a 38% increase at 8 weeks compared to the control group. The MSC, PRP, and CoTa group showed an average tensile strength increase of 301% at 4 weeks compared to the control group and a 100% increase compared to the PRP and CoTa group. At 8 weeks, the MSC, PRP, and CoTa group exhibited a 117% increase to the control group and 58% increase in comparison to the PRP and CoTa group. The PRP and CoTa group also displayed an increase in the modulus of toughness when compared to the control group. At 4 weeks this increase was 122% and at 8 weeks, 85%. The MSC, PRP, and CoTa group also presented an increase in the modulus of toughness. At 4 weeks, this increase was 320% compared to the control and 90% compared to PRP and CoTa. At 8 weeks this increase was 142% in comparison with the control and 31% with PRP and CoTa. This data shows promise for the use of a

combined treatment for MSC and PRP. In both the tensile strength and the modulus of toughness the researchers found that the combined group displayed a significant increase, particularly at early time periods when compared with a control group and with PRP and CoTa alone. This research implies an improved treatment method for faster and better fascial healing. However, this does not necessarily imply there would also be improved healing characteristics in Achilles tendons.

Teng, Zhou, Xu, and Bi (2016) conducted a study looking at the combination of PRP and bone marrow mesenchymal stem cells (BMSCs) to enhance tendon-bone healing. This study was on the anterior cruciate ligament in a rabbit model. Three groups were formed: a control group, a group with only PRP, and a group with PRP and BMSCs. Specimens were harvested at 8 weeks. The results revealed that the combination of PRP and BMSCs has a higher load at failure (36.22 ± 8.77 N) than the other groups (19.56 ± 2.45 N for control and 24.08 ± 1.16 N for PRP). No difference in stiffness, however, was found. Their study also revealed that PRP improved BMSC osteodifferentiation in vitro. Finally, their study proved that the combination of PRP and BMSCs promoted tendon-bone healing.

In a study conducted by Yuksel et al. (2016), the Achilles tendon of three groups of rats: a bone marrow-derived MSC group, a PRP group, and a control group, were compared at 4 weeks. The ultimate tensile strength (UTS) of each tendon was calculated, and then each group was averaged together. The UTS of the MSC, PRP, and control groups values are as follows respectively: 5.41 ± 0.84 (MPa), 4.85 ± 0.05 (MPa), and

4.41 ± 0.07 (MPa). It can be seen that the MSC group has the highest UTS, followed by the PRP group. The strain at UTS was also looked at. The results are as follows: MSC group was 0.78 ± 0.13 (mm/mm), the PRP group was 0.60 ± 0.08 (mm/mm), and the control group was 0.45 ± 0.12 (mm/mm). The same trend follows as with the ultimate tensile strength, the MSC group has the highest strain at UTS, followed by the PRP group. This concludes that both the MSC and PRP groups had increased recovery. It has also indicated that MSCs alone are more effective than PRP alone.

1.2.4 Achilles Tendon Finite Element Modeling

Living tissue is a complex material and therefore requires a complex model. A verified model of an Achilles tendon could be an extremely useful tool in predicting the outcomes of different treatment types and loading scenarios. The following literature review outlines what has already been done in terms of modeling the Achilles tendon.

Tang et al. (2011) created a finite element (FE) model of an Achilles tendon in ANSYS. The goal of this research was to develop a method to find the optimized parameters for the chosen material models to create an accurate representation of the tendon. The researchers verified their model through experimentation. Tendons are considered to be a visco-hyperelastic material. This means that the relationship between stress and strain is time-dependent and not constant. To model these characteristics two material models were used, a 3-parameter Mooney-Rivlin model and a 64-parameter Prony series model. By integrating the optimization toolboxes of ANSYS and MATLAB, Tang et al. were able to find the optimized parameters for both material models. The solid

model of the tendon was simplified to an elliptical shape using dimensions measured from the experimental tendons. The elements used in the model were 8-node hexahedron Solid 185 brick elements. For boundary conditions, the model was constrained along the axial direction on the left side, while a displacement was placed on the right side in the axial direction. The reaction force on the constrained left side was used for the verification. Sprague-Dawley rats were used for the experiment and load-relaxation tests and tensile tests were performed. The force-displacement curves and the force-relaxation curves of the experimental and simulated data were similar, indicating that the FE model of the tendon is a reliable model and the verification was successful.

Bajuri et al. (2016) also constructed an FE model in an attempt to simulate the mechanical behavior of the Achilles tendon at four different healing time points. The material model used was a hyperelastic fiber-reinforced continuum model introduced by Gasser, Ogden and Holzapfel (GOH) and the parameters for the model were optimized using MATLAB. The tendons were modeled as a perfect cylinder and two plane symmetry was used in the models. Other than symmetry as a boundary condition, a load was also placed on the end of each model to simulate a tensile test. The FE models were run in ABAQUS with nonlinear geometry used to account for the large deformations that occur in tensile testing. To verify the FE models, the strains received from ABAQUS were compared to the strains in the experimental data. The study calculated the determinant of coefficient, R^2 , value between each respective FE model and the experimental data. These values ranged from $0.9924 < R^2 < 0.9964$. Since 1 is considered a perfect R^2 value, these calculations show very promising results using the GOH model.

1.3 SCOPE OF WORK

In consideration of the literature review including Achilles tendon repair options, treatment options, and finite element models, several objectives were determined and experimental protocols, as well as computer models, were created. The purpose of this work was to determine the best overall treatment method as well as compare healing rates of each method. A secondary goal was to create a finite element model that could be verified by the experimental data as well as look at elastography of a tendon and determine if a more accurate finite element model could be conducted using localized strain. The following sections present an overview of each subsequent chapter.

1.3.1 Experimental Design

This study focused on the repair of an Achilles tendon rupture. Creating a design that is both simple and repeatable is a crucial step. References for this can be found in Section 1.2. A rat model was used to minimize variability and lessen chances of rejection. As seen in Table 1.1, four different groups were created with the following variability: group one received standard Achilles tendon repair with a CollaTape (collagen) carrier (CoTa), group two received CollaTape and platelet-rich plasma (PRP), group three had CollaTape and mesenchymal stem cells (MSC), and finally group four obtained CollaTape, platelet-rich plasma, and mesenchymal stem cells (CPM). After 1 or 2 weeks each group was sacrificed and a standard tensile test was performed to determine and compare the mechanical properties of the tendons in each group.

Table 1.1: Treatment Types and Times

	Treatment Type	Recovery (weeks)
Group One	collagen	1, 2
Group Two	collagen +PRP	1, 2
Group Three	collagen +MSC	1, 2
Group Four	collagen + PRP + MSC	1, 2

1.3.2 Elastography

Elastography is a noninvasive way to study and characterize the strain of a material through a complete testing cycle. This study used elastography on a treated tendon to review the heterogeneity within the material and compare the strains obtained through elastography with the experimental data. The localized strains found with this method were also incorporated into a finite element model to examine whether a more accurate linear model could be created.

1.3.3 Finite Element Modeling

In order to analyze the Achilles tendon through finite element analysis, first a model must be created in a modeling program. In this study SolidWorks was used to create a 3D model of an Achilles tendon. This was done by choosing one of the specimens from each group which best represented the average. Once the model was built, it was imported into ANSYS so an analysis could be completed. Before any data could be collected from the model, boundary conditions and a few parameters had to be determined; these can be found Section 2.8. After everything was set, the model was run

and then a validation was conducted. The finite element model was verified by comparing the reaction force in the model to the recorded force from the experimental data and comparing the average modulus of elasticity of the model to the experimental, for a prescribed displacement input.

1.3.4 Results and Analysis

Data from each of the eight different groups from the experimental procedure were collected from the tensile testing. This data was analyzed and then compared to determine which group had the best mechanical properties after one and two weeks of healing. The properties looked at include maximum stress, strain at maximum stress, modulus of elasticity, and strain energy. The computer models were also compared to the experimental data as a validation.

1.3.5 Conclusions and Recommendations

All treatment groups' mechanical properties improved from 1 to 2 week recovery. The cross-sections of the treatment groups were notably larger than the virgin tissue controls, similarly noted by Young et al. (1998). The MSC group at 2 week recovery time had the closest average stress-strain curve to its controls. The linear finite element models were not a reliable way to model the Achilles tendon. Finally, a histology analysis of the tendon materials to note any differences in the material would be beneficial, as well as a cyclic loading analysis to better simulate loading in the body.

CHAPTER II

EXPERIMENTAL METHODS

The following chapter explains in detail the methods and protocols used in the gathering and preparing of platelet-rich plasma (PRP) and mesenchymal stromal cells (MSC). The protocols for pre and post-surgery for the rats is also described, as well as the methods used for preparing specimens for mechanical testing.

2.1 TEST SPECIMEN AND PROTOCOL

Male Lewis rats weighing between 200–300 g were used to investigate the healing effects of collagen tape, PRP, and MSCs both as separate treatments and as a combined treatment at 1 and 2 weeks recovery. The rats were obtained from Charles River Laboratories International, Inc., in Wilmington, Massachusetts. They were housed for one week prior to the experimental procedures at the animal care facilities at Youngstown State University.

2.2 TREATMENT METHODS

There are several different treatment methods used in this study to compare the healing effects. This section outlines the processes to obtain, grow, and store each treatment additive.

2.2.1 Collagen Matrix

CollaTape™ (CoTa) absorbable collagen was purchased from Zimmer Biomet for this study. According to Zimmer Biomet's website, CoTa "resorbs in fewer than 30 days" (Zimmer Biomet). The Collatape is a sponge-like wound dressing that is soft, white, and pliable. It was 8 mm x 13 mm in size. The mesh was applied following surgical repair of the tendon by wrapping it around the tendon before the skin was sutured closed.

2.2.2 Platelet-Rich Plasma (PRP)

A procedure by Maekawa, et al. (2003) for collecting platelets was followed. At sacrifice, heart blood (5-10 ml) was collected from each rat using a 21 G needle with a 10 ml syringe that contained 100 µl of αMEM containing 10 U/ml heparin, then transferred to an EDTA vacutainer tube. The blood was centrifuged for 10 minutes at 200 xg. The PRP layer was then removed and centrifuged at 700 xg for 10 additional minutes. The platelet poor upper layer was then aspirated and saved at -20 °C. Dimethylsulfoxide (DMSO, 5%) was added to the remaining 1 ml of PRP and re-suspended. This mixture was then slowly frozen in a cryo vial until -80 °C was reached. The platelets were then stored in liquid nitrogen.

To use the platelets, the platelet poor plasma was thawed and warmed to 37 °C. The PRP was thawed until the ice pellet could be dislodged and placed into 1 ml of the pre-warmed platelet poor plasma in a 15 ml conical tube. This mixture was then centrifuged at 4 °C at 700 xg for 10 minutes. The plasma was then removed and discarded. Finally, the platelet pellet was re-suspended in 1 ml of the remaining plasma

and 0.1 ml was injected subcutaneously adjacent to the repaired incision site after surgery.

2.2.3 Bone Marrow-derived Mesenchymal Stromal Cells (MSC)

Procedures by Dai et al. (2005) and Javazon et al. (2001) were followed for harvesting and storing stromal cells. First, bone marrow cells were harvested from the femoral and tibial bones of 2 male Lewis rats of approximately 200-300 g. This was done by first inserting a 21 gauge needle and using 30 ml of α MEM containing 10 U/ml of heparin to flush the bones. The clumps were allowed to settle for 5 minutes before all but 0.5 ml of supernatant was collected. The supernatant was then centrifuged at 400 xg for 10 minutes. The pellet was re-suspended in 10 ml of complete medium. The medium was α MEM containing 20% FCS, 2 mM L-glutamine, 100 U/ml penicillin, 100 μ g/ml streptomycin, and 25 ng/ml amphotericin B. Using acetic acid, the nucleated cells were then counted. The cells were then diluted to 1×10^6 cell/ml in complete medium. 10 ml was then placed in a T75 culture flask. The cells were then incubated for 4 days. After the 4 days, the non-adherent cells were removed and the cells were fed every 3 days. The culture dish was washed with PBS at 80% confluence. The cells were then treated with trypsin/EDTA. The procedure, known as trypsinization, is as follows: use approximately 3 ml of 0.25% trypsin/1.0 mM EDTA, treat for 7 min at 37 °C, tap the flask to dislodge the cells and then stop the reaction with 30 ml of complete medium. The cells were then split into two flasks and the expansion of MSCs was continued. After passage three, the cells were collected by trypsinization and centrifuged at 400 xg for 10 minutes and then

re-suspended. The cells were frozen in complete medium containing 10% DMSO for storage.

The MSCs to be used were slightly thawed and then the frozen pellet was placed in 5 ml of 37 °C complete medium and mixed. They were then plated in a T25 tissue culture flask. The cells were once again incubated to recover overnight and then removed by trypsinization, as described previously. The cells were then centrifuged at 400 xg for 10 minutes. Then, 10^6 cells/ml they were either re-suspended in 0.5 ml of saline or PRP for treatment of animals following surgery, or they were re-suspended in complete medium at 10^6 cells/ml and saved for differentiation assays. Following surgery, 100 μ l containing 10^5 cells was injected subcutaneously adjacent to the repaired Achilles tendon.

2.3 STUDY DESIGN

The study was performed to evaluate and compare four different treatment methods for repairing a ruptured Achilles tendon. The study consisted of 80 rats total that were separated into 8 different groups that contained 10 rats each. Additional rats (10) were used for harvesting PRP and MSCs, and their tendons were harvested for normal controls. The control group (group one) received only collatape (CoTa) during repair. Group two received CoTa and PRP, group three received CoTa and MSCs, and group four received CoTa, PRP, and MSCs. Table 1.1 shows the different groups. Each treatment method then had 10 rats for the two recovery time periods of 1 and 2 weeks each.

2.3.1 Sample Size Determination

A two factor completely randomized design statistical analysis was done to determine the sample size for this experiment. The equation for determining sample size is shown in Equation 2-1.

$$\phi = \sqrt{\frac{nbD^2}{2a\sigma^2}} \quad 2-1$$

Where ϕ is a parameter based upon the following variables: n is the number of units in each experimental group, a and b are the number of levels in each factor ($a=4$ for number of treatments and $b=2$ for number of times of interest), D is the difference between means considered to be significant, and σ^2 is the variance of the strain at ultimate tensile strength. The critical response being looked at was the strain at ultimate tensile strength. The two independent factors were treatment type and recovery time. Treatment type had four levels, which were: collagen, collagen and PRP, collagen and MSC, and collagen, PRP, and MSCs. Recovery time had two different levels: 1 week and 2 weeks. The analysis was run with a 95% confidence interval ($\alpha = 0.05$) and a power of 80% ($1-\beta = 0.8$). The number of units in each experimental group was chosen to be 10. The standard deviation used was 0.13 mm/mm. This was based off of a previously done experiment by Yuksel, S. et al. (2016). This standard deviation was chosen because the experiment was done on rat Achilles tendons at four weeks and used bone marrow-derived mesenchymal stem cells, which are the same type of stem cells as the current experiment. The researchers also used a steady testing speed on the tendons, which was also used in this study. The statistical analysis was done in Minitab and Figure 2.1 is the plot given by Minitab of the statistical analysis.

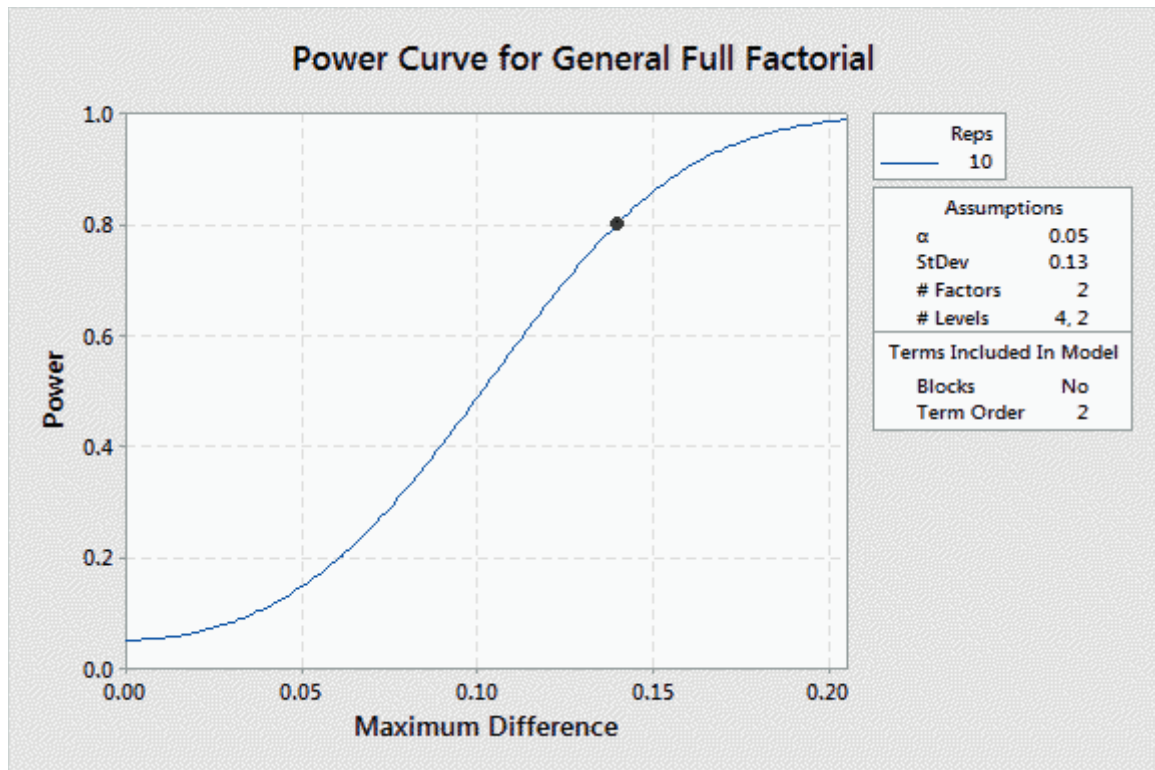


Figure 2.1: Minitab Sample Size Determination

A general full factorial design was chosen in Minitab to determine the difference between means. As shown on the graph in Figure 2.1, for a power of 80% to be achieved, a difference of means no smaller than 0.139 will be considered statistically significant.

Table 2.1 displays the number of rats in each group for each time period.

Table 2.1: Number of Rats per Group per Time Period

	One Week	Two Weeks
Group One	10	10
Group Two	10	10
Group Three	10	10
Group Four	10	10

2.4 ACHILLES TENDON INCISION AND REPAIR

The rats were put under with isoflurane (3-5%) inhalation anesthesia for induction, which was delivered through a vaporizer in a polycarbonate induction chamber, seen in Figure 2.2. They were also given isoflurane (1-3%) for maintenance. Maintenance anesthesia was delivered through a nose cone, as in Figure 2.3. Rats were kept under 20 to 40 minutes and were monitored by assessing respiratory rate, toe pinch reflex, and tissue color. They received 0.015 mg/kg of buprenorphine in 100 μ l, injected subcutaneously following surgery and at 12 and 24 hours after.



Figure 2.2: Inhalation Anesthesia

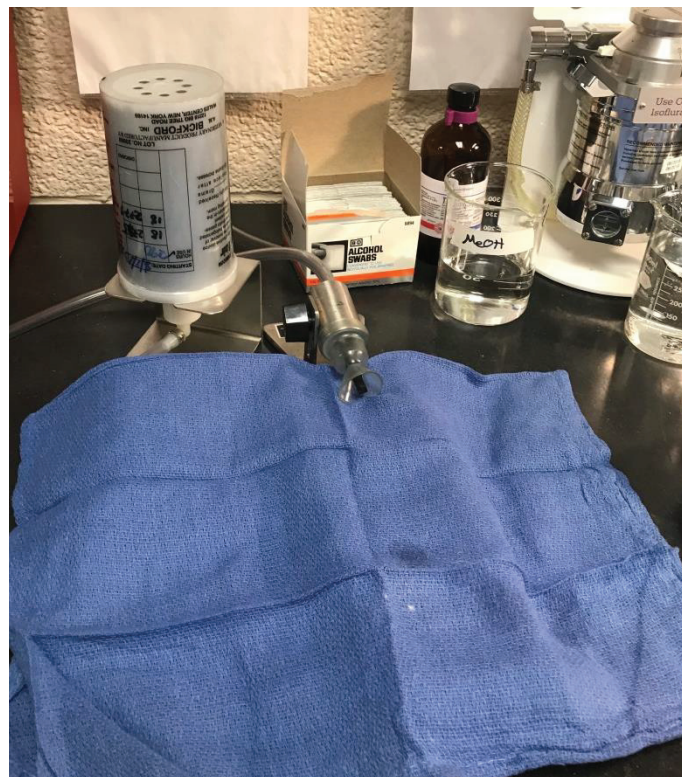


Figure 2.3: Nose Cone and Surgery Site

Aseptic techniques were followed throughout the surgical procedures and all surgical equipment was sterilized by an autoclave or with a dry sterilization unit. Instruments were wiped with a 70% ethanol solution, wiped dry, and re-sterilized in a hot bed sterilizer between each surgery, as shown in Figure 2.4.



Figure 2.4: Dry Sterilization Unit

Once the animals were under anesthesia, the skin and underlying fascia on the right hind leg was opened with a surgical blade, as shown in Figure 2.5. This exposed the Achilles tendon and a full thickness transection of the tendon was made 6 mm proximal to the calcaneus bone. The plantaris tendon was left intact to act as a splint. A modified Kessler suture was used to approximate the transected tendon ends. Collatape was wrapped around the tendon and the skin and underlying fascia was repaired using a 5-0

running Vicryl suture. Each rat was then either injected subcutaneously adjacent to the wound site with PRP, MSC, or the combination of both or received nothing based upon what group it was in. Group one received nothing, group two received an injection of PRP, group three received an injection of MSCs, and group four received an injection of PRP and MSCs. Each group contained ten animals. Figure 2.6 shows a completed Achilles tendon transection surgery.



Figure 2.5: Achilles Tendon Surgery



Figure 2.6: Post Surgery

2.5 POST PROCEDURE MONITORING

Once surgery was completed, the rats were placed in clean bedding and monitored once per day for 1 week. This was done to look for signs of infection and autophagia, which was not noted in any of the rats. After the first week of recovery, animals were monitored 2 to 3 times per week.

2.6 RECOVERY OF ACHILLES TENDON

The rats were allowed to recover for either 1 or 2 weeks and then the Achilles tendons were harvested. The rats were euthanized using anesthesia with isofluorane. This was followed by pneumothorax and the collection of blood through a heart puncture. Since there were different time intervals at which the tendons were harvested, it was possible that the tendons extracted at a later time point could be larger than those extracted at an earlier time point due to growth of the rats. To take this into account, the Achilles tendon from both hind limbs of every rat were removed, with the left Achilles

tendon acting as a control. The tendons were then wrapped in gauze and phosphate-buffered saline and frozen until testing day.

2.7 MECHANICAL TESTING

A standard tensile analysis was used to determine the mechanical properties of the tendons. Each group produced 20 specimens, which gave a total of 160 specimens for testing. The testing was performed using an Instron Tensiometer Model 5697, Figure 2.7, equipped with a 100 N load cell with 0.25% accuracy over the entire range.



Figure 2.7: Instron Testing Machine

The mechanical grips used included: custom design miniature clamping grips with a coarse grit sandpaper adhered to both inner sides, shown in Figure 2.8. These grips were used to clamp the upper muscle/tendon connection. The bottom portion of the tendon was gripped using a custom designed tendon vice, shown in Figure 2.9 and Figure 2.10.



Figure 2.8: Upper Grips



Figure 2.9: Bottom Grips Open

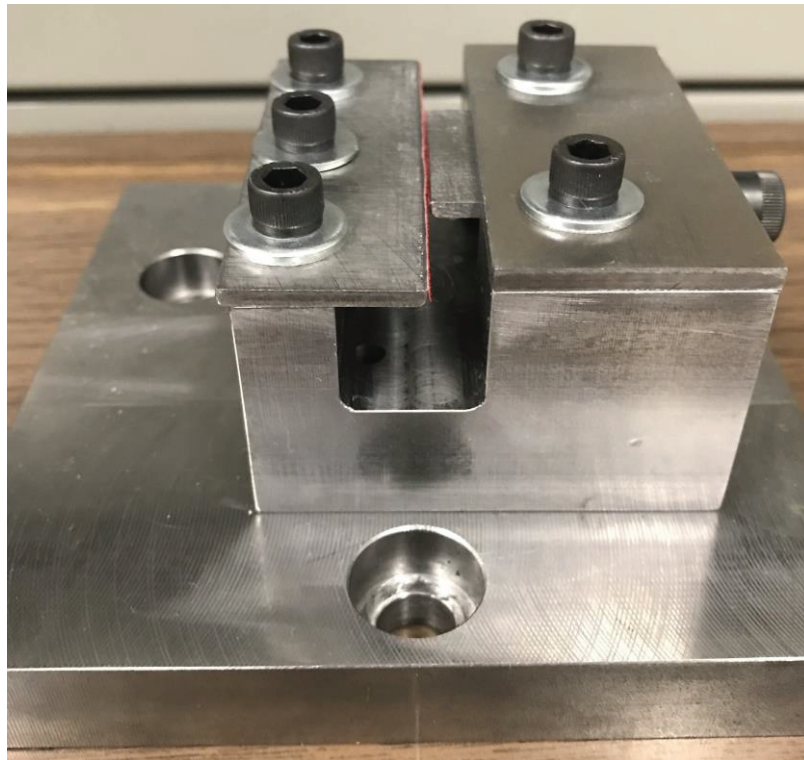


Figure 2.10: Bottom Grips Closed

A major hurdle during the designing of this procedure was eliminating slippage during testing. Originally, the top grip was to be used for both the bottom and top grips; however the tendon continually slipped out. Sandpaper was then super glued to both the top and bottom of the tendon, which eliminated slipping at the top, but not at the bottom. Epoxying the calcaneal tendon-bone connection was then considered, however a time constraint was noted. This led to the current design of the bottom tendon grip, which utilizes both the sandpaper from the first design and the tendon-bone connection from the second design. Therefore in the final design to eliminate slippage during testing, sandpaper was super glued to both sides of the upper muscle/tendon portion of the specimen, as shown in Figure 2.11. Part of the calcaneal bone was left attached to the Achilles tendon to use as a stop to keep the tendon from slipping through the grips. The bone was slid under the metal plates in the bottom grip and the tendon was pinched between the two plates, as shown in Figure 2.12. Course grit sandpaper was also placed on the metal plates to combat slipping. This strategy was specially chosen to eliminate slippage during testing.



Figure 2.11: Tendon Prepped with Sandpaper

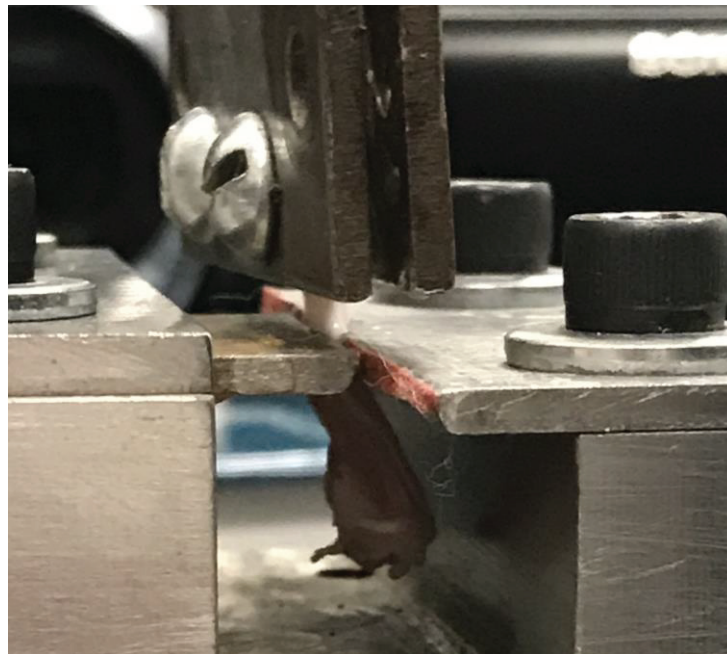
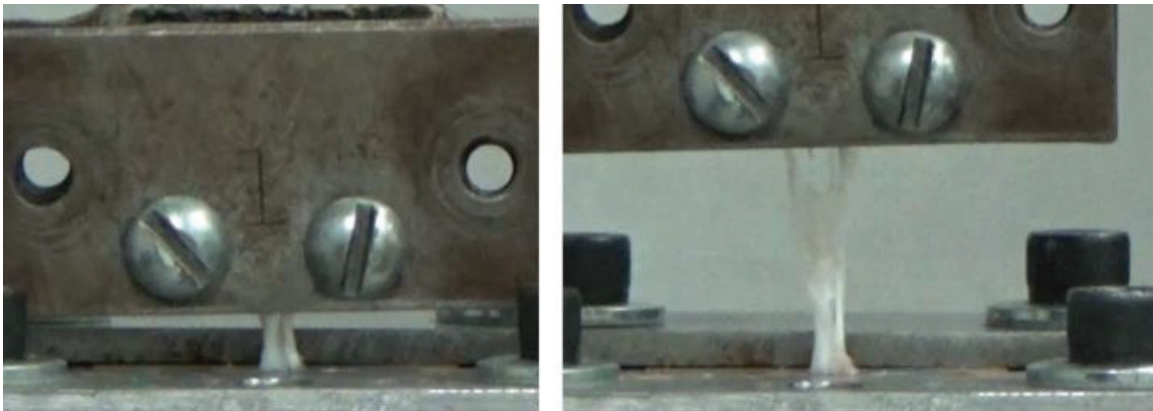


Figure 2.12: Tendon Pinched in Bottom Clamp

Prior to testing, the length; width at the top, middle, and bottom; and the thickness at the top, middle, and bottom of the Achilles tendons, were measured using digital calipers on each sample. To create a more accurate finite element model, pictures and recordings of the tensile tests were taken of the front and side of each tendon.

Figure 2.13 shows a specimen in the Instron prior to testing. First, a preload of 1 N was applied to the tendon to eliminate slack in the tendon. Then, a constant extension rate of 10mm/min was used during the testing of each specimen. The sample was stretched until failure, which occurred when the tendon was nearly completely torn in half. The force and extension data was recorded with Bluehill 3 software (Instron Corp).



(a)

(b)

Figure 2.13: Tendon Before and After Testing (a) Before Tensile Testing (b) After Tensile Testing

Using the data collected from the tensile testing, the following mechanical properties were calculated: engineering stress, ultimate tensile strength, engineering strain, strain at ultimate tensile strength, modulus of elasticity, and modulus of toughness.

The engineering stress, σ , was calculated by taking the forces recorded at each time step, F , and dividing by the original cross sectional area of the tendon, A_{CS} , as seen in Equation 2-2.

$$\sigma = F/A_{CS} \quad 2-2$$

The ultimate tensile strength was simply the maximum stress the tendon endured. The engineering strain, ε , was determined by taking the extension recorded, ΔL , and dividing by the original length of the specimen, L_i , Equation 2-3.

$$\varepsilon = \Delta L/L_i \quad 2-3$$

A stress-strain curve was then plotted using the engineering stress and engineering strains calculated at each time step. From that graph, the modulus of elasticity was computed using a linear curve-fit on the linear portion of the graph. The modulus of toughness, u , was found by calculating the area under the stress-strain curve from zero to the point of failure, ε_{max} , using Equation 2-4. This area was found by integrating the engineering stress, σ , with respect to the engineering strain, ε . A polynomial curve-fit equation was used to characterize the stress to failure in order to calculate the modulus of toughness.

$$u = \int_0^{\varepsilon_{max}} \sigma d\varepsilon \quad 2-4$$

Figure 2.14 is a stress-strain curve from control tendon 77c. The modulus of elasticity, E , strain energy, u , and maximum stress, σ_{max} , are all labeled.

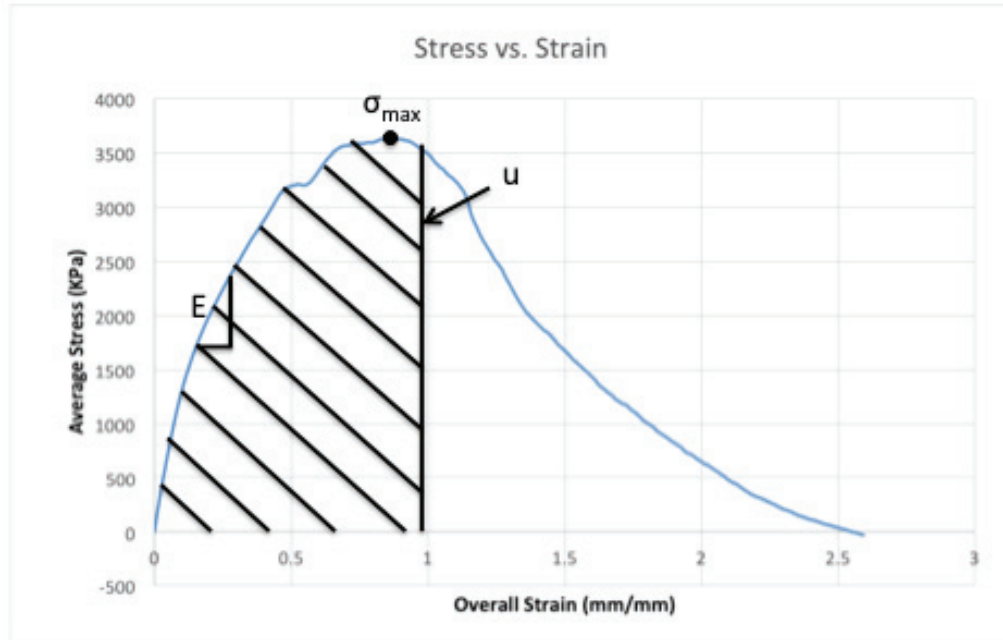


Figure 2.14: Strain-Strain Curve of Control Tendon

2.8 FINITE ELEMENT ANALYSIS

A specimen from each treatment group, CoTa, PRP, MSC, and CPM, which best represented the average was chosen. A 3D model for each treatment group was created using SolidWorks 2015 by using the dimensions found previously. These models, a sample shown in Figure 2.15, were then imported into ANSYS Workbench 19.1 for analysis.

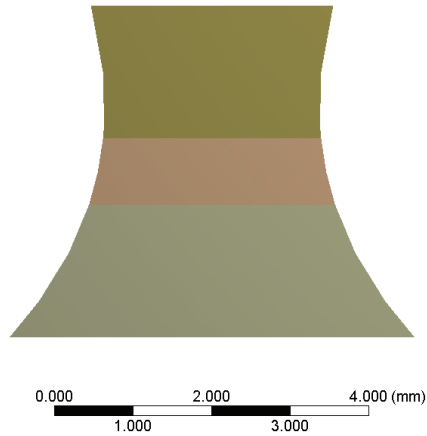


Figure 2.15: Tendon Geometry Model (Tendon 45 from 1 Week Recovery Collagen Group)

2.8.1 Material Model

Since the Achilles tendon is a nonlinear material, the models were divided into 3 different sections. In ANSYS, 3 different linear isotropic material models were created using the averaged modulus of elasticity of each respective group. To create the material models for a tendon model, first the average modulus of elasticity of the control groups was found. Secondly, the average modulus of elasticity for the treatment group was found. From there, a code was created in MATLAB, found in Appendix A, to create a bell curve using the averaged control modulus as the two upper points and the averaged treated modulus as the base for the lower point. Once the polynomial was created, MATLAB then extracted the modulus halfway between the highest and lowest points on the curve. In the 1 week recovery tendons the modulus at the middle point was used in the top and bottom section of the tendons and the lowest point on the curve was used in the center to represent the wound. Testing the 2 week recovery tendons however, it was found that most often; they did not break at the wound site, but above or below it. For the

2 week recovery tendons, to simulate this scenario, the lowest point on the bell curve was applied to the top and bottom portions of the model and the modulus of elasticity found between the control and treated modulus was applied to the wound site in the middle. As for Poisson's ratio, Vergari et al. (2011) found that as an initial approximation, tendons can be considered an incompressible material. This would make the Poisson's ratio nearly 0.5. In ANSYS a Poisson's ratio of 0.49 was used for all models.

2.8.2 Boundary Conditions

A fixed boundary condition was placed on the bottom part of the tendon and a displacement support was placed on the top to simulate the tensile test for all models. The displacement value was chosen such that ANSYS modeled the tendon that corresponded to a displacement that was half was up the linear portion of the stress-strain curve for the tendon being modeled. Figure 2.16 shows the boundary conditions on one of the models.

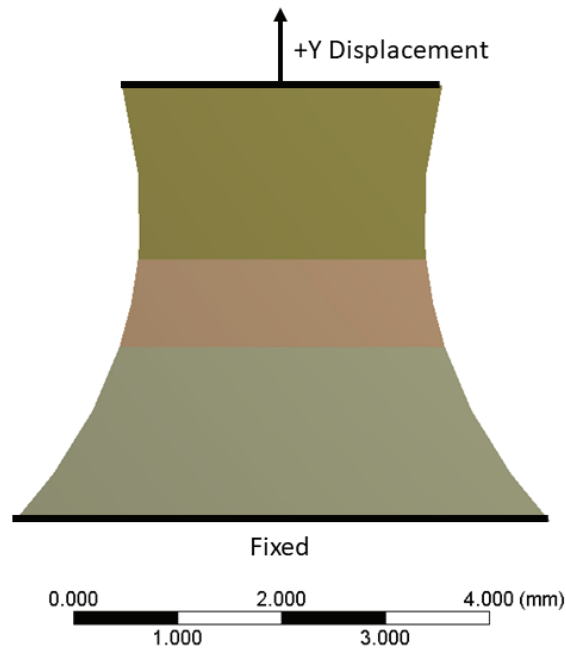


Figure 2.16: Boundary Conditions

2.8.3 Meshing

All models were meshed using second order quadrilateral elements. A larger mesh was favored for convergence of models, however at least 4 elements were placed in the thickness, shown in Figure 2.17. Table 2.2 shows the number of elements for each model. The front view of the final meshed model of tendon 45 in the 1 week recovery collagen group can be seen in Figure 2.18.

Table 2.2: Elements in FEA Models

	Number of Elements in Model
Collagen 1 Week Recovery (45)	1216
PRP 1 Week Recovery (37)	1152
MSC 1 Week Recovery (49)	1248
CPM 1 Week Recovery (2)	1632
Collagen 2 Week Recovery (71)	1944
PRP 2 Week Recovery (32)	1980
MSC 2 Week Recovery (27)	1980
CPM 2 Week Recovery (44)	1944

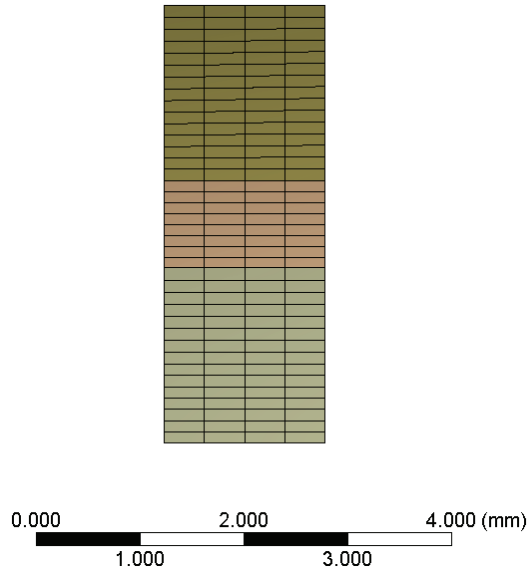


Figure 2.17: Side of Tendon Mesh

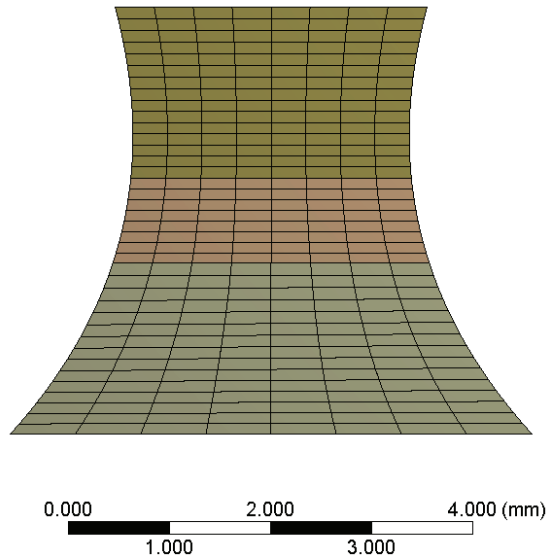


Figure 2.18: Front of Tendon Mesh

2.9 ELASTOGRAPHY

Elastography is a non-invasive way to calculate the strain in an object. By videotaping the mechanical testing of the tendons, localized strain could be calculated

through elastography. The mechanical tests were filmed under normal lighting, using a SONY high definition camera filming at 30 frames per second, fps. Calculating the strains from these films requires a few steps. Firstly, the video was broken into each individual frame. Then, the pixels movements were tracked through each frame. Finally, the strain elastogram was obtained from the pixels movements.

Based on Marie et al. (2010), an optical flow algorithm was used to estimate the pixels movements throughout the frames. This was done by solving a brightness conservation equation, shown in Equation 2-5. $I(x,y,t)$ is the image brightness function with x and y as the rows and columns and t is the frame interval or time.

$$\frac{\partial I}{\partial x} \frac{dx}{dt} + \frac{\partial I}{\partial y} \frac{dy}{dt} + \frac{\partial I}{\partial t} = 0 \quad 2-5$$

As stated in the research by Marie et al. (2012), Equation 2-5 does not guarantee a unique solution, however. Therefore, constraints in the form of a regularization term must be imposed. By minimizing the objective function in Equation 2-6, an optical flow solution (u,v) can be achieved.

$$obj(u, v) = (I_x u + I_y v + I_t)^2 + \lambda(u_x^2 + u_y^2 + v_x^2 + v_y^2) \quad 2-6$$

A strain tensor shown in Equation 2-7, where $(\epsilon_{xx}, \epsilon_{yy})$ are the normal strains and $(\epsilon_{xy}, \epsilon_{yx})$ are the shear strains, was used to aid in the strain elastogram computation.

$$\epsilon = \begin{bmatrix} \epsilon_{xx} = \frac{\partial u}{\partial x} & \epsilon_{yx} = \frac{1}{2} \left(\frac{\partial u}{\partial y} + \frac{\partial v}{\partial x} \right) \\ \epsilon_{xy} = \frac{1}{2} \left(\frac{\partial v}{\partial x} + \frac{\partial u}{\partial y} \right) & \epsilon_{yy} = \frac{\partial v}{\partial y} \end{bmatrix} \quad 2-7$$

The researchers noted that the derivatives of Equation 2-7 were calculated by a convolution operation using an optical flow solution $u=(u,v)^T$. The derivatives can be found in Equation 2-8 and Equation 2-9, where S_x and S_y are the Sobel filters.

$$\frac{\partial u}{\partial x} = S_x^*u, \quad \frac{\partial v}{\partial x} = S_x^*v \quad 2-8$$

$$\frac{\partial u}{\partial y} = S_y^*u, \quad \frac{\partial v}{\partial y} = S_y^*v \quad 2-9$$

An image was then calculated for each strain component.

2.9.1 Elastography of Tendon 45

Tendon 45 from the collagen treated group at 1 week recovery was chosen for an elastography analysis. Dr. Yong Zhang from the Department of Computer and Information Sciences at Youngstown State University ran the video of the tensile test through his elastography program. Figure 2.19 shows the tendon at the beginning, middle, and end of testing and the corresponding strain elastography images. In Figure 2.19 (a) the points marked 1-6 were chosen to conduct a localized strain analysis. An overall strain analysis was done as well. The lighter portions of the elastography images in Figure 2.19 (d-f) correlate with higher strains. The dark portion at the top of the images is the clamp used for testing, hence why there is no strain shown in the elastography.

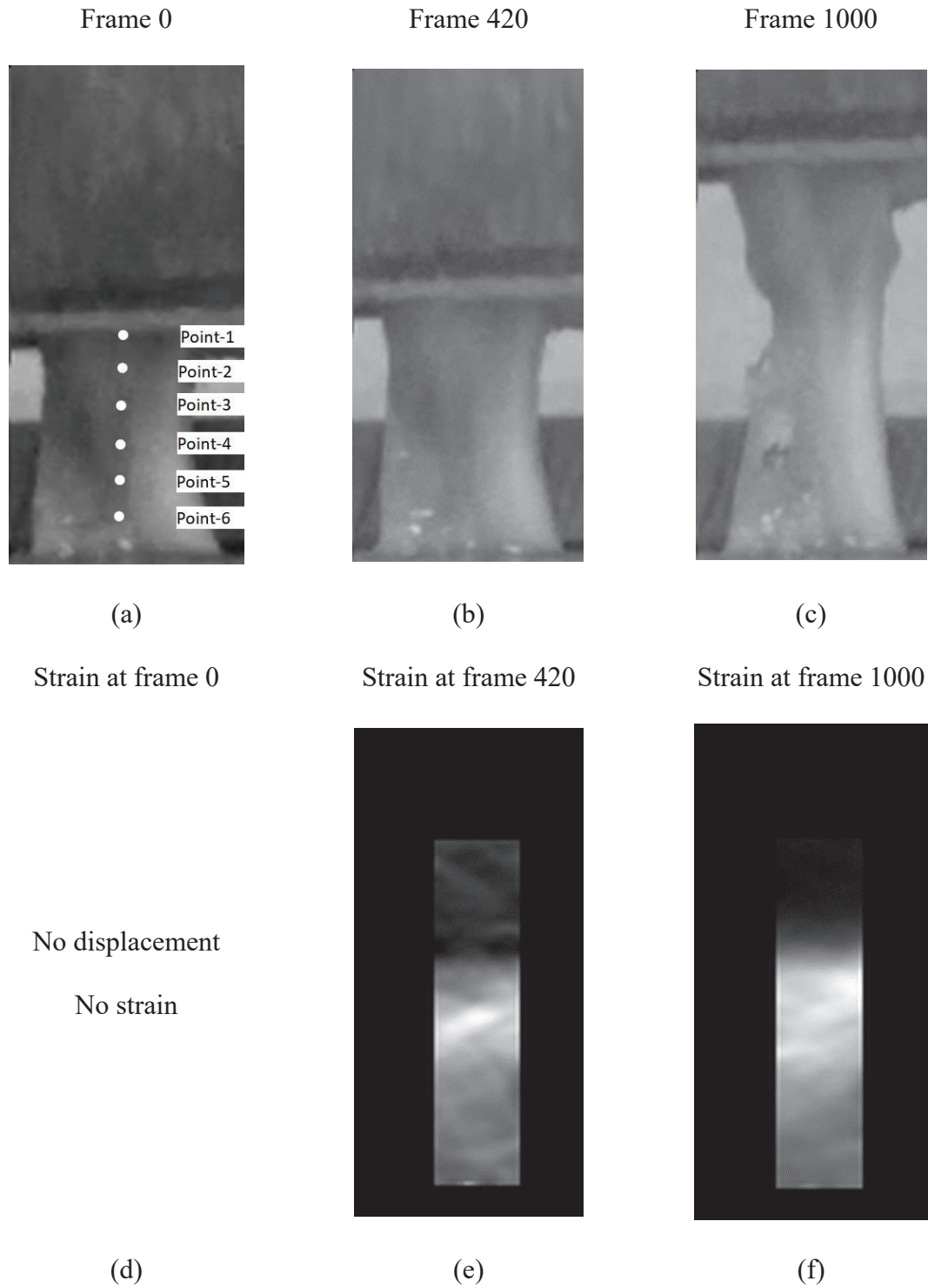


Figure 2.19: Images of Tendon During Testing and Corresponding Elastography
Images (a) Tendon Prior to Test, Marked with Six Points to be Traced During Elastography (b) Tendon During Test at Frame 420 (c) Tendon at Frame 1000 Near End of Test (d) No Displacement Before Testing (e) Elastography Image at Mid Test (f) Elastography Image at End of Test

2.9.2 Finite Element Analysis using Elastography

Using the elastography from tendon 45 in the 1 week recovery collagen group, an FE model was created using similar steps described in Section 2.8. Since there were six different locations where the strain was calculated, six different sections were created in the tendon model to correlate to the moduli of elasticity found. The sizes of the sections were all equal widths. Figure 2.20 shows the six different sections on the model.

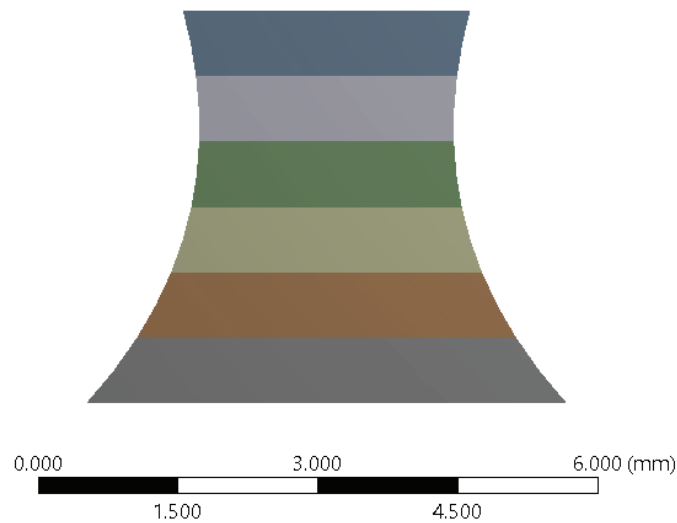


Figure 2.20: Geometry of Elastography Model

The boundary conditions and the meshing were done the same way as described in Section 2.8. The total amount of elements in the model was 1480.

The modulus of elasticity for each point shown previously in Figure 2.19 (a) was found and is shown in Table 2.3. The graphs used to find the modulus of elasticity of each of the six points can be found in Appendix B.

Table 2.3: Modulus of Elasticity at Each Point in Elastography

	Point 1	Point 2	Point 3	Point 4	Point 5	Point 6
Modulus of Elasticity (kPa)	4548.5222	3455.493	6125.422	8349.1	19177.83	10381.132

These moduli were used in the six different linear isotropic material models created in ANSYS 16.1 and the poison's ratio used was 0.49.

2.10 STATISTICAL ANALYSIS

The following sections explain the methods used to perform different statistical analyses. The first section, Section 1.13.1, explains whether or not there is a statistical difference between the left and right Achilles tendons of Lewis rats. Once that was determined, Section 1.13.2 explains the method used to find a statistical difference between each treatment method at both time points.

2.10.1 Left Tendon vs. Right Tendon

To use the left tendon of each rat confidently as a virgin tissue control, a small study was done to confirm that there is no statistical difference between the left and right Achilles tendons of rats. Five Lewis rats were used and both Achilles tendons from each rat were extracted. Tensile testing was done following the procedure discussed previously. A One-Way ANOVA was used to find any statistical difference between the left and right tendons. Table 2.4 shows the averages of the left and right tendons and the P-value for the max force, modulus of elasticity, strain at UTS, and strain energy.

Table 2.4: Statistical Analysis of Left vs Right Tendon

Group	Average Max Force (N)	Average Modulus of Elasticity (KPa)	Average Strain at UTS (mm/mm)	Average Strain Energy (KPa)
Left Tendon	43	36728.23	0.513	4778
Right Tendon	38.6	29376.50	0.663	6404
P-Value	0.684	0.644	0.587	0.533

A 95% confidence interval was used for this analysis. Looking at the P-values for all the data, it should be noted that there is no statistical difference between the left and right tendons in any of the areas studied. There is, however, variation within the individual groups. To combat this, the measurements for all the tendons in the treatment study were measured from scaled picture in SolidWorks 2015 rather than with calipers. This produced more accurate measurement and therefore more accurate results.

2.10.2 Differences between Treatment Methods through Time

A two-way ANOVA statistical analysis was chosen for this study. The two-way ANOVA is able to take the independent variables, treatment and recovery time, into consideration. It also checks to see if there is an interaction between the independent variables on the dependent variable. This would signify that one of the independent variables is dependent on the other independent variable. To receive accurate results from a two-way ANOVA, six different assumptions must be met.

1. The dependent variable should be measured at a continuous level.
2. The two independent variables should consist of two or more categorical sections.
3. There should be independence of observation.
4. There should be no significant outliers.
5. The dependent variable should be normally distributed.

6. There needs to be equal variances between groups.

The first three assumptions are met by way of the experimental design (Laerd Statistics).

After checking the data for outliers and a normal distribution, it was found that the maximum stress, strain at failure, strain at UTS, total strain energy, elastic strain energy, and the modulus of elasticity all possessed outliers or skewed distributions. To combat that, a log base 10 transformation was used. According to McDonald (2014), this is a common transformation used in biology statistics. As for the final assumption, if a model contains fixed factors and the samples sizes are equal or almost equal then the ANOVA results are only slightly varied by unequal variances (Minitab). Since this study has fixed factors and equal or almost equal sample sizes, it was assumed that the samples had equal variances or that the results would not be heavily varied otherwise. The results of this analysis can be found in Chapter 3.

CHAPTER III

RESULTS AND CONCLUSIONS

The following sections detail the results of this study as well as a statistical analysis done to verify any statistically significant differences. The results obtained were also compared to those seen in literature.

3.1 DIFFERENCES IN TENDON SIZES

The treated tendons all had much larger cross-sectional areas. The average cross-sectional area of each group was compared to the cross sectional area of their controls. Table 3.1 shows the comparison of cross-sectional areas in percentage of the 1 week recovery tendons. Table 3.2 shows the differences of the cross sectional areas for the 2 week recovery.

Table 3.1: Average Cross Sectional Areas at 1 Week Recovery

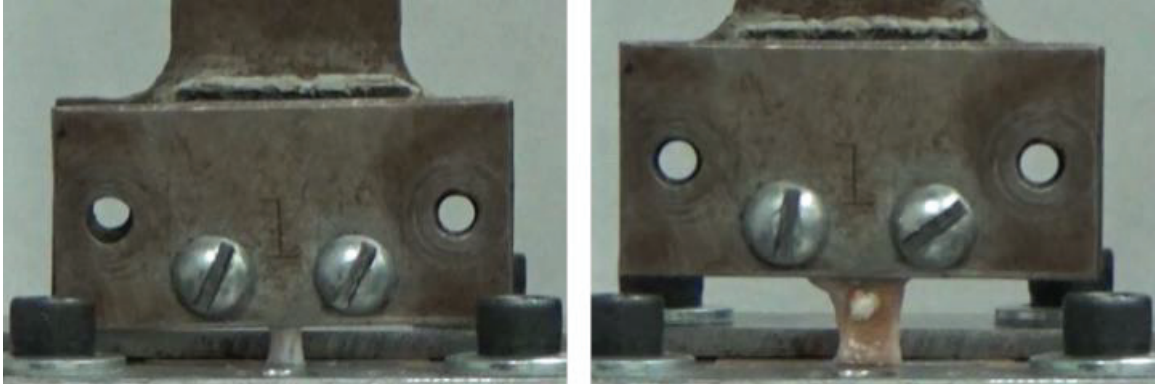
	Average Cross-Sectional Areas (mm ²)	Standard Deviation	Percent Difference Between Control
Collagen Treated	20.75	5.5	
Collagen Controls	7.77	2.07	62.5%
PRP Treated	22.95	7.34	
PRP Controls	8.08	2.21	64.8%
MSC Treated	21.71	2.6	
MSC Controls	7.65	2.01	64.8%
CPM Treated	21.86	3.9	
CPM Controls	7.31	2.24	66.6%

Table 3.2: Average Cross-Sectional Area of 2 Week Recovery

	Average Cross-Sectional Areas (mm ²)	Standard Deviation	Percent Difference Between Control
Collagen Treated	21.40	5.14	
Collagen Controls	7.8	2.92	63.6%
PRP Treated	25.95	4.87	
PRP Controls	7.33	2.26	71.8%
MSC Treated	23.66	4.72	
MSC Controls	8.46	2.63	64.2%
CPM Treated	26.54	4.41	
CPM Controls	8.53	3.32	67.9%

Although the treated cross-sectional areas are larger than the controls, they do not significantly change from 1 to 2 week recovery.

The calculations for finding the mechanical properties of the tendons requires the cross-sectional area of each tendon. In Figure 3.1 tendon 45 and 45c can be seen. The cross-sectional areas of the treated tendons at both recovery times were swollen due to the surgeries. It was therefore decided that the treated cross-sectional areas were invalid and the left leg controls' cross sectional areas were used for calculations.



(a)

(b)

Figure 3.1: (a) Left Untreated Tendon (b) Right MSC Treated Tendon 1 Week Recovery

3.2 MECHANICAL TESTING RESULTS

Four of the eighty treated tendons tested were removed from the analysis. One of them was redone. Because of this, the collagen treatment group at 1 week recovery only had nine samples and the PRP group at 1 week recovery had eight samples. All other groups had ten samples. It should also be noted that any sutures that were found intact were removed for mechanical testing purposes.

Figure 3.2 is the stress-strain curve of one tendon in the collagen only group at 2 weeks recovery. Figure 3.3 is the stress-strain curve to failure of tendon 50. A trendline was added to estimate the equation of the curve so that the strain energy could be obtained. From there, the linear most portion of the graph was plotted, shown in Figure 3.4, and a linear trendline was added to estimate the slope of the line, thereby obtaining the modulus of elasticity.

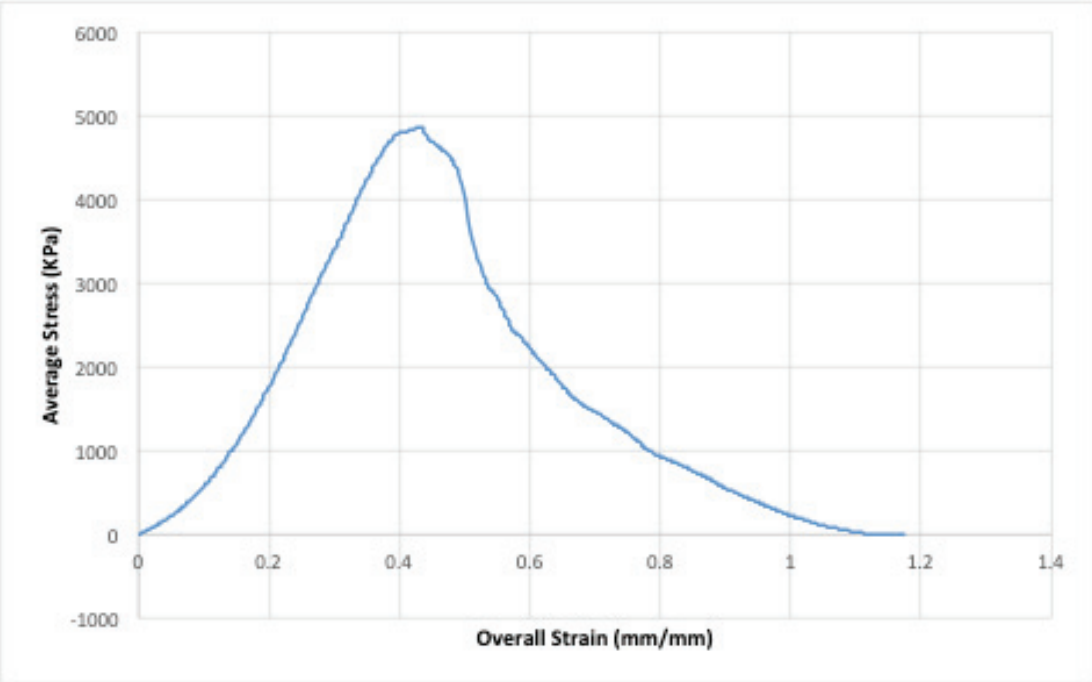


Figure 3.2: Stress-Strain of Tendon 50

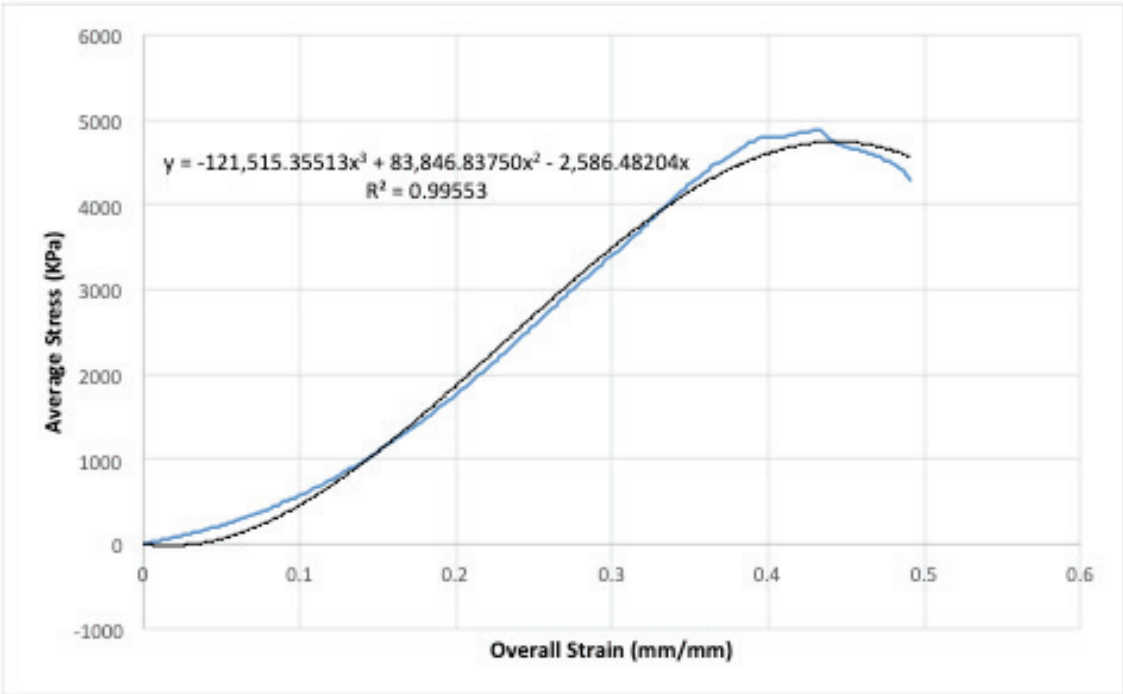


Figure 3.3: Stress-Strain to Failure of Tendon 50

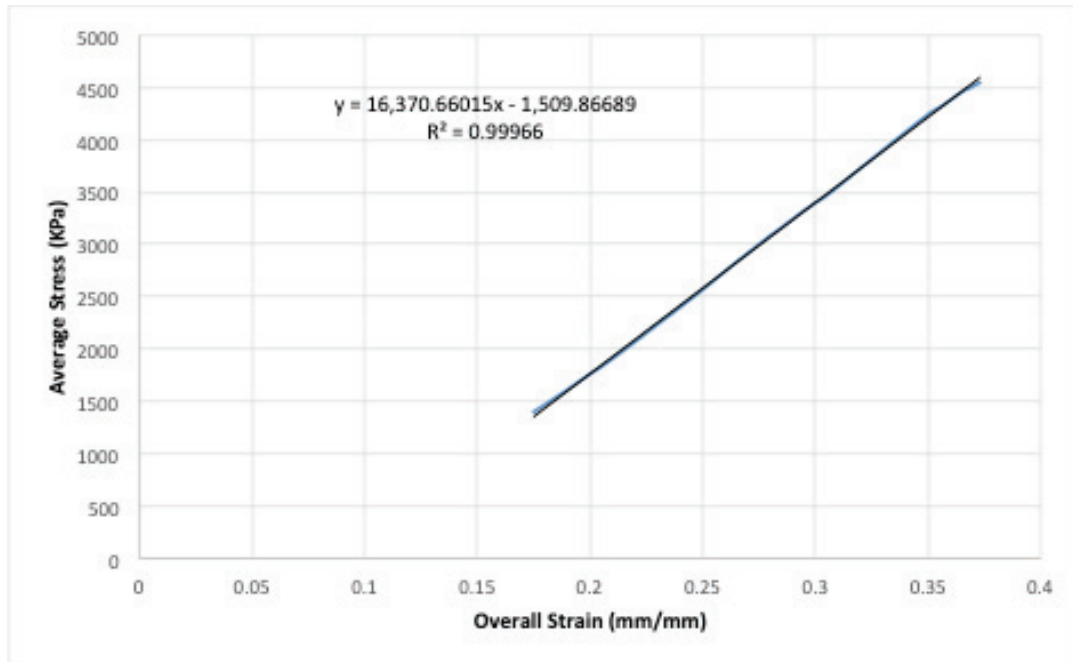


Figure 3.4: Modulus of Elasticity of Tendon 50

3.2.1 Location of Failure

The tendons that only had 1 week to recover normally failed at the wound site. Figure 3.5 is tendon 25, which was from the 1 week recovery collagen group. It can be seen that the tendon failed at the wound site.



(a)

(b)

Figure 3.5: 1 Week Recovery Failure Site (a) Tendon Prior to Testing (b) Tendon Post Failure

Figure 3.6 is of tendon 26c, showing one of the common ways of failure for the control tendons. Many of the control tendons strained until they could no longer hold any load. In this scenario they would strain at the top.



Figure 3.6: Control Tendon Strained to Failure (a) Tendon Prior to Testing (b) Tendon Post Failure

Another common way for the control tendons to fail was by tearing and straining at the bottom. Figure 3.7 shows an example of this failure.



Figure 3.7: Control Tendon Torn at Bottom (a) Tendon Prior to Testing (b) Tendon Post Failure

Many of the 2 week recovery tendons did not fail at the wound site, but either above or below. Figure 3.8 is an example of a common failure of the 2 week recoveries. It can be seen that the tendon tore above the wound.

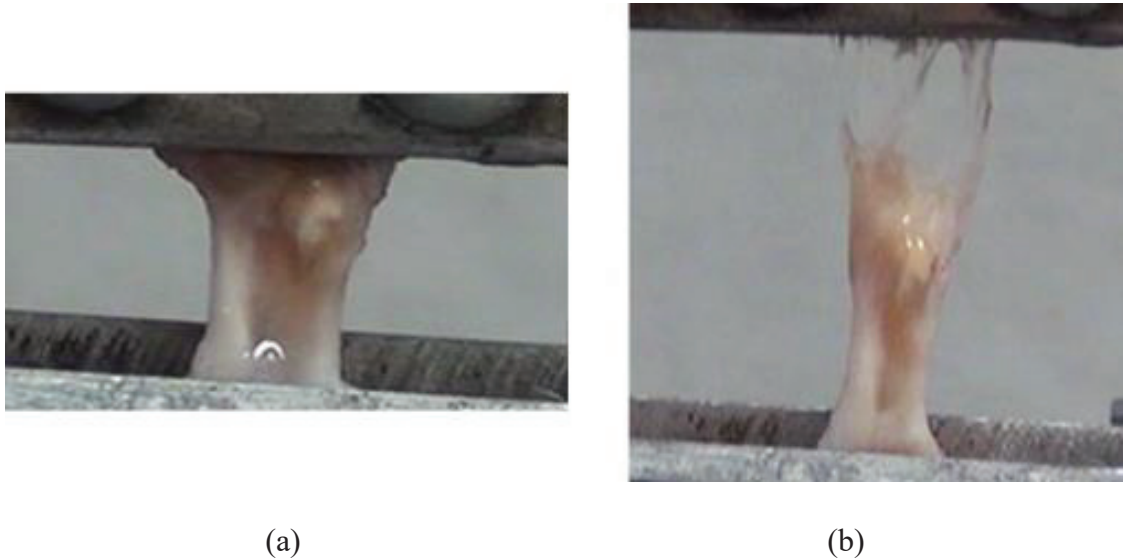


Figure 3.8: 2 Week Recovery Failure Site (a) Tendon Prior to Testing (b) Tendon Post Failure

3.2.2 Average Mechanical Properties of Each Treatment Group

Table 3.3 shows the average of the mechanical properties of each treatment group, collagen, PRP and collagen, MSC and collagen, and MSC, PRP, and collagen, at 1 week recovery time. Table 3.4 shows the same properties but at 2 weeks recovery time. These averages were found by averaging the properties of each individual tendon. For example, for the maximum stress, the maximum stress of each tendon was averaged together for each treatment group at each recovery time. The material properties for each individual tendon can be found in Appendix C.

Table 3.3: Average Mechanical Properties at 1 Week Recovery

	Collagen	PRP + Collagen	MSC + Collagen	Both + Collagen	Control
Max Stress (kPa)	2898.62	2665.44	2452.29	2716.32	6,504.96
Max Force (N)	20.39	16.32	18.03	21.43	47.67
Strain at Failure (mm/mm)	0.50	0.54	0.58	0.55	0.53
Total Strain Energy (kPa)	810.39	920.89	949.32	930.96	1,885.60
Strain at UTS (mm/mm)	0.47	0.50	0.52	0.52	0.51
Average Modulus of Elasticity (kPa)	8493.52	8501.46	8895.47	7483.42	16,045.15
Elastic Strain Energy (kPa)	597.98	509.64	267.24	521.95	1,148.65

Table 3.4: Average Mechanical Properties at 2 Weeks Recovery

	Collagen (with outlier)	Collagen (without outlier)	PRP + Collagen	MSC + Collagen	Both + Collagen	Control
Max Stress (kPa)	4,380.06	4,541.31	4,686.70	4,418.34	4095.25	6,504.96
Max Force (N)	30.90	31.31	33.57	30.14	31.43	47.67
Strain at Failure (mm/mm)	0.80	0.60	0.57	0.55	0.52	0.53
Total Strain Energy (kPa)	1853.00	1553.08	1859.64	1,355.29	1008.04	1,885.60
Strain at UTS (mm/mm)	0.74	0.55	0.56	0.51	0.49	0.51
Average Modulus of Elasticity (kPa)	11,717.73	12,834.56	13,374.25	14,292.80	12616.47	16,045.15
Elastic Strain Energy (kPa)	1,108.16	1,093.13	956.37	634.14	669.81	1,148.65

It should be noted that in the collagen group at 2 weeks recovery time, an outlier was detected three standard deviations from the mean using Minitab. This data was recorded both with and without the outlier so its affects can be seen. At 1 week recovery time it can be seen that the tendons have not yet fully recovered. Differences between the treatment groups can be seen at this recovery time. The total strain energy of the collagen only group is 43% that of the control group while the PRP, MSC, and CPM are 49%, 50.35%, and 49.37% of the control group respectively. A difference can also be seen in the strain at failure between the different treatment groups at 1 week recovery. This can be better seen in the average stress-strain curves of the groups in Section 3.2.3.

Figure 3.9 shows a box plot of the modulus of elasticity of each treatment group at 1 week recovery and Figure 3.10 shows the same thing at 2 weeks recovery. Although each treatment groups modulus of elasticity is similar at 1 week recovery, MSC has the highest average modulus of elasticity (8,895 kPa), with PRP being second (8,501 kPa), collagen being third (8,494 kPa), and CPM has the smallest modulus of elasticity (7,483 kPa). At 2 week recovery all treatment groups' modulus of elasticity improved. The MSC group still maintains the highest modulus of elasticity at 14,293 kPa. Collagen, PRP, and CPM's moduli of elasticity are 11,718 kPa, 13,374 kPa, and 12,616 kPa respectively.

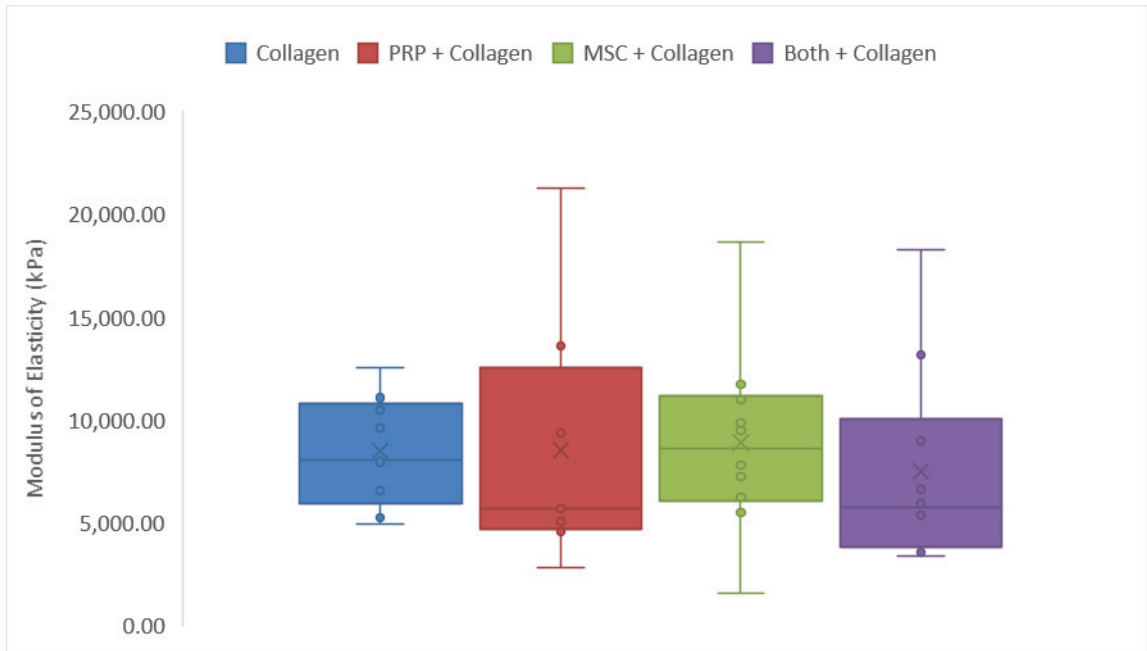


Figure 3.9: Plot of Modulus of Elasticity at 1 Week Recovery

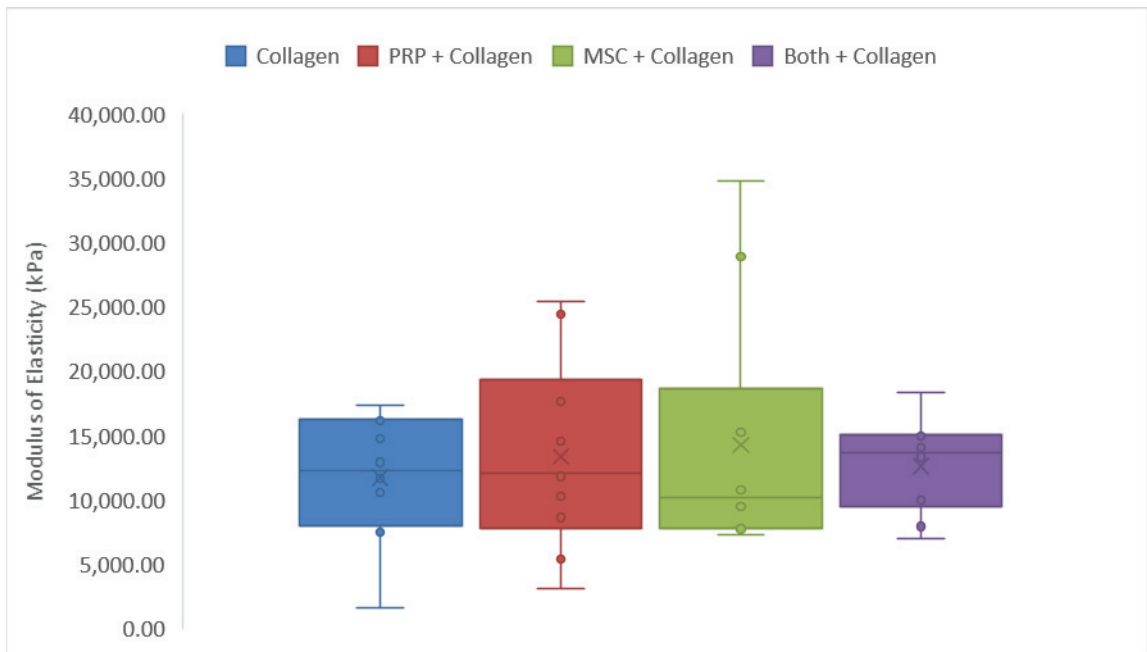


Figure 3.10: Plot of Modulus of Elasticity at 2 Week Recovery

Box plots of the maximum stress, maximum force, strain to failure, strain at UTS, strain energy, and elastic strain energy can be found in Appendix D.

3.2.3 Mechanical Properties Based on Averaged Stress-Strain Curves

Figure 3.11 is the average stress-strain curve at 1 week recovery with the cross sections measured from the treated tendons. Figure 3.12 is the average stress-strain curve at 1 week recovery with the control cross sections applied to the treated tendons. Using the control cross-sections, the collagen only treatment no longer has the greatest maximum stress. The PRP, MSC, and CPM groups all withstand greater strain compared to the collagen only group. This is an advantageous quality in the early stages of tendon healing. The MSC group also has a higher modulus of elasticity at 1 week recovery than the other treated groups.

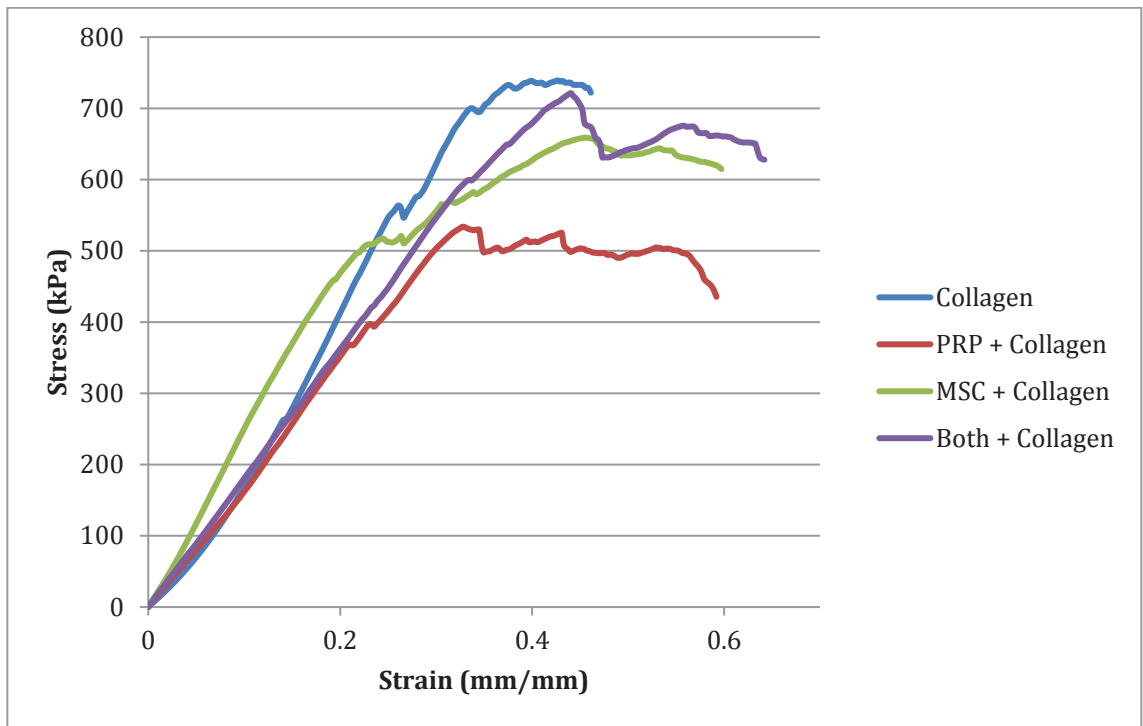


Figure 3.11: 1 Week Recovery: Stress-Strain to Failure, Original Treated Cross-Section

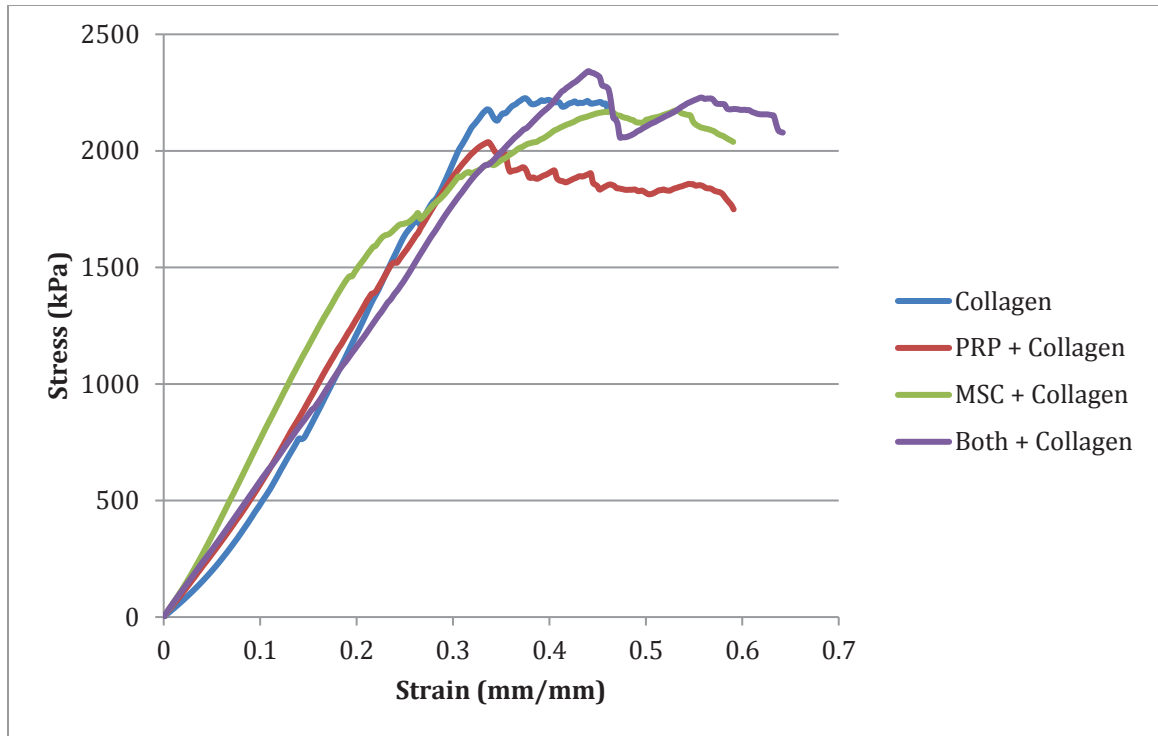


Figure 3.12: 1 Week Recovery: Stress-Strain to Failure, Control Cross-Section

Table 3.5 shows the mechanical properties of each treatment group at 1 week recovery. Table 3.6 shows the mechanical properties of each 1 week recovery control based on their right leg treatment counterpart. These properties were taken from the average stress-strain curves using the control cross-sections. Table 3.7 shows the percent differences between the treatment groups and their respective control groups as well as between the PRP, MSC, and CPM treatments and the collagen treatment at 1 week recovery. When comparing with the control group, a negative percent difference indicates the treatment has a larger material property value. A negative percent difference when comparing with the collagen group indicates the collagen group has a larger material value. Looking at the MSC group, there is only a 0.57% difference in the strain at UTS between the MSC and control groups. The MSC group has a larger strain to failure by

3.01% compared to the control group. The CPM group only has a 1.85% difference in strain to failure between the control group. When looking at percent differences between the PRP, MSC, and CPM groups with collagen, all three groups have larger strain to failure and total strain energy than collagen. Only the MSC group however, has a significantly larger modulus of elasticity (20.83%).

Table 3.5: Average Mechanical Properties of Treated Tendons 1 Week Recovery from Average Stress-Strain Curves

	Collagen	PRP + Collagen	MSC + Collagen	Both + Collagen
Max Stress (kPa)	2225.57	2037.15	2173.44	2342.17
Max Force (N)	15.21	13.28	15.85	18.74
Strain at Failure (mm/mm)	0.46	0.59	0.59	0.64
Total Strain Energy (kPa)	618.15	823.80	925.25	988.86
Strain at UTS (mm/mm)	0.38	0.34	0.53	0.44
Average Modulus of Elasticity (kPa)	6722.21	6788.46	8122.50	5890.12
Elastic Strain Energy (kPa)	312.21	298.16	133.11	428.18

Table 3.6: Average Mechanical Properties of Control Tendons 1 Week Recovery from Average Stress-Strain Curves

	Collagen Control	PRP + Collagen Control	MSC + Collagen Control	Both + Collagen Control
Max Stress (kPa)	4895.73	5237.40	3819.21	3737.39
Max Force (N)	32.20	34.54	30.71	29.43
Strain at Failure (mm/mm)	0.60	0.96	0.54	0.65
Total Strain Energy (kPa)	1725.89	2828.96	2004.43	1778.82
Strain at UTS (mm/mm)	0.51	0.90	0.53	0.54
Average Modulus of Elasticity (kPa)	10582.11	8250.90	11465.80	10428.77
Elastic Strain Energy (kPa)	938.82	1528.62	466.93	516.52

Table 3.7: Percent Difference between Treatments and Controls and Treatments and Collagen 1 Week Recovery

	Percent Difference Control				Percent Difference Collagen		
	Collagen	PRP + Collagen	MSC + Collagen	CPM + Collagen	PRP + Collagen	MSC + Collagen	CPM + Collagen
Max Stress (kPa)	54.54%	61.10%	43.09%	37.33%	-8.47%	-2.34%	5.24%
Max Force (N)	52.76%	61.54%	48.40%	36.32%	-12.66%	4.19%	23.22%
Strain at Failure (mm/mm)	22.10%	38.26%	-3.01%	1.85%	27.46%	22.61%	38.46%
Total Strain Energy (kPa)	64.18%	70.88%	35.82%	44.41%	33.27%	42.31%	59.97%
Strain at UTS (mm/mm)	26.53%	62.70%	0.57%	17.93%	-10.29%	41.38%	17.34%
Average Modulus of Elasticity (kPa)	36.48%	17.72%	29.16%	43.52%	0.99%	20.83%	-12.38%
Elastic Strain Energy (kPa)	66.74%	80.49%	71.49%	17.10%	-4.50%	-57.37%	37.14%

Figure 3.13 is the averaged stress-strain graph of the treatment group at 2 weeks recovery, with the outlier removed from the collagen group. This data used the original cross sections of the treated tendons. Figure 3.14 is that same graph as Figure 3.13, but uses the cross sections of the control tendons. At 2 weeks it seems the collagen only group has around the same strain at failure as the PRP group. A notable difference in the graphs is in Figure 3.14. Collagen has a smaller modulus of elasticity than the other groups. A comparison of the treatment groups' force-extension can be found in Appendix D.

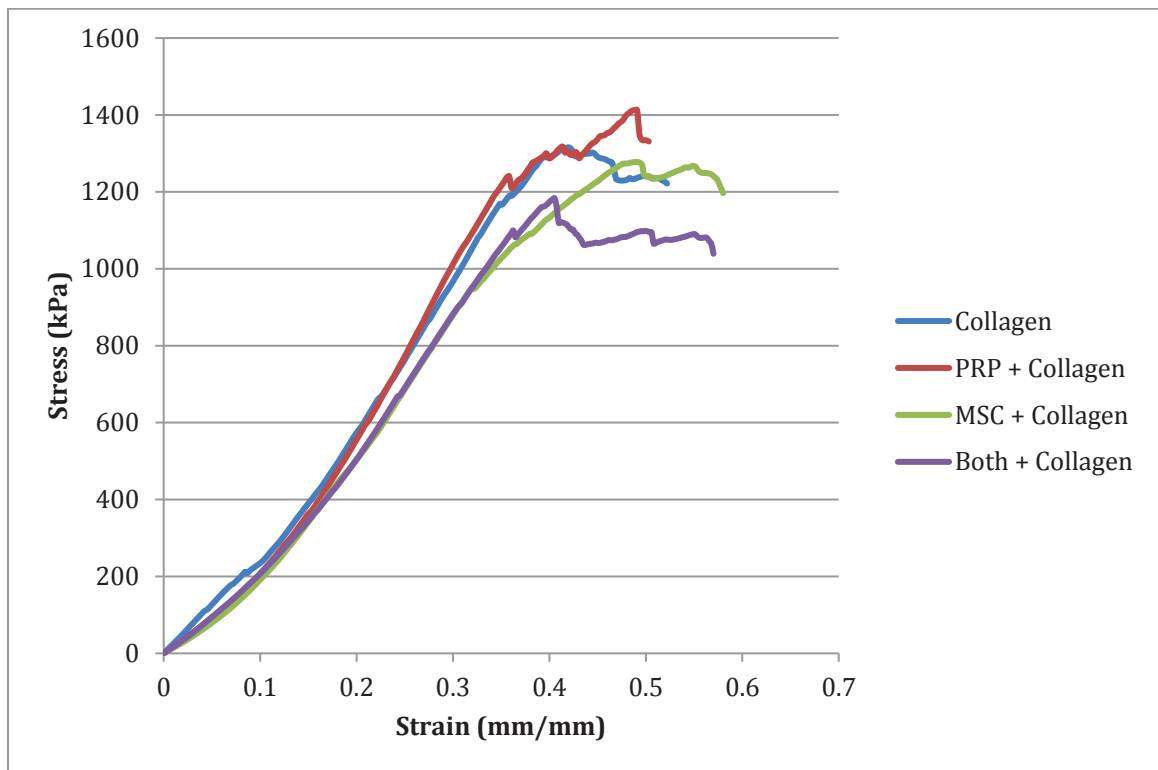


Figure 3.13: 2 Week Recovery: Stress-Strain to Failure, Original Treated Cross-Section

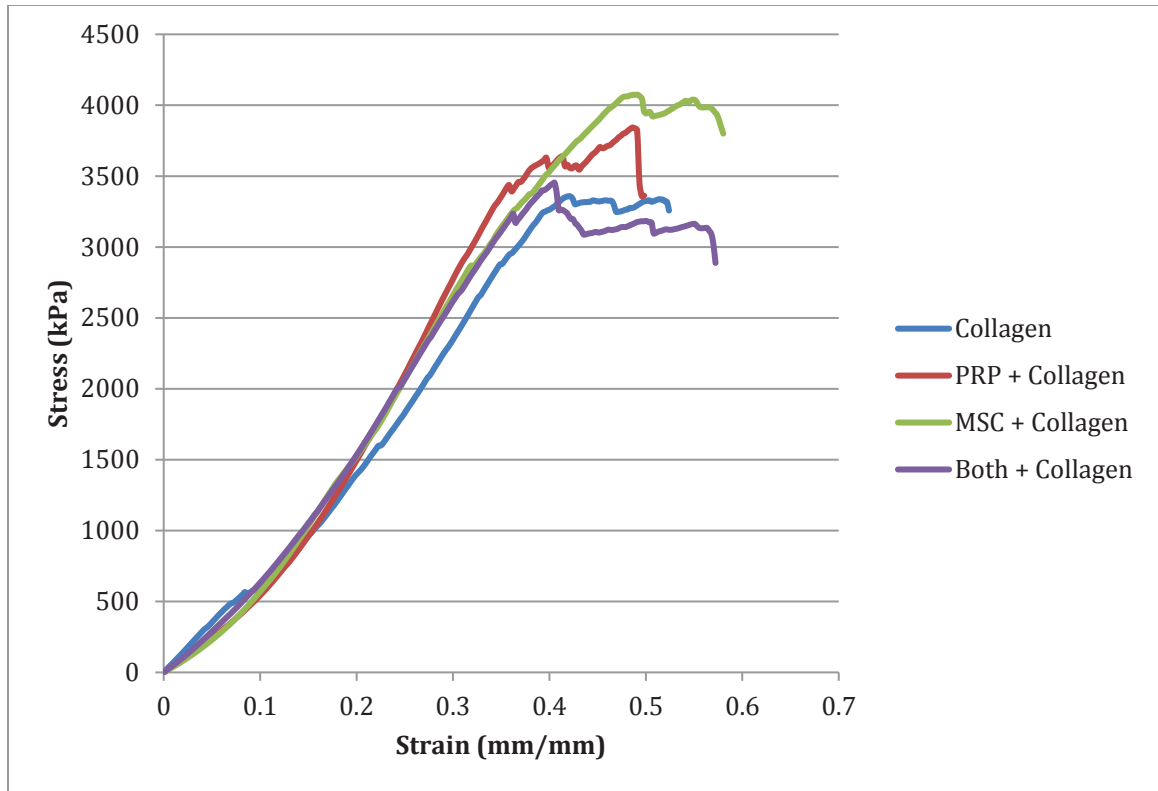


Figure 3.14: 2 Week Recovery: Stress-Strain to Failure, Control Cross-Section

Stress-strain curves of each individual tendon can also be found in Appendix D.

Table 3.8 shows the mechanical properties of each treatment group at 2 week recovery. Table 3.9 shows the mechanical properties of each 2 week recovery control based on their right leg treatment counterpart. These properties were taken from the average stress-strain curves using the control cross-sections. They show the collagen group both with and without the outlier to show its affects. Table 3.10 shows the percent differences between the treatment groups and their respective control groups as well as between the PRP, MSC, and CPM treatments and the collagen treatment at 2 week recovery. When comparing with the control group, a negative percent difference indicates

the treatment has a larger material property value. A negative percent difference when comparing with the collagen group indicates the collagen group has a larger material value. At 2 week recovery it can be seen that the MSC group still has a larger strain to failure than its control group (7.55%). Looking at the percent difference between the treatment groups and their controls, the MSC group generally has lower percent differences all around than the other treatment groups, indicating that it is closest to its control. When looking at the percent differences between the PRP, MSC, and CPM groups and collagen, it can be seen that the three treatment groups all have higher modulus of elasticity, maximum stresses, and maximum forces.

Table 3.8: Average Mechanical Properties of Treated Tendons 2 Week Recovery from Average Stress-Strain Curves

	Collagen (with outlier)	Collagen (without outlier)	PRP + Collagen	MSC + Collagen	CPM + Collagen
Max Stress (kPa)	3,159.32	3,358.51	3,842.89	4,074.14	3,453.26
Max Force (N)	23.09	24.43	26.99	27.45	25.30
Strain at Failure (mm/mm)	0.56	0.52	0.50	0.58	0.57
Total Strain Energy (kPa)	1,013.67	1,005.25	1,010.00	1,344.17	1,183.33
Strain at UTS (mm/mm)	0.56	0.42	0.49	0.49	0.41
Average Modulus of Elasticity (kPa)	7,904.35	9,085.53	12,471.19	10,752.88	10,479.81
Elastic Strain Energy (kPa)	612.12	638.94	540.27	839.93	523.56

Table 3.9: Average Mechanical Properties of Control Tendons 2 Week Recovery from Average Stress-Strain Curves

	Collagen Control (with outlier)	Collagen Control (without outlier)	PRP + Collagen Control	MSC + Collagen Control	CPM + Collagen Control
Max Stress (kPa)	3,967.98	4,092.99	5,396.53	4,542.98	4755.20
Max Force (N)	30.03	29.84	39.16	33.98	35.00
Strain at Failure (mm/mm)	0.94	0.90	0.64	0.54	0.82
Total Strain Energy (kPa)	2667.96	2702.02	2229.02	1,585.69	2580.70
Strain at UTS (mm/mm)	0.91	0.64	0.56	0.42	0.58
Average Modulus of Elasticity (kPa)	9,573.13	10,965.97	11,667.29	10,567.15	9,085.25
Elastic Strain Energy (kPa)	797.23	811.15	1138.02	725.65	845.02

Table 3.10: Percent Difference between Treatments and Controls and Treatments and Collagen 2 Week Recovery

	Percent Difference Control				Percent Difference Collagen		
	Collagen	PRP + Collagen	MSC + Collagen	CPM + Collagen	PRP + Collagen	MSC + Collagen	CPM + Collagen
Max Stress (kPa)	17.94%	28.79%	10.32%	27.38%	14.42%	21.31%	2.82%
Max Force (N)	18.15%	31.07%	19.21%	27.72%	10.51%	12.38%	3.56%
Strain at Failure (mm/mm)	41.70%	22.66%	-7.55%	30.21%	-5.38%	10.34%	8.80%
Total Strain Energy (kPa)	62.80%	54.69%	15.23%	54.15%	0.47%	33.72%	17.72%
Strain at UTS (mm/mm)	34.54%	12.50%	-16.07%	29.81%	15.70%	15.99%	-3.53%
Average Modulus of Elasticity (kPa)	17.15%	-6.89%	-1.76%	-15.35%	37.26%	18.35%	15.35%
Elastic Strain Energy (kPa)	21.23%	52.53%	-15.75%	38.04%	-15.44%	31.46%	-18.06%

3.2.4 Differences Between 1 and 2 Week Recovery

Figure 3.15 shows the average stress-strain curve of the collagen group at 1 week recovery, 2 week recovery, and the left control tendons for the 1 and 2 week recovery times. This graph shows that there is notable improvement in the tendons between 1 and 2 week recovery, as expected. Both the stress and strain to failure have increased from 1 to 2 weeks. It is not, however, to the same magnitude as the controls. Table 3.11 gives the percent differences in material properties between the collagen group at 1 week recovery and 2 week recovery, based off the average stress-strain curves. The greatest increase was in the elastic strain energy, which increased from 1 week to 2 week by 51.14%. The smallest increase was in the strain at UTS, which was 10.62%.

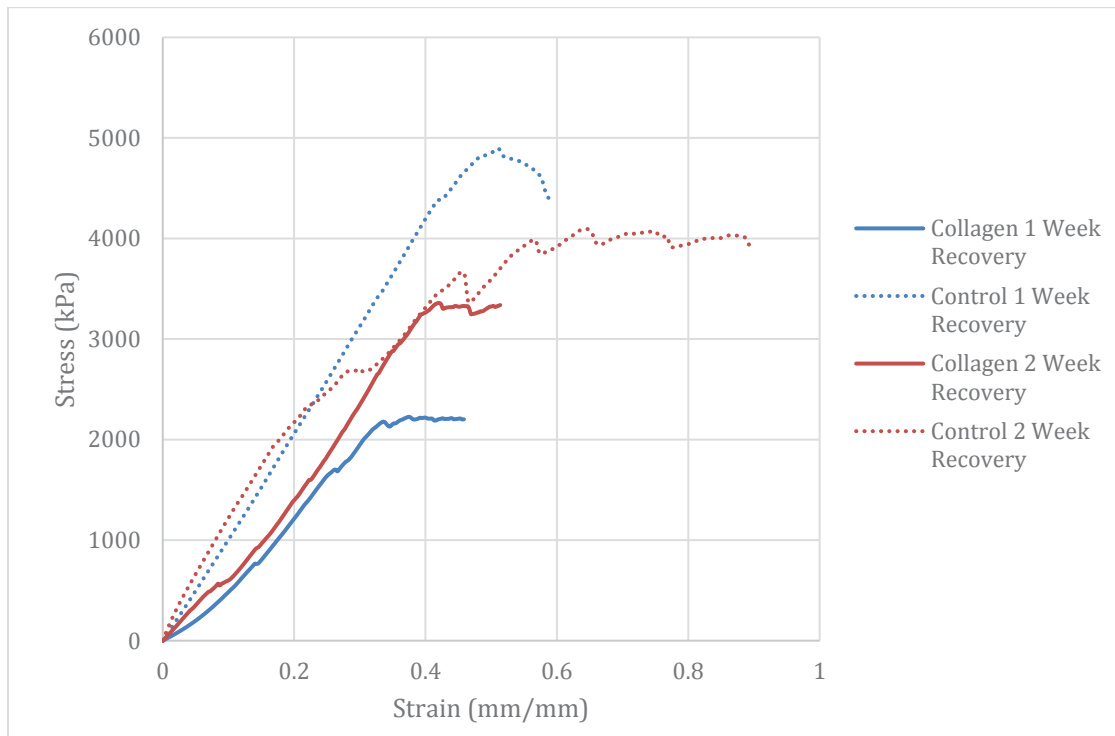


Figure 3.15: Stress-Strain to Failure Collagen at 1 and 2 Week Recovery and Controls

Table 3.11: Percent Difference Between Collagen Group at 1 and 2 Weeks Recovery

	Collagen 1 Week Recovery	Collagen 2 Week Recovery (without outlier)	Percent Difference
Max Stress (kPa)	2,225.57	3,358.51	33.73%
Max Force (N)	15.21	24.43	37.74%
Strain at Failure (mm/mm)	0.46	0.52	11.51%
Total Strain Energy (kPa)	618.15	1,005.25	38.51%
Strain at UTS (mm/mm)	0.38	0.42	10.62%
Average Modulus of Elasticity (kPa)	6,722.21	9,085.53	26.01%
Elastic Strain Energy (kPa)	312.21	638.94	51.14%

Figure 3.16 shows the stress-strain to failure graphs of the PRP group at 1 and 2 week recovery and the corresponding controls at 1 and 2 week recovery. Just as with the collagen group, significant improvement can be seen from 1 to 2 week recovery in the PRP group. The stress had increased as well as the modulus of elasticity, which can be seen in Table 3.12. The most significant increase from 1 to 2 weeks recovery with the PRP group is in the maximum force, which had an increase of 50.79%. The modulus of elasticity of the 2 week recovery is close to that of the 2 week controls. The strain to failure of the 2 week recovery is also closer to the control's strain to failure than the 1 week recovery. The other material properties have still not reached those of the controls at 2 weeks, however.

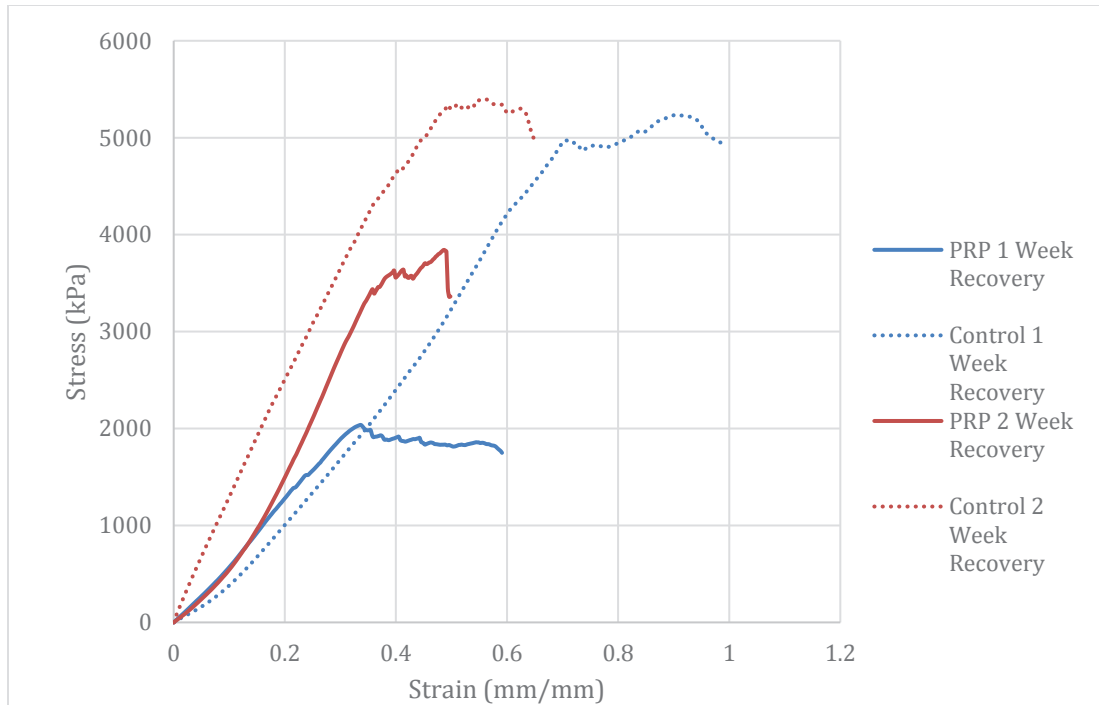


Figure 3.16: Stress-Strain to Failure PRP Group at 1 and 2 Week Recovery and Controls

Table 3.12: Percent Difference Between PRP Group at 1 and 2 Weeks Recovery

	PRP + Collagen 1 Week Recovery	PRP + Collagen 2 Week Recovery	Percent Difference
Max Stress (kPa)	2,037.15	3,842.89	46.99%
Max Force (N)	13.28	26.99	50.79%
Strain at Failure (mm/mm)	0.59	0.50	-19.20%
Total Strain Energy (kPa)	823.80	1,010.00	18.44%
Strain at UTS (mm/mm)	0.34	0.49	30.70%
Average Modulus of Elasticity (kPa)	6,788.46	12,471.19	45.57%
Elastic Strain Energy (kPa)	298.16	540.27	44.81%

Figure 3.17 shows the stress-strain to failure curve of the MSC groups at 1 and 2 weeks recovery next to their control counter parts. There is a significant increase between the 1 and 2 week recovery graphs. The stress has nearly doubled from 1 to 2 weeks and the 2 week recovery graph follows parallel with the 2 week control graph. Although it is still not as strong as the controls, it shows great promise with further healing time. Both the 1 and 2 week recovery graphs show similar strains to failure as their control counter parts. This insinuates that the tendons reach their full strain to failure by 1 week healing time. Table 3.13 presents the percent difference between the material properties of the MSC groups at 1 and 2 week recovery. The largest difference is within the elastic strain energy, being 84.15% at 2 weeks.

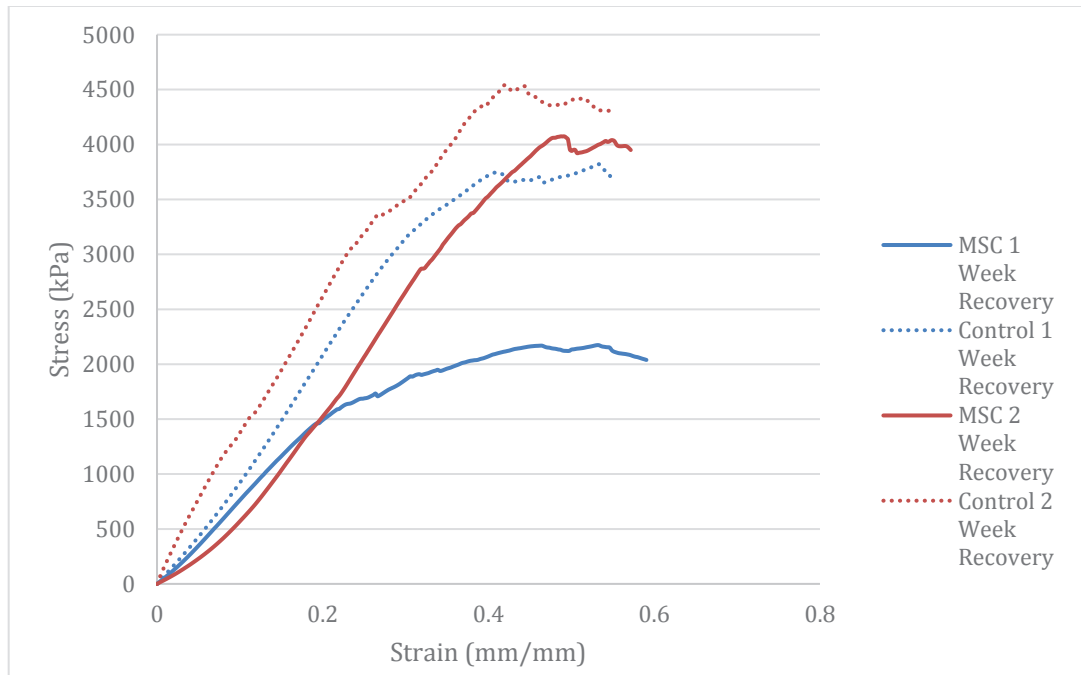


Figure 3.17: Stress-Strain to Failure MSC Group at 1 and 2 Week Recovery and Controls

Table 3.13 Percent Difference Between MSC Group at 1 and 2 Weeks Recovery

	MSC + Collagen 1 Week Recovery	MSC + Collagen 2 Week Recovery	Percent Difference
Max Stress (kPa)	2,173.44	4,074.14	46.65%
Max Force (N)	15.85	27.45	42.28%
Strain at Failure (mm/mm)	0.59	0.58	-2.15%
Total Strain Energy (kPa)	925.25	1,344.17	31.17%
Strain at UTS (mm/mm)	0.53	0.49	-8.95%
Average Modulus of Elasticity (kPa)	8,122.50	10,752.88	24.46%
Elastic Strain Energy (kPa)	133.11	839.93	84.15%

Figure 3.18 depicts the stress-strain to failure graphs of the CPM treatment groups at 1 and 2 weeks recovery along with their controls. As with the other treatment groups, this group also shows improvement from 1 to 2 weeks recovery. At 2 weeks recovery the CPM treated group has a modulus of elasticity similar to the 2 week controls and generally has the same shape as the control graph, though it is not to the same magnitude as the control. Table 3.14 gives the percent difference between the CPM treated groups at 1 week and 2 weeks. The modulus of elasticity increased 43.8% from 1 to 2 weeks recovery.

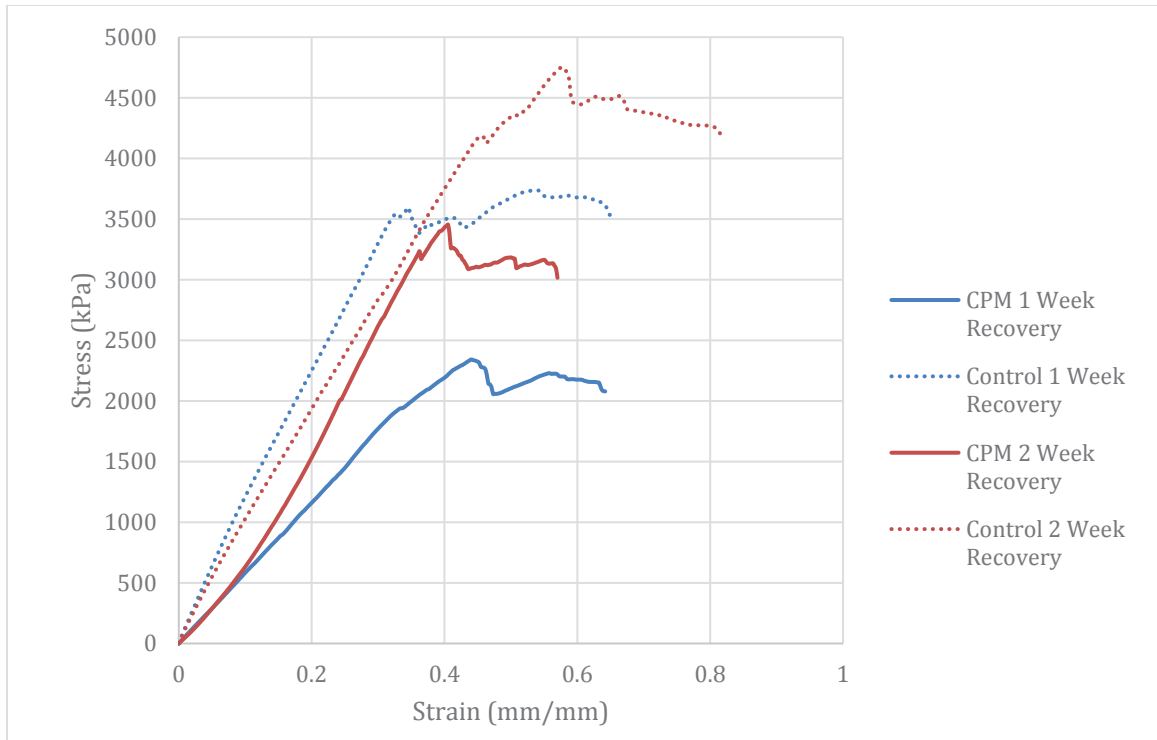


Figure 3.18: Stress-Strain to Failure CPM Group at 1 and 2 Week Recovery and Controls

Table 3.14: Percent Difference Between CPM Group at 1 and 2 Weeks Recovery

	Both + Collagen 1 Week Recovery	Both + Collagen 2 Week Recovery	Percent Difference
Max Stress (kPa)	2,342.17	3,453.26	32.17%
Max Force (N)	18.74	25.30	25.92%
Strain at Failure (mm/mm)	0.64	0.57	-12.61%
Total Strain Energy (kPa)	988.86	1,183.33	16.43%
Strain at UTS (mm/mm)	0.44	0.41	-8.72%
Average Modulus of Elasticity (kPa)	5,890.12	10,479.81	43.80%
Elastic Strain Energy (kPa)	428.18	523.56	18.22%

All the treatment groups improved from 1 to 2 weeks recovery. Both the PRP and MSC groups reached near the same strain to failure as their controls by 2 weeks and even by 1 week recovery for the MSC group. By 2 weeks recovery the MSC stress-strain curve closely resembles the 2 week controls curve. The PRP and CPM curves by 2 weeks are starting to reach the stress-strain curves of the controls, but not to the magnitude of the MSC group. The force-extension graphs comparing the 1 and 2 week recovery times with the 1 and 2 week controls for all the treatment types can be found in Appendix D.

3.3 STATISTICAL ANALYSIS OF TREATMENT GROUPS

The two-way ANOVA was run comparing 1 week and 2 week treatment recovery time points and the treatment groups, CoTa, PRP, MSC, and CPM. Since the standard deviation for the groups were larger than typically found in literature, a 90% confidence interval was used in this statistical analysis. Tukey's post hoc test was used in interpreting the data since there are more than 3 groups being looked at. It should be noted that although a log transformation was used on the modulus of elasticity data to help with the skewed data, it still is not considered a normal distribution, though it is closer than before.

The analysis was first run on the maximum stress between the groups. It was found that the only statistically significant difference was between the controls and the 1 week recovery groups. A significant difference in maximum force was found between the controls and the 1 and 2 week recovery group. Statistically, no differences were found between any of the groups in regards to strain at failure and strain at UTS. The only

statistically significant difference found with respect to the total strain energy and modulus of elasticity was between the control and the collagen at 1 week recovery. Looking at the statistical analysis of the elastic strain energy, there was a statistically significant difference between the MSC at 1 and 2 week recovery and the controls and between the MSC 2 week recovery and the collagen 2 week recovery (MSC 634.14 ± 628.11 , collagen 1108 ± 967.02 , $p < 0.1$).

The statistical analysis was run again, but this time with the outlier previously described in the collagen 2 week recovery group removed. The only change that occurred was that the difference in the elastic strain energy between the MSC 2 week recovery and collagen 2 week recovery was no longer statistically significant.

Due to the large standard deviations in the material properties of the tendons, nothing of interest was found through the statistical analysis, even with using a 90% confidence interval. There are notable differences between the treatment groups, as expressed in Section 3.2, even though they are not considered statistically significant.

The large standard deviations experienced in this study could partially be due to the large group of individuals working on this project. There were multiple people injecting the treatment after surgery, extracting the tendons, and performing the mechanical testing. This could bring variation into the study. Having a couple people performing each task would decrease the variability within the study. Practicing each aspect of the study, such as extracting the tendons and performing the mechanical testing

would also lessen the variability in the study as the researchers perfected their work. The differing in the rats' weights was initially a concern with the variability; because of this the weights were checked for any correlation between them and the mechanical properties. No correlation was found.

3.4 RESULTS COMPARED TO LITERATURE

In a study conducted by Chong et al (2007), they looked at using MSCs to repair the Achilles tendon in a rabbit model. They found that at three weeks the MSC group had a 32% increase in the modulus of elasticity compared with the fibrin carrier control group. In this study, the modulus of elasticity for the MSC group at 2 weeks recovery increased 38% from the 1 week recovery and has a 10% increase compared to the collagen group at 2 weeks recovery.

Young et al. (1998) looked at the differences in the cross-sectional areas of the MSC treated tendons versus nontreated tendons in a rabbit model. At 4, 8, and 12 weeks the averaged measured cross-sectional areas ($\text{mm}^2 \pm \text{SD}$) of the treated group, respectively were found to be: 15.1 ± 6.8 , 10.4 ± 3.7 , and 7.4 ± 2.8 . To compare, the following is the recorded averaged cross-sectional areas of the control group at the same respective time periods: 8.4 ± 1.9 , 6.3 ± 1.9 , and 5.4 ± 2.6 . The researcher noted that the treated tendons have a larger cross-sectional area at every time interval. In this study at both recovery times the collagen groups have the smallest cross-sectional areas, although the differences in cross-section are not as large. This is similar to the researchers findings.

3.5 FINITE ELEMNT ANALYSIS RESULTS

Nine finite element analyses were run, one for each treatment group at each time point and one using the results from the elastography. Figure 3.19 shows the tendon 45 model (a) undeformed and (b) deformed.

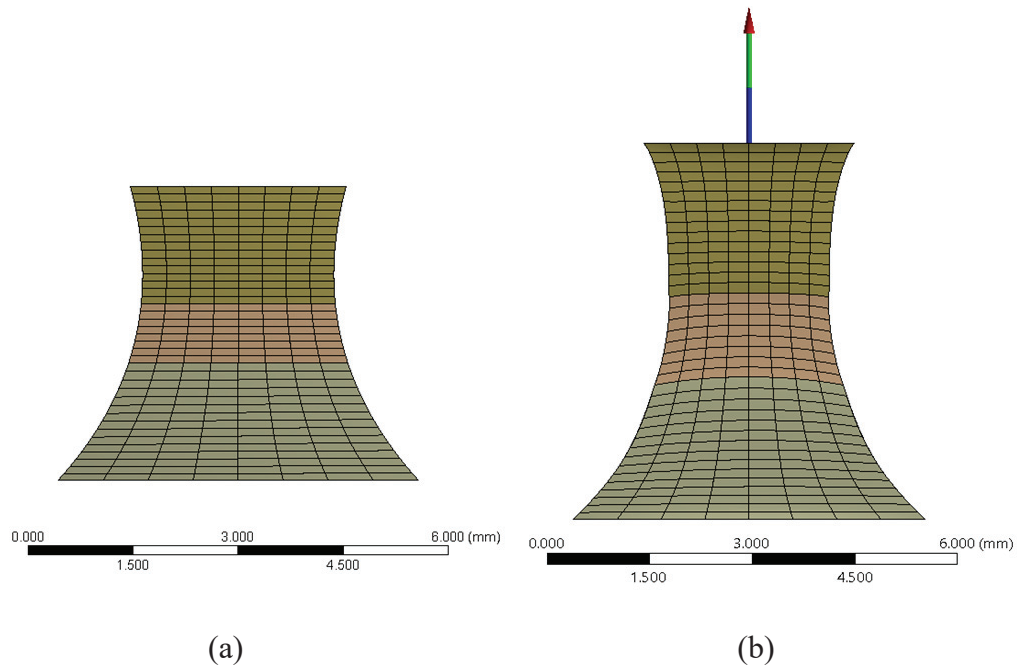


Figure 3.19: Deformed Model (a) Undeformed Tendon Model (b) Deformed Tendon Model

Table 3.15 gives the total percent difference between the actual and simulated tendons for the 1 week recovery and Table 3.16 shows these values for the 2 week recovery groups. The percent difference considers the average modulus of elasticity used in the simulation and the force required to extend the model the determined amount. These values were then compared to the actual values and the errors were added to find the total error of each model.

Table 3.15: Percent Difference Between Actual and Simulated Force and Modulus of Elasticity at 1 Week Recovery

	Collagen 1 Week Recovery (45)	PRP 1 Week Recovery (37)	MSC 1 Week Recovery (49)	CPM 1 Week Recovery (2)
Extension (mm)	1.29	1.31	1.46	1.91
Experimental Force (N)	7.09	9.39	5.74	9.71
FEA Force (N)	5.79	9.41	5.75	7.95
Experimental Modulus of Elasticity (kPa)	4,923.10	9,354.50	7,780.46	5,624.94
FEA Modulus of Elasticity (kPa)	5,689.77	10,086.38	7,767.96	6,138.17
Total Percent Difference	33.91%	8.04%	0.33%	27.25%

Table 3.16: Percent Difference Between Actual and Simulated Force and Modulus of Elasticity at 2 Week Recovery

	Collagen 2 Week Recovery (71)	PRP 2 Week Recovery (32)	MSC 2 Week Recovery (27)	CPM 2 Week Recovery (44)
Extension (mm)	1.56	1.21	2.02	1.83
Experimental Force (N)	15.72	7.81	16.12	18.26
FEA Force (N)	11.46	10.28	15.28	18.44
Experimental Modulus of Elasticity (kPa)	7,494.98	12,286.17	15,298.65	14,614.49
FEA Modulus of Elasticity (kPa)	9,161.81	8,728.20	15,442.43	14,617.78
Total Percent Difference	49.34%	60.59%	6.15%	1.01%

Looking at Table 3.15 and Table 3.16, it is clear attempting to use multiple linear material models to simulate a nonlinear effect for the Achilles tendon is unreliable. Half

of the models have small percent errors while the other half have larger, unacceptable errors. The large errors occur in both the 1 week and 2 week recovery models.

3.5.1 Finite Element Analysis Using Elastography

Figure 3.20 shows the elastography model (a) undeformed and (b) deformed. This model of tendon 45 deforms differently than the one shown in Figure 3.19. Due to the three extra sections and more refined moduli of elasticity.

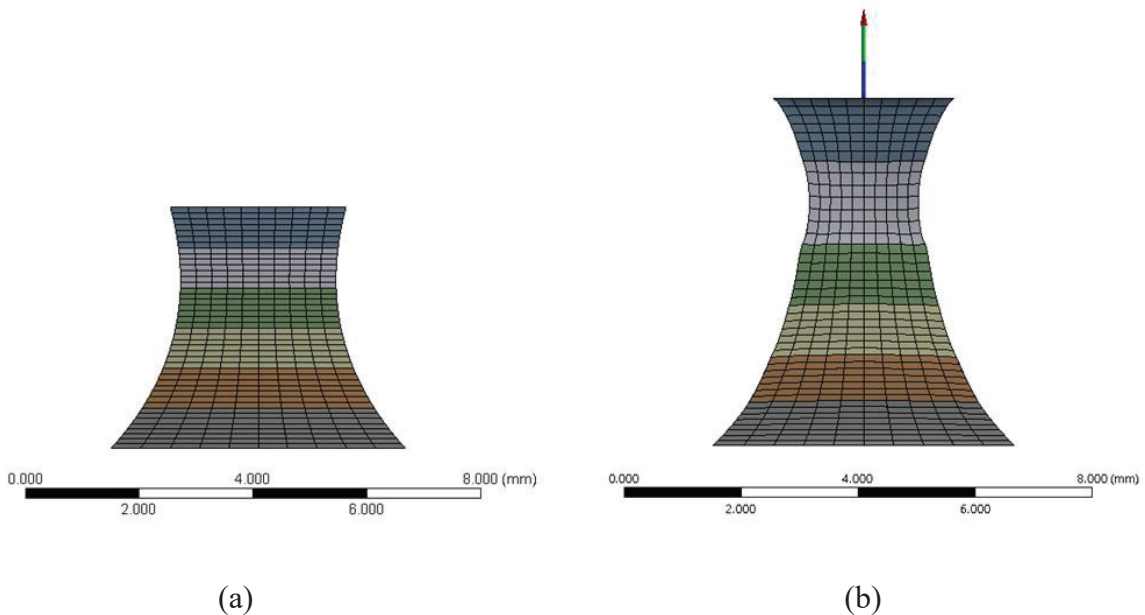


Figure 3.20: Deformed Elastography Model (a) Undeformed Model (b) Deformed Model

Table 3.17 shows the results of the elastography model compared to the experimental values. The error in this model is extremely high. This could be because only six points are being looked at in the tendon. Since tendons are nonlinear materials, each point has a different modulus of elasticity, as seen in Table 2.3. Adding more points to the elastography and the FE model would allow for a more accurate average modulus

of elasticity and therefore a more accurate model. Another possibility is modeling an Achilles tendon with linear material models does not accurately capture what happens during testing.

Table 3.17: Results of FEA of Elastography Model

	Elastography (45)
Extension (mm)	1.17
Experimental Force (N)	6.34
FEA Force (N)	5.3362
Experimental Modulus of Elasticity (kPa)	4,923.10
FEA Modulus of Elasticity (kPa)	8674.35
Total Percent Difference	92.09%

3.5.2 Finite Element Analysis Compared to Literature

Many studies involving modeling the Achilles tendon use nonlinear material models, an example is Bajuri et al. (2016). The researchers used the Gasser-Ogden-Holzapfel (GOH) model to simulate the material properties of a healing tendon. To assess the accuracy of their FEA model they graphed the results and compared them to experimental tensile data. They found an R^2 value of 0.9964 at 3 days healing and 0.9959 at 21 days healing. Khayyeri et al. (2016) also used the GOH model to simulate a tensile test and found it had high accuracy with a RMS of 0.617. The researchers also created a model using a visco-hyper-poro-elastic model and found that it had high accuracy predicting an entire load cycle with an RMS of 0.503. The material structure of Achilles

tendons are intricate and complex. A linear model is just too simplistic to accurately model their behavior reliably.

3.6 ELASTOGRAPHY OF A TENDON

The overall strain from the elastography was graphed with the overall stress obtained from the tensile test and can be seen in Figure 3.21, along with the mechanical stress-strain curve. The optical and mechanical stress-strain curves line up very nicely and show that the elastography from the testing video is a valid way of obtaining the strain in the tendons.

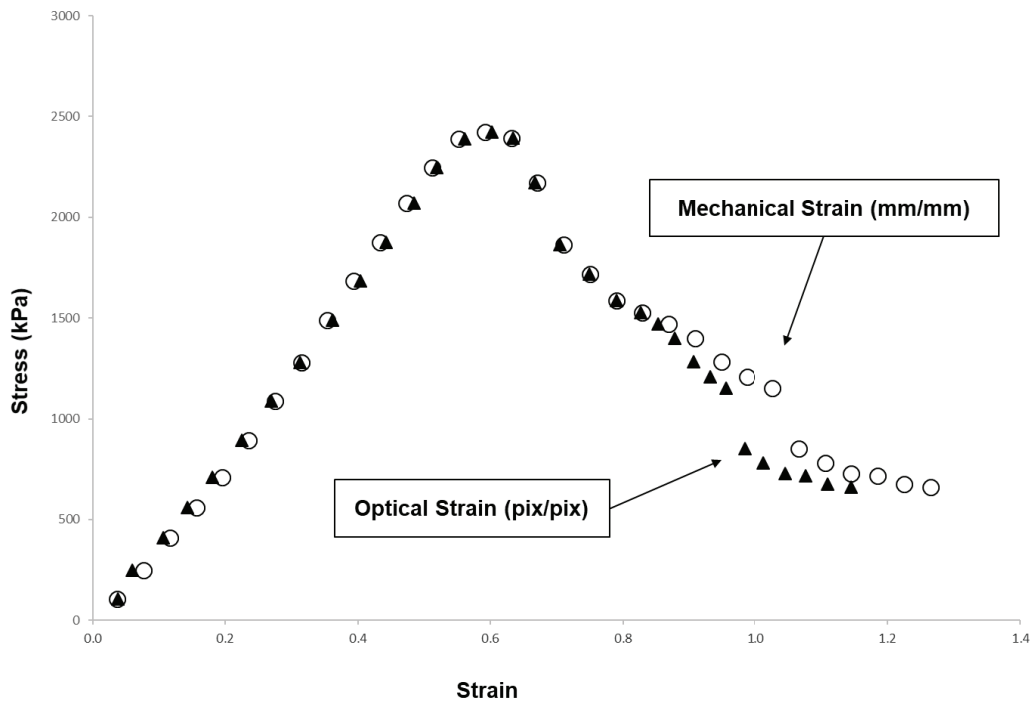


Figure 3.21: Mechanical vs Optical Strain

Stress-strain curves of three of the six location points, points 2, 4, and 5 as well as the overall strain can be seen in Figure 3.22. Figure 3.23 is of the strain at each point and

the overall strain through time. Notice how at each point from top to bottom of the tendon experiences less strain. This was noticeable during the tensile testing of the tendons. Some of the tendons experienced strain, but no tearing. In these cases the tendons always experienced strained at the top. The change from liner to plastic deformation occurs at around 13 seconds.

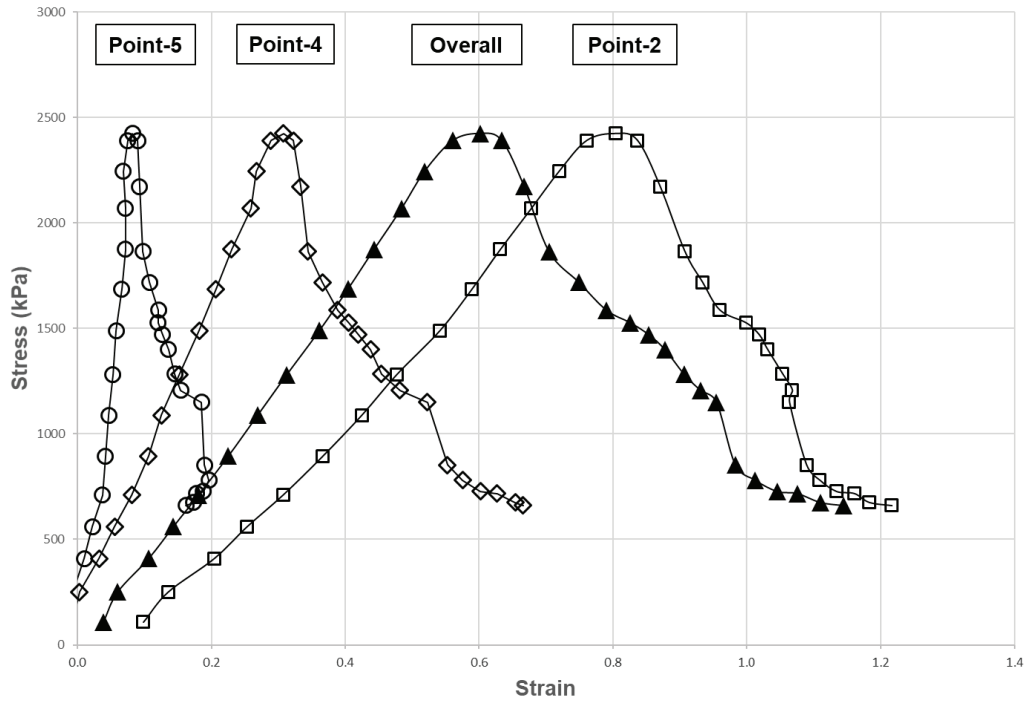


Figure 3.22: Optical Strain at Points

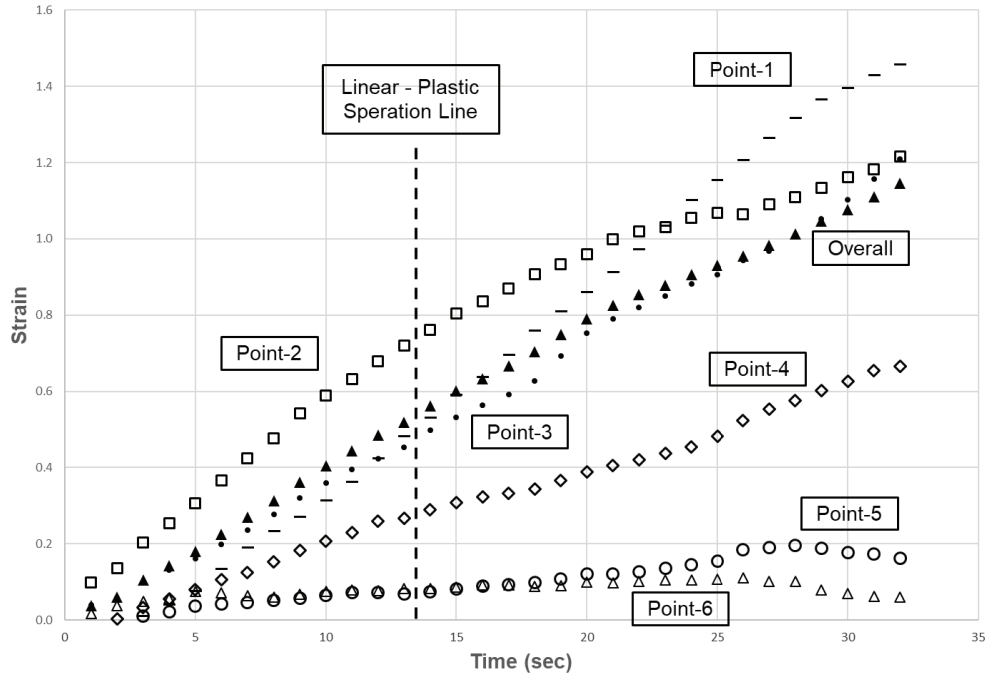


Figure 3.23: Optical Strain at Points vs Time

The overall modulus of elasticity from the elastography data was 4,432.73 kPa. The modulus of elasticity obtained from the testing was 4,923.1 kPa. This gives a percent error of 9.96% error.

3.7 FUTURE WORK

Future work should be done to better understand the effects of PRP, MSC, and CPM on the healing Achilles tendon. Firstly, a histology analysis should be done of the Achilles tendons at 1 and 2 weeks recovery to see if they have any differing effects on the material. A second study would be to give multiple injections of the treatments at varying times to see if more than one dose has any effects on the healing properties. A third suggested study would be a cyclic loading study. The tissue would undergo a predetermined amount of cycles of loading before being stretched to failure. This would

better simulate how tendons are loaded in the body. An investigation into an elastography FEA model with more than six points of interest to determine whether a more accurate linear model could be constructed would be beneficial as well.

APPENDIX A

%% Mod of Elasticity for FEA

```
clear all
clc
close all
```

%Distance on Tendon

```
x1 = 0;
x2 = 2.7025;
x3 = 5.405;
```

%Modulus of Elasticity

```
y1 = 16442.77; %Control
y2 = 2383.31; %Treated
y3 = 16442.77; %Control
```

```
xraw = [x1 x2 x3];
yraw = [y1 y2 y3];
```

%2nd order poly

```
p = polyfit(xraw,yraw,2);
```

```
a = p(1);
b = p(2);
c = p(3);
```

%Intermediate points for section 2 and 4 on FEA tendon

```
xint = x2/2
yint = a*xint^2 + b*xint + c
```

APPENDIX B

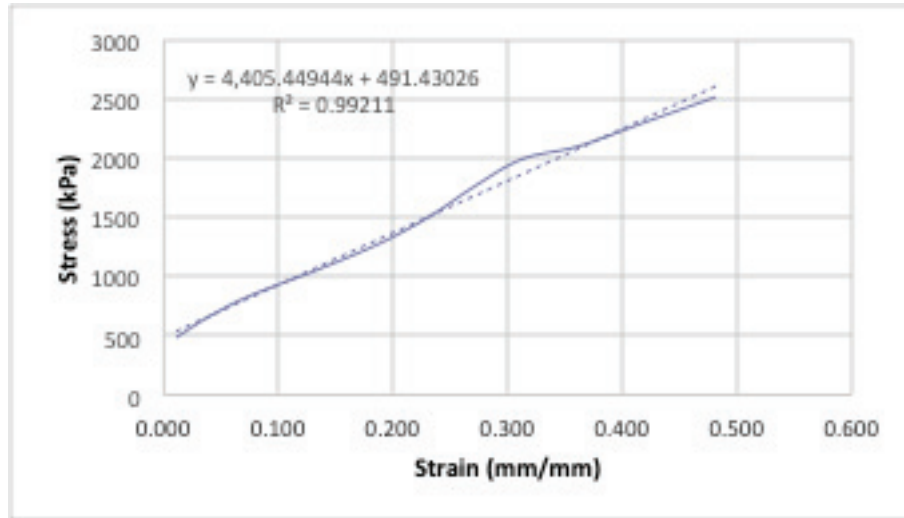


Figure B.1: Modulus of Elasticity for Elastography Point 1

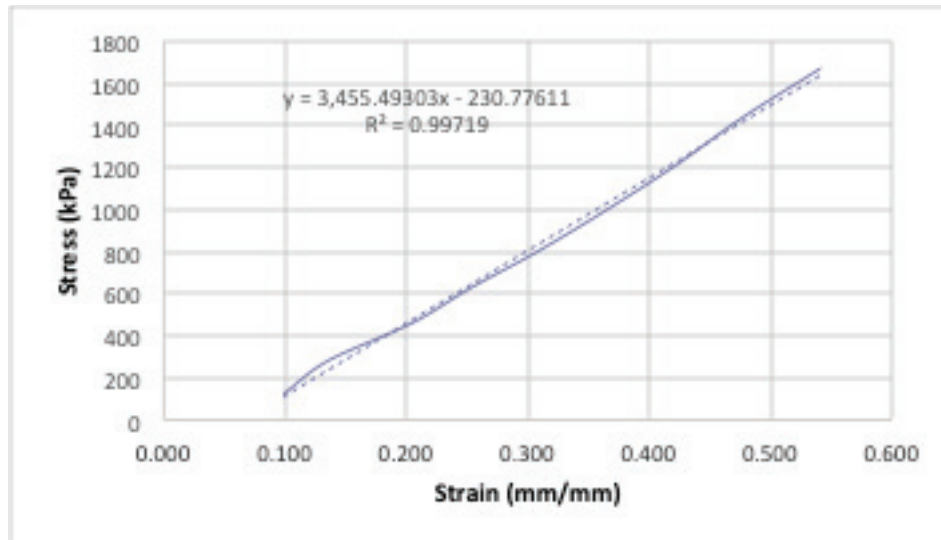


Figure B.2: Modulus of Elasticity of Elastography Point 2

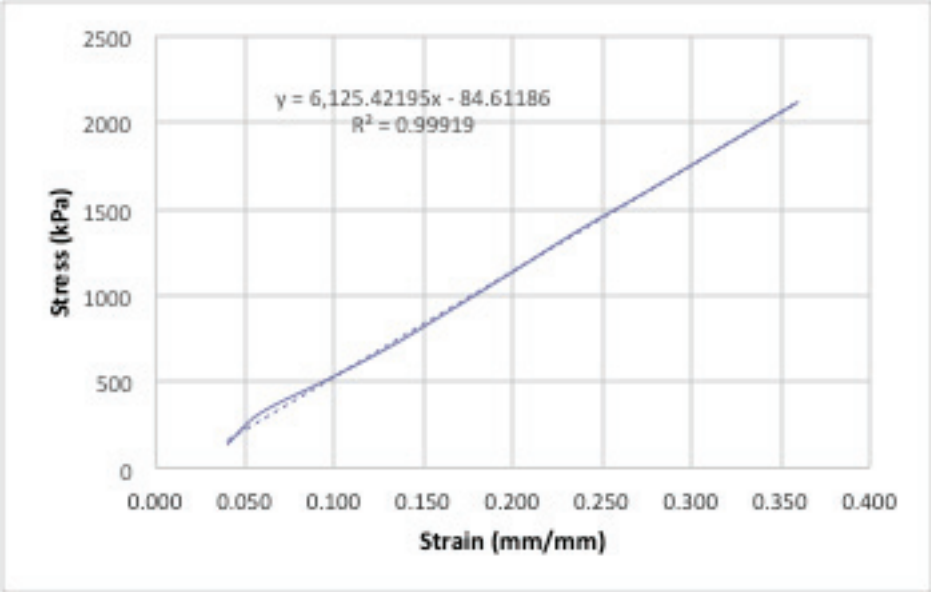


Figure B.3: Modulus of Elasticity of Elastography Point 3

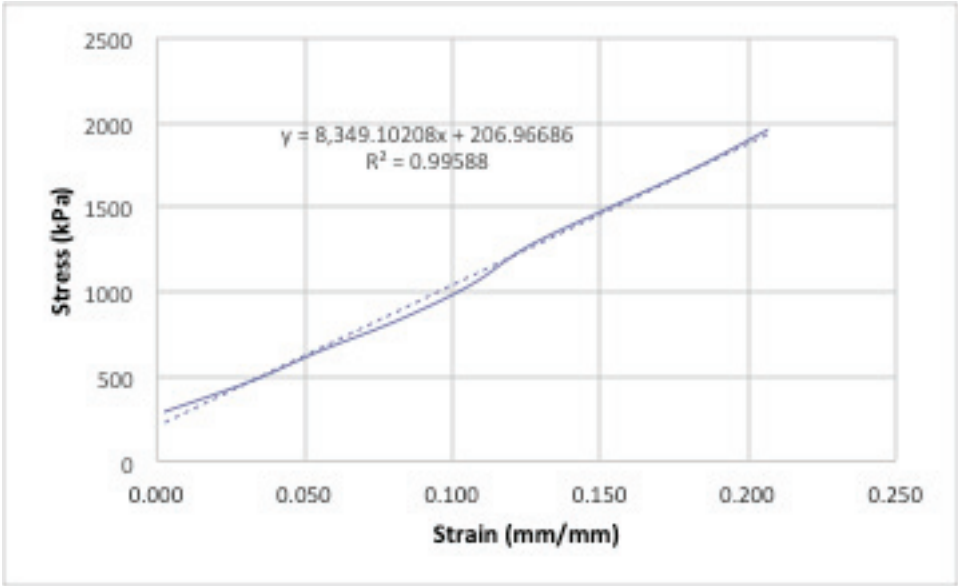


Figure B.4: Modulus of Elasticity of Elastography Point 4

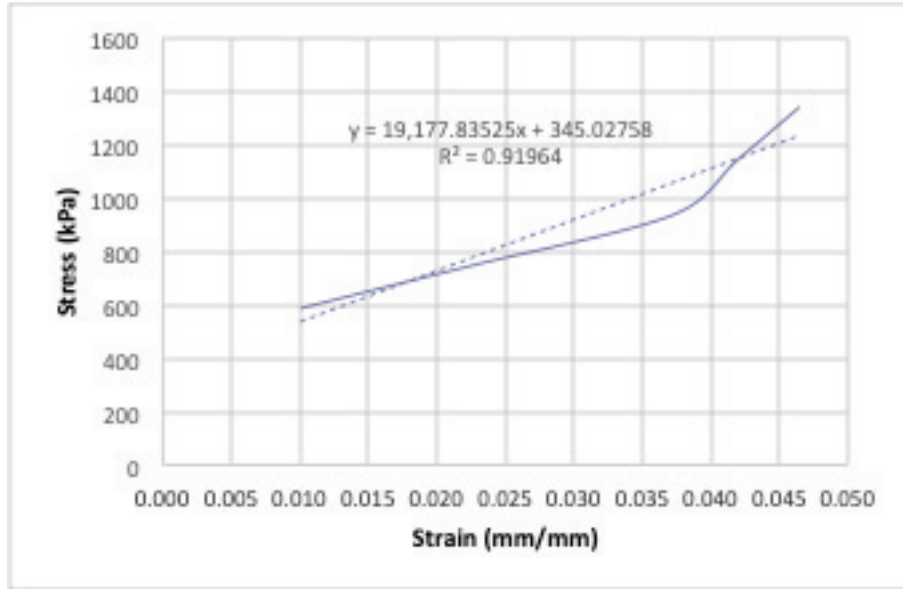


Figure B.5: Modulus of Elasticity of Elastography Point 5

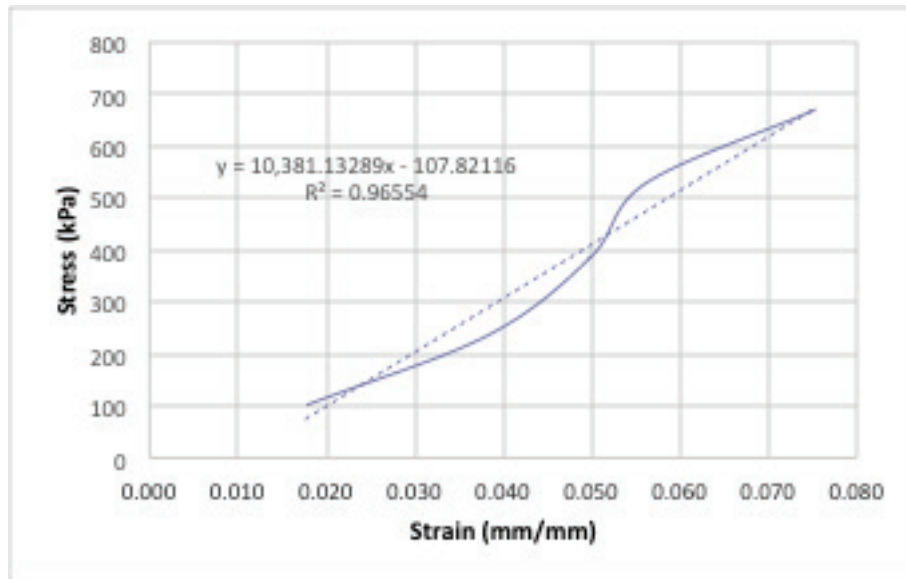


Figure B.6: Modulus of Elasticity of Elastography Point 6

APPENDIX C

Table C.1: Collagen Treated Tendons Material Properties 1 Week Recovery

	21	25	26m	36m	45
Max Stress (kPa)	3,302.33	3,372.26	2,752.02	2,686.74	2,437.00
Max Force (N)	20.44	15.74	20.06	21.39	13.92
Strain @ Failure (mm/mm)	0.5128	0.4551	0.6670	0.4975	0.6549
Total Strain Energy(kPa)	916.28	796.65	1,167.37	636.95	871.87
Strain at UTS (mm/mm)	0.45	0.39	0.62	0.44	0.61
Average Modulus of Elasticity (kPa)	10,481.30	11,065.11	8,069.94	7,952.81	4,923.10
Elastic Strain Energy (kPa)	746.35	414.68	413.65	594.53	740.13
Mass	250.00	238.00	309.00	258.30	253.00
Time in Freezer	3.00	2.00	3.00	6.00	6.00
Length (mm)	7.49	6.50	12.63	7.89	4.21
CS Area (mm ²)	6.19	4.67	7.29	7.96	5.71

Table C.2: Collagen Treated Tendons Material Properties 1 Week Recovery Cont.

	47	61m	74	76
Max Stress (kPa)	1,531.41	1,700.07	1,746.56	6,559.21
Max Force (N)	16.96	24.03	15.82	35.13
Strain @ Failure (mm/mm)	0.2018	0.5527	0.3478	0.6536
Total Strain Energy(kPa)	81.93	548.03	304.87	1,969.52
Strain at UTS (mm/mm)	0.19	0.52	0.33	0.64
Average Modulus of Elasticity (kPa)	9,590.85	5,241.12	6,575.87	12,541.54
Elastic Strain Energy (kPa)	118.09	250.29	282.35	1821.72
Mass	333.00	345.00	262.00	251.50
Time in Freezer	3.00	3.00	3.00	3.00
Length (mm)	12.43	9.03	4.67	3.25
CS Area (mm ²)	11.08	14.14	9.06	5.36

Table C.3: PRP and Collagen Tendon Material Properties at 1 Week Recovery

	2,291.19	1,625.55	1,863.88	4,196.77
Max Stress (kPa)	18.40	11.70	10.06	24.31
Max Force (N)	0.2719	0.5674	0.5887	0.6032
Strain @ Failure (mm/mm)	419.19	1,686.35	701.27	1,347.48
Total Strain Energy (kPa)	0.17	0.53	0.50	0.59
Strain at UTS (mm/mm)	13,605.11	4,561.68	5,719.08	9,354.50
Average Modulus of Elasticity (kPa)	419.19	428.99	257.32	691.50
Elastic Strain Energy (kPa)	313.00	240.00	251.10	258.00
Length (mm)	3.00	3.00	3.00	2.00
CS Area (mm ²)	9.84	5.89	5.11	5.65

Table C.4: PRP and Collagen Tendon Material Properties at 1 Week Recovery Cont.

	67	72	75m	79m
Max Stress (kPa)	2,656.85	5,955.01	1,401.08	1,333.19
Max Force (N)	21.76	17.47	14.61	12.20
Strain @ Failure (mm/mm)	0.7819	0.4067	0.6561	0.4797
Total Strain Energy (kPa)	1,069.27	1,263.75	498.95	380.87
Strain at UTS (mm/mm)	0.76	0.36	0.64	0.43
Average Modulus of Elasticity (kPa)	5,048.81	21,244.96	2,806.12	5,671.45
Elastic Strain Energy (kPa)	513.68	1054.75	448.92	262.76
Length (mm)	312.00	258.00	247.00	303.00
CS Area (mm ²)	3.00	3.00	3.00	3.00

Table C.5: MSC and Collagen Tendon Material Properties at 1 Week Recovery

	4m	7	20m	49	53
Max Stress (kPa)	1,331.05	3,264.74	1,023.04	2,572.80	2,699.84
Max Force (N)	9.22	25.08	9.74	16.37	22.68
Strain @ Failure (mm/mm)	0.1637	0.6448	0.2042	0.6387	0.5163
Total Strain Energy (kPa)	127.74	1,155.56	150.24	974.27	1,020.44
Strain at UTS (mm/mm)	0.16	0.64	0.19	0.61	0.27
Average Modulus of Elasticity (kPa)	9,868.59	6,238.23	9,477.94	7,780.46	11,716.47
Elastic Strain Energy (kPa)	104.53	511.76	44.74	427.95	254.31
Length (mm)	11.66	8.00	8.69	7.19	8.73
CS Area (mm ²)	6.92	7.68	9.52	6.36	8.40

Table C.6: MSC and Collagen Tendon Material Properties at 1 Week Recovery Cont.

	56	68	77	78	81m
Max Stress (kPa)	1,314.86	4,105.73	1,024.83	2,372.57	4,813.44
Max Force (N)	11.92	20.32	14.47	25.74	24.73
Strain @ Failure (mm/mm)	0.9556	0.6762	0.8793	0.5196	0.5642
Total Strain Energy (kPa)	986.43	1,911.48	534.23	705.42	1,927.44
Strain at UTS (mm/mm)	0.84	0.66	0.85	0.51	0.45
Average Modulus of Elasticity (kPa)	7,239.05	10,954.96	1,569.70	5,479.31	18,629.94
Elastic Strain Energy (kPa)	87.46	486.26	272.48	374.70	108.26
Length (mm)	8.38	6.05	5.24	6.91	7.99
CS Area (mm ²)	23.29	4.95	14.12	10.85	5.14

Table C.7: Combined Tendon Material Properties at 1 Week Recovery

	2	11m	15m	34	39
Max Stress (kPa)	2,685.04	5,151.39	3,116.85	3,298.55	3,078.80
Max Force (N)	22.21	24.08	15.30	33.82	28.92
Strain @ Failure (mm/mm)	0.6524	0.4178	0.7446	1.0559	0.3240
Total Strain Energy (kPa)	1,058.80	1,195.33	1,648.34	2,213.55	396.28
Strain at UTS (mm/mm)	0.60	0.42	0.72	0.96	0.32
Average Modulus of Elasticity (kPa)	5,624.94	18,227.03	8,969.03	3,938.17	13,126.37
Elastic Strain Energy (kPa)	490.64	595.96	747.71	1046.56	480.08
Length (mm)	8.57	11.31	4.42	4.19	10.21
CS Area (mm ²)	8.27	4.67	4.91	10.25	9.39

Table C.8: Combined Tendon Material Properties at 1 Week Recovery Cont.

	60	64	66	69	80m
Max Stress (kPa)	3,416.04	1,052.43	2,095.12	2,170.00	1,098.96
Max Force (N)	22.17	9.68	31.60	15.78	10.74
Strain @ Failure (mm/mm)	0.5266	0.5021	0.4784	0.4733	0.3692
Total Strain Energy (kPa)	938.25	333.30	793.53	486.17	246.08
Strain at UTS (mm/mm)	0.50	0.42	0.47	0.45	0.37
Average Modulus of Elasticity (kPa)	6,636.53	3,417.74	5,926.71	5,389.32	3,578.34
Elastic Strain Energy (kPa)	763.68	142.97	312.99	445.59	193.29
Length (mm)	7.99	8.48	6.67	9.63	8.10
CS Area (mm ²)	6.49	9.20	15.08	7.27	9.77

Table C.9: Collagen Tendon Material Properties at 2 Week Recovery

	6 redo	12	23	24m	30
Max Stress (kPa)	5,157.48	3,531.93	1,950.77	5,823.53	10,687.16
Max Force (N)	40.49	19.52	15.29	37.22	46.92
Strain @ Failure (mm/mm)	0.6384	0.4463	0.5288	0.6192	1.1157
Total Strain Energy (kPa)	1,966.30	515.29	378.55	1,918.16	5,484.02
Strain at UTS (mm/mm)	0.48	0.45	0.52	0.53	1.03
Average Modulus of Elasticity (kPa)	14,745.65	16,184.92	8,116.50	12,938.06	17,350.92
Elastic Strain Energy (kPa)	864.30	778.87	493.92	1529.95	3678.73
Length (mm)	6.67	12.49	11.55	6.93	5.31
CS Area (mm ²)	7.85	5.53	7.84	6.39	4.39

Table C.10: Collagen Tendon Material Properties at 2 Week Recovery Cont.

	35m	40	48	50	71
Max Stress (kPa)	3,414.33	2,928.82	2,603.48	4,872.76	2,830.32
Max Force (N)	33.76	27.18	25.00	33.17	30.45
Strain @ Failure (mm/mm)	0.4020	2.5439	0.6430	0.4912	0.5234
Total Strain Energy (kPa)	726.74	4,552.28	904.91	1,231.78	851.97
Strain at UTS (mm/mm)	0.39	2.48	0.64	0.43	0.47
Average Modulus of Elasticity (kPa)	11,690.36	1,666.28	10,618.98	16,370.66	7,494.98
Elastic Strain Energy (kPa)	633.12	1243.49	351.93	848.71	658.61
Length (mm)	12.25	4.72	10.51	7.48	7.18
CS Area (mm ²)	9.89	9.28	9.60	6.81	10.76

Table C.11: PRP and Collagen Tendons Material Properties at 2 Week Recovery

	1m	5m	10m	32	33
Max Stress (kPa)	1,723.03	5,026.29	6,815.20	2604.67	5,241.82
Max Force (N)	15.89	35.31	46.14	23.56	35.13
Strain @ Failure (mm/mm)	1.0541	0.6972	0.5677	0.3102	0.2831
Total Strain Energy (kPa)	1,099.33	6,119.84	2,096.24	389.32	622.59
Strain at UTS (mm/mm)	1.05	0.64	0.57	0.31	0.27
Average Modulus of Elasticity (kPa)	3,110.34	10,297.44	17,676.05	12,286.17	24,449.14
Elastic Strain Energy (kPa)	420.30	1601.20	1154.31	351.84	575.39
Length (mm)	2.00	2.00	2.00	2.00	4.00
CS Area (mm ²)	9.22	7.03	6.77	6.77	6.70

Table C.12: PRP and Collagen Tendon Material Properties at 2 Week Recovery Cont.

	46	51m	52	55	73
Max Stress (kPa)	7,454.03	2,370.00	2,674.33	8,270.93	3,858.74
Max Force (N)	46.58	30.68	21.29	44.03	37.06
Strain @ Failure (mm/mm)	1.0981	0.5725	0.2575	0.5214	0.3615
Total Strain Energy (kPa)	4,707.17	617.98	354.20	2,003.48	586.26
Strain at UTS (mm/mm)	1.08	0.56	0.25	0.52	0.36
Average Modulus of Elasticity (kPa)	8,664.38	5,419.93	11,823.68	25,421.75	14,593.65
Elastic Strain Energy (kPa)	2,192.52	661.50	337.41	1588.20	681.08
Length (mm)	4.00	2.00	2.00	2.00	2.00
CS Area (mm ²)	6.25	12.94	7.96	5.32	9.60

Table C.13: MSC and Collagen Tendon Material Properties at 2 Week Recovery

	9	18 redo	27	28m	38
Max Stress (kPa)	5,121.58	9,136.32	5,932.02	1,439.21	6,922.83
Max Force (N)	36.81	47.76	39.95	13.33	42.05
Strain @ Failure (mm/mm)	0.6839	0.5511	0.4566	0.4416	0.7327
Total Strain Energy (kPa)	1,721.47	2,204.49	1,249.11	395.65	2,629.56
Strain at UTS (mm/mm)	0.63	0.53	0.39	0.30	0.73
Average Modulus of Elasticity (kPa)	10,793.60	34,796.07	15,298.65	7,346.93	11,268.67
Elastic Strain Energy (kPa)	1211.28	1574.69	28.45	83.49	1622.90
Length (mm)	5.74	8.18	9.69	9.83	5.13
CS Area (mm ²)	7.19	5.23	6.73	9.26	6.07

Table C.14: MSC and Collagen Tendon Material Properties at 2 Week Recovery Cont.

	41m	42m redo	54m	57m	59m
Max Stress (kPa)	2,335.47	5,224.19	4,443.20	1,732.53	1,896.10
Max Force (N)	28.25	33.41	29.09	15.52	15.20
Strain @ Failure (mm/mm)	0.5097	0.3355	0.9232	0.3169	0.5776
Total Strain Energy (kPa)	760.75	962.82	2,676.89	255.00	697.19
Strain at UTS (mm/mm)	0.49	0.30	0.89	0.31	0.47
Average Modulus of Elasticity (kPa)	7,779.90	28,864.33	9,464.15	9,555.88	7,759.83
Elastic Strain Energy (kPa)	304.34	444.20	812.27	123.80	135.94
Length (mm)	9.04	12.69	12.69	8.86	9.19
CS Area (mm ²)	12.10	6.39	6.55	8.96	8.02

Table C.15: Combined Treatment Tendon Material Properties at 2 Week Recovery

	3m	14m	16	17m	19
Max Stress (kPa)	2,846.50	3,813.56	4,788.23	2489.96	3,680.78
Max Force (N)	33.64	30.65	35.29	12.91	23.61
Strain @ Failure (mm/mm)	0.4762	0.7088	0.4740	0.3737	0.6050
Total Strain Energy (kPa)	654.27	608.95	1114.9818	598.44	1,186.97
Strain at UTS (mm/mm)	0.37	0.69	0.45	0.34	0.58
Average Modulus of Elasticity (kPa)	15,297.29	10,625.72	14,969.91	13,326.78	6,981.63
Elastic Strain Energy (kPa)	438.16	331.34	1055.36	306.19	1043.75
Length (mm)	9.29	7.77	7.05	13.00	7.04
CS Area (mm ²)	11.82	8.04	7.37	5.18	6.41

Table C.16: Combined Treatment Tendon Material Properties at 2 Week Recovery

	22	43	44	58	62m
Max Stress (kPa)	4,048.78	3,586.77	6,305.84	6,415.43	2,976.64
Max Force (N)	26.04	28.72	49.02	46.77	27.68
Strain @ Failure (mm/mm)	0.7275	0.4363	0.5900	0.4129	0.4094
Total Strain Energy (kPa)	1,510.44	778.93	1,928.21	1,182.48	516.71
Strain at UTS (mm/mm)	0.70	0.39	0.57	0.37	0.40
Average Modulus of Elasticity (kPa)	7,966.67	14,045.04	14,614.49	18,312.85	10,024.34
Elastic Strain Energy (kPa)	802.85	474.89	1124.04	572.09	549.48
Length (mm)	4.34	10.37	7.64	6.84	12.11
CS Area (mm ²)	6.43	8.01	7.77	7.29	9.30

APPENDIX D

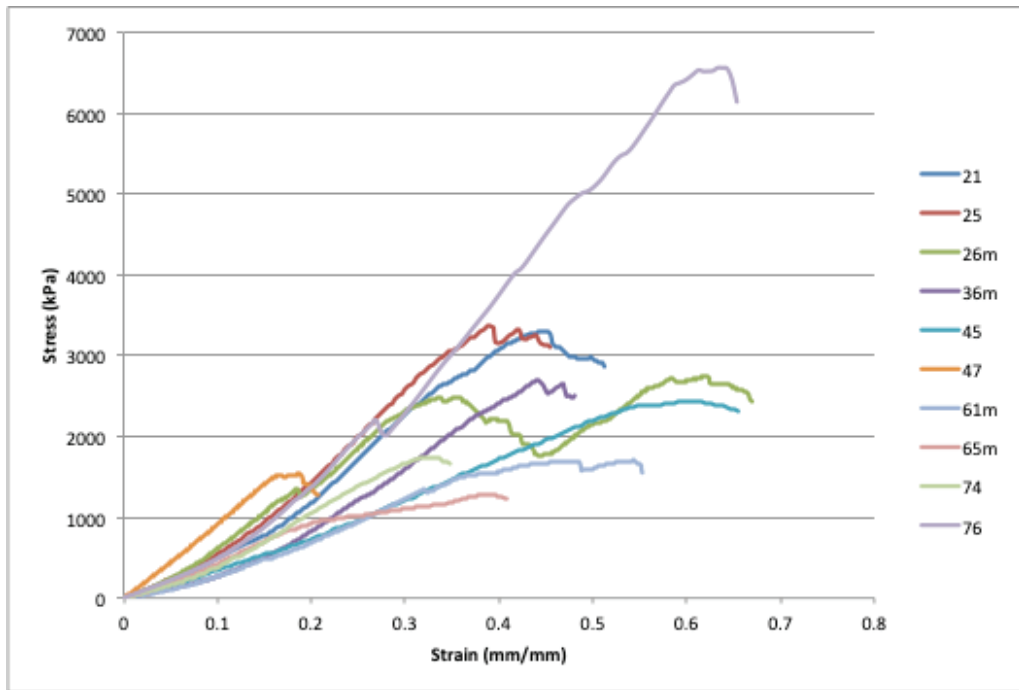


Figure D.1: Stress-Strain Curve to Failure of Collagen Group at 1 Week Recovery

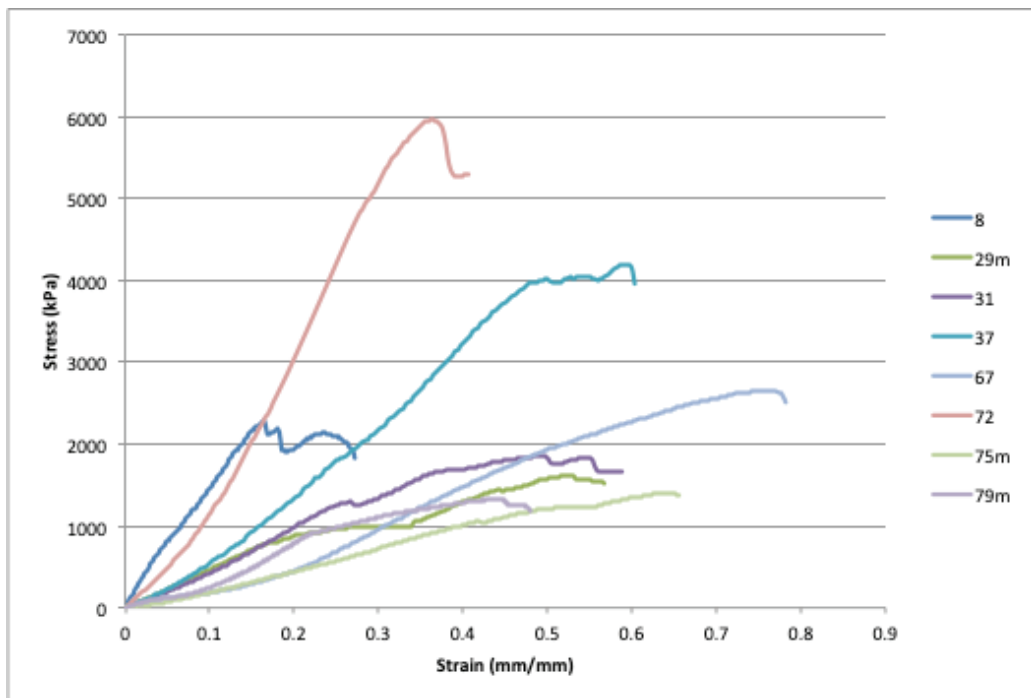


Figure D.2: Stress-Strain Curve to Failure of PRP Group at 1 Week Recovery

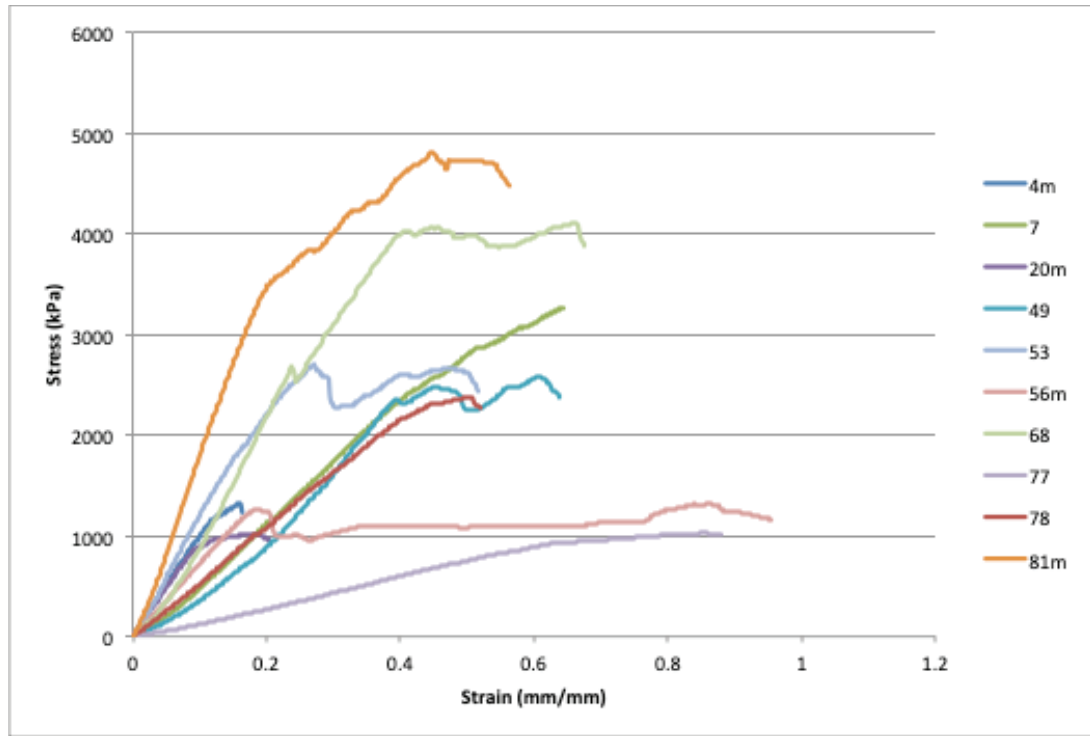


Figure D.3: Stress-Strain Curve to Failure of MSC Group at 2 Weeks Recovery

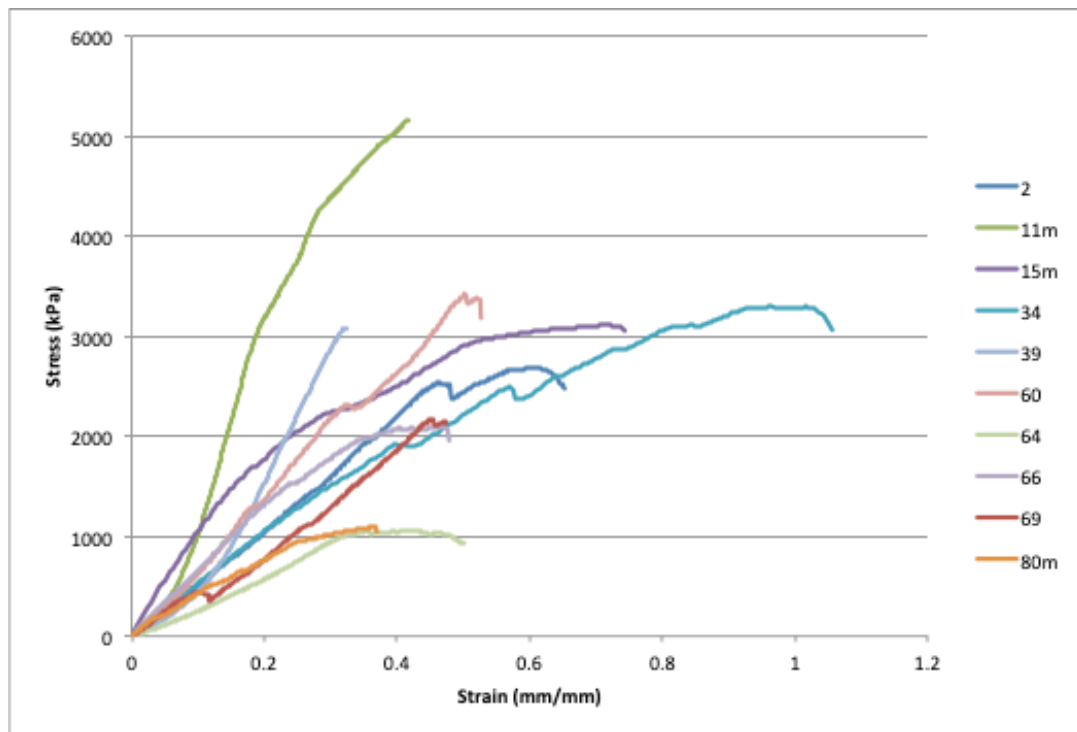


Figure D.4: Stress-Strain Curve to Failure of Combined Group at 1 Week Recovery

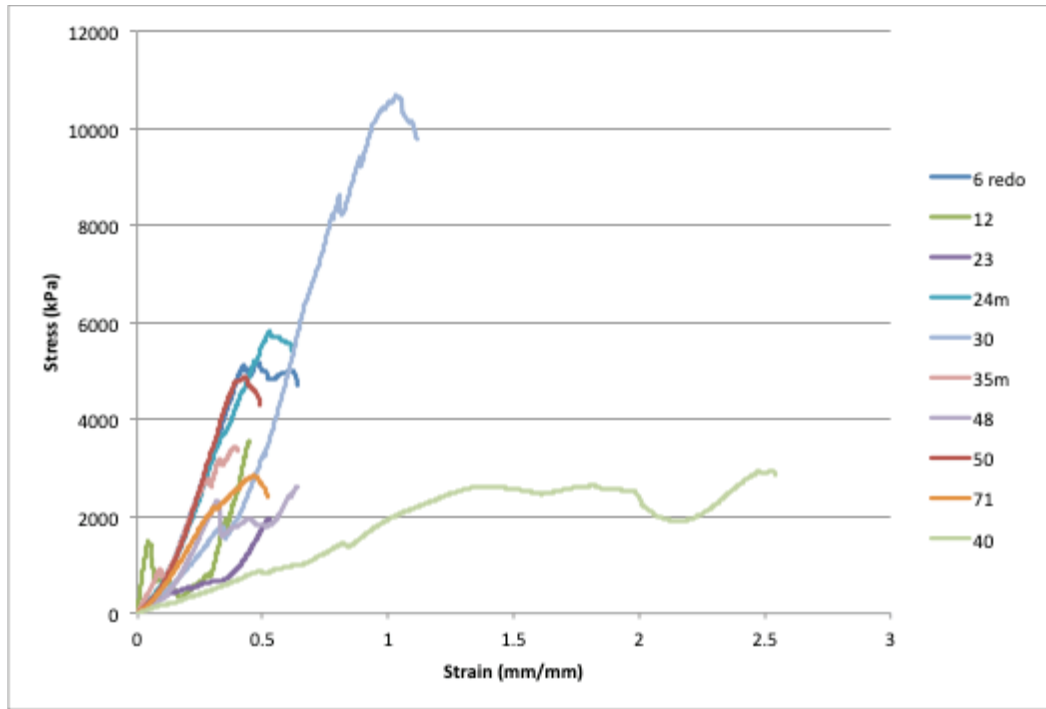


Figure D.5: Stress-Strain to Failure of Collagen Group at 2 Weeks Recovery (with Outlier)

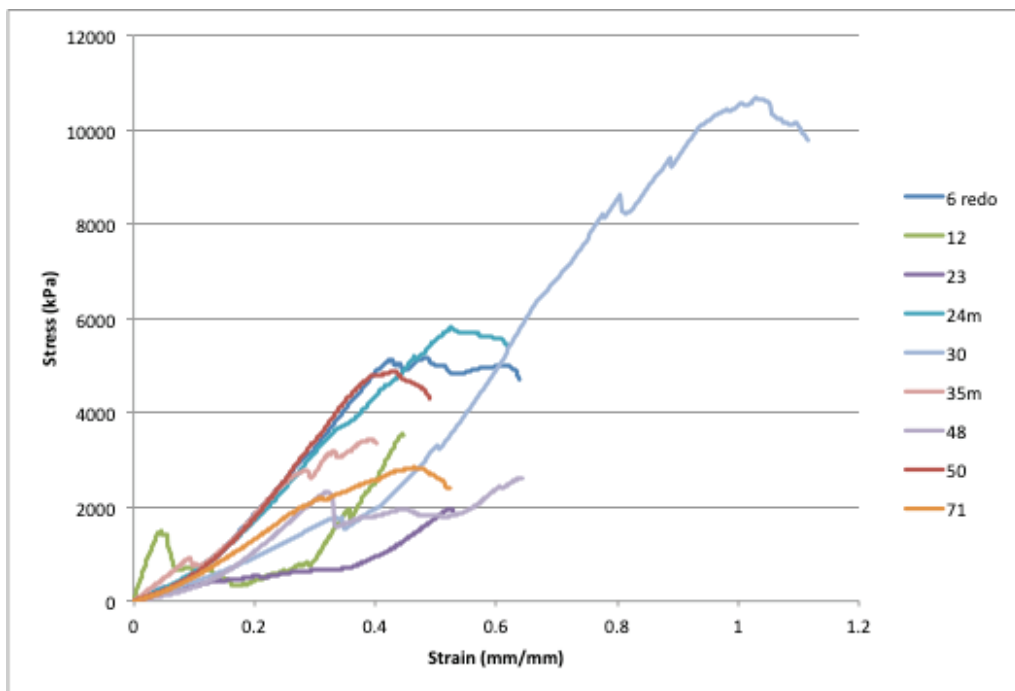


Figure D.6: Stress-Strain Curve to Failure of Collagen Group at 2 Weeks Recovery (without Outlier)

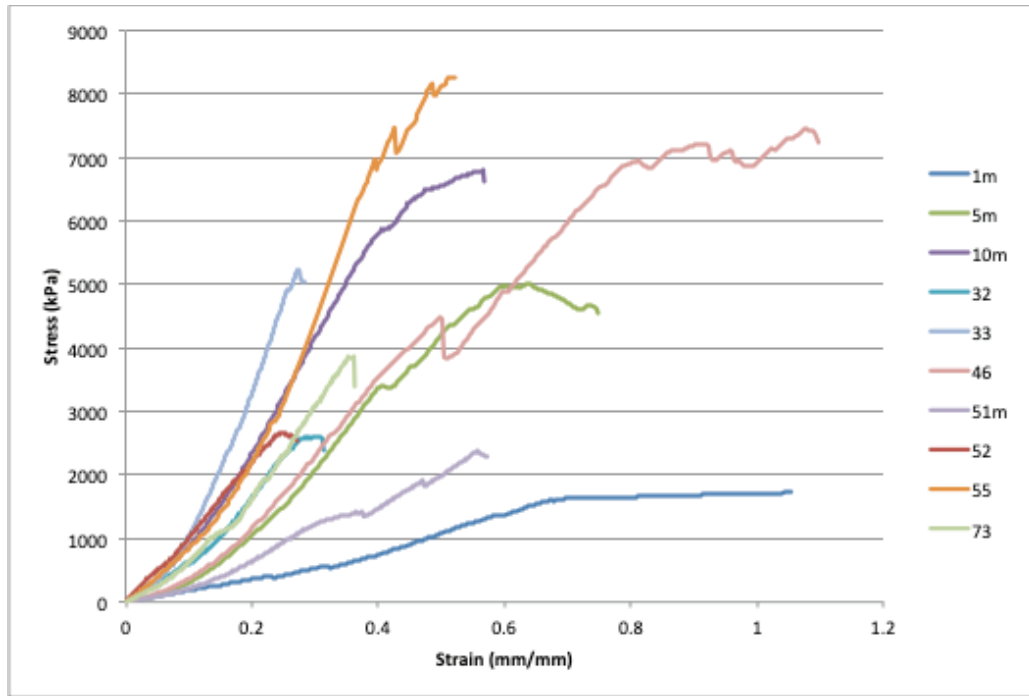


Figure D.7: Stress-Strain Graph to Failure of PRP Group at 2 Weeks Recovery

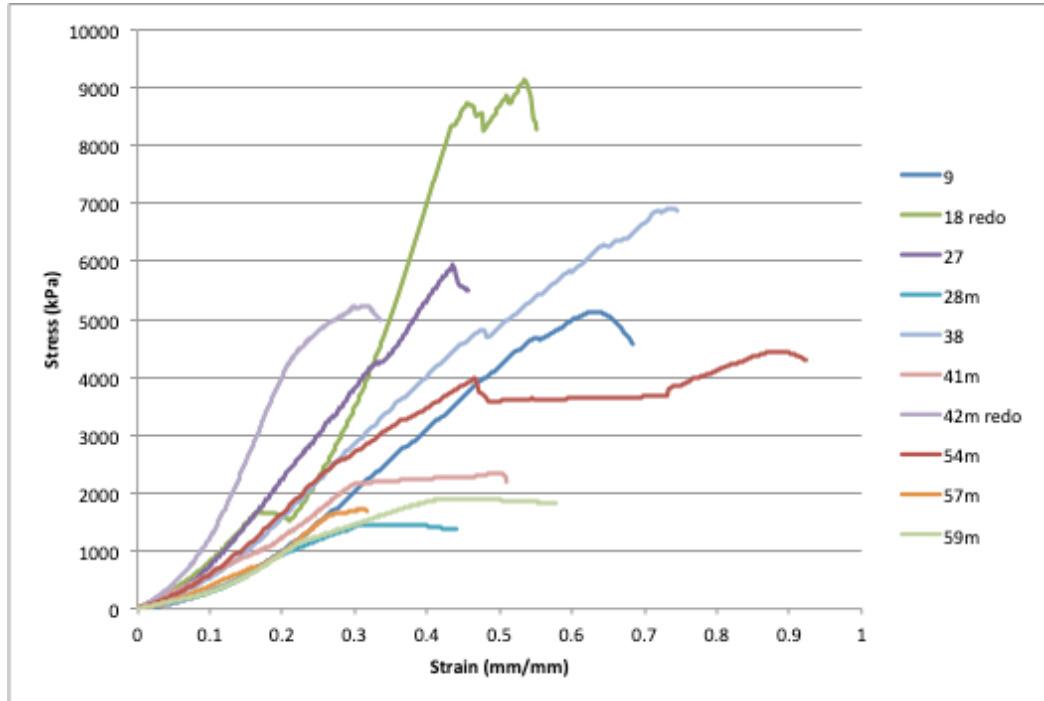


Figure D.8: Stress-Strain Curve to Failure of MSC Group at 2 Weeks Recovery

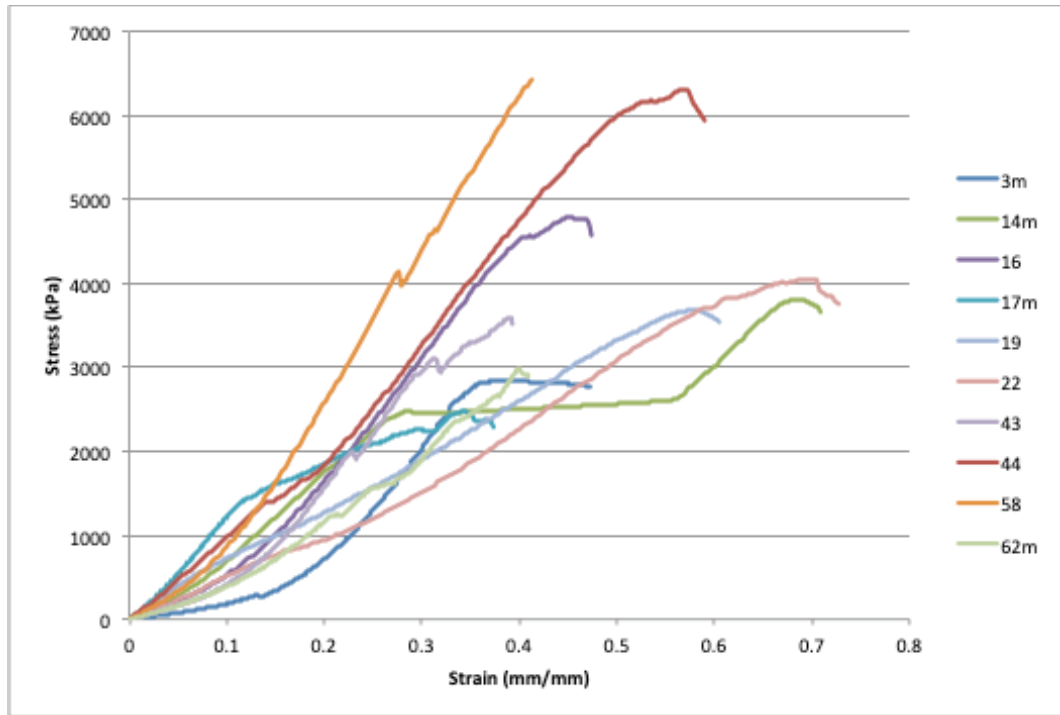


Figure D.9: Stress-Strain Curve to Failure of Combination Group at 2 Weeks Recovery

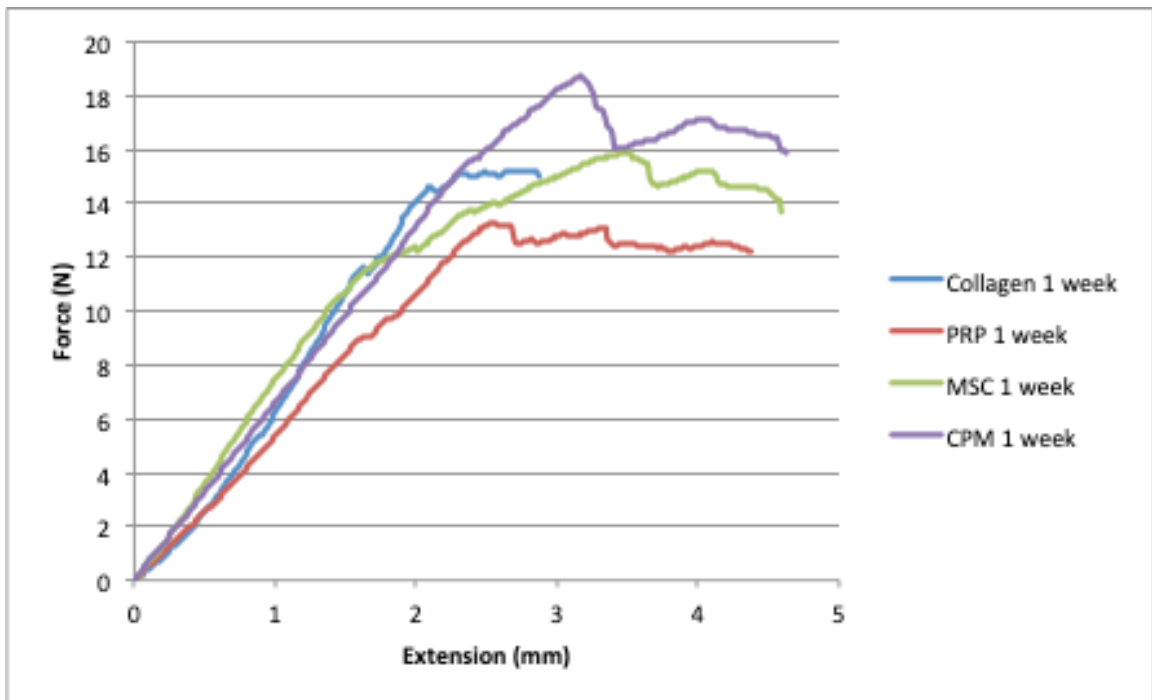


Figure D.10: Force-Extension to Failure of all Treatments at 1 Week Recovery

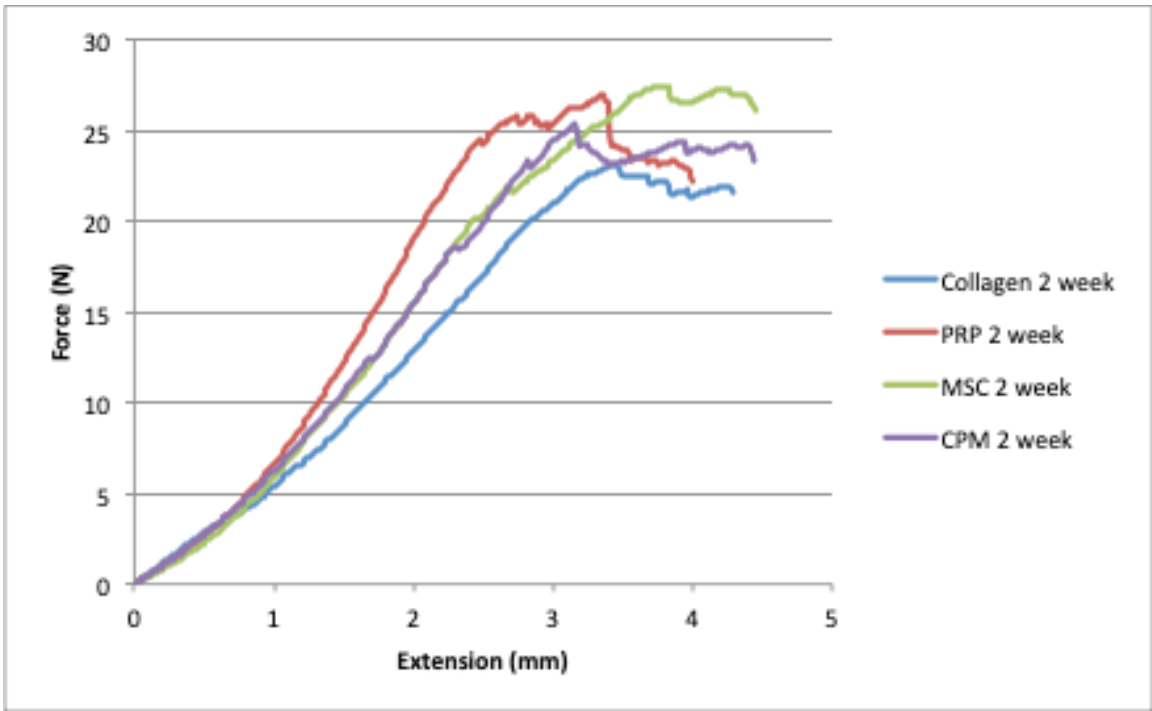


Figure D.11: Force-Extension to Failure of all Treatments at 2 Weeks Recovery

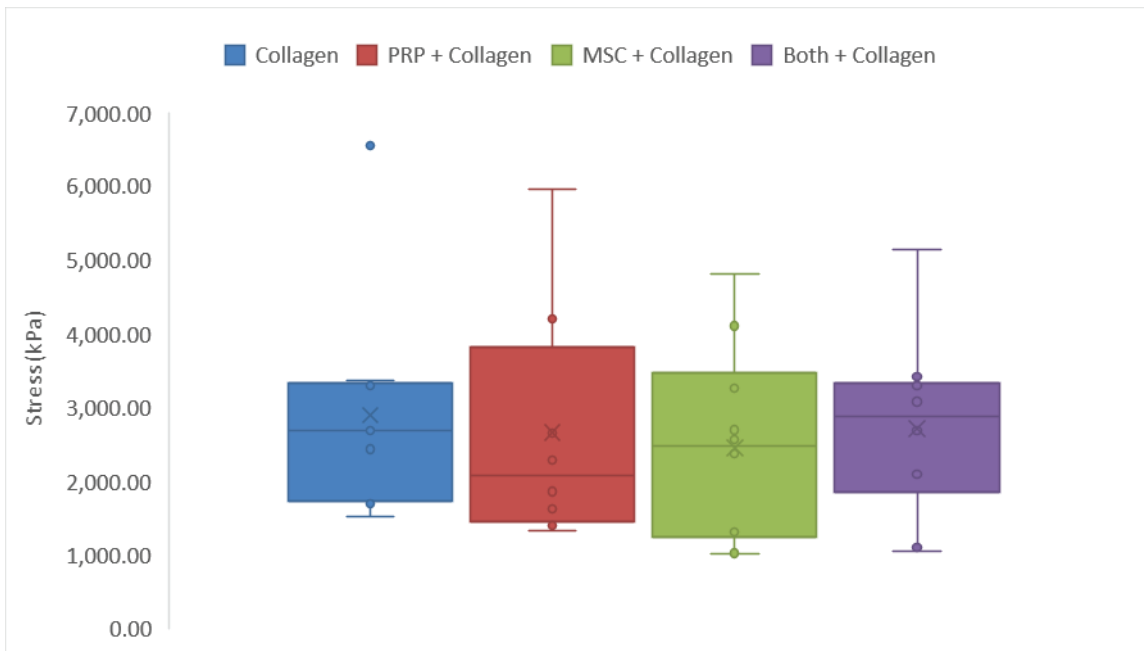


Figure D.12: Maximum Stress at 1 Week Recovery

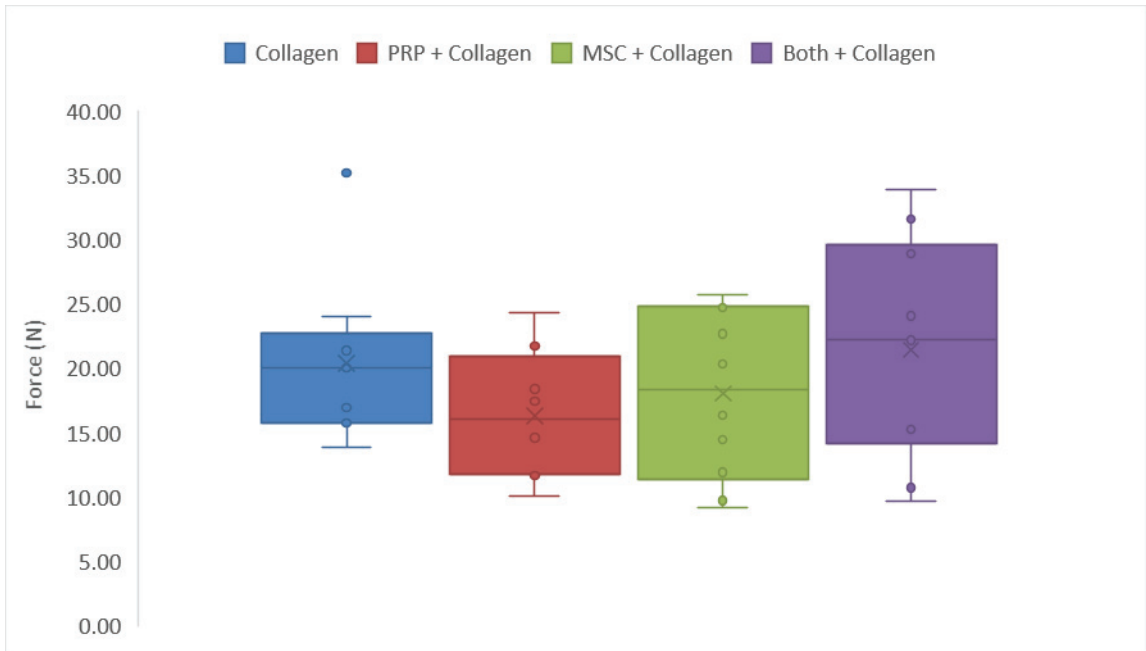


Figure D.13: Maximum Force at 1 Week Recovery

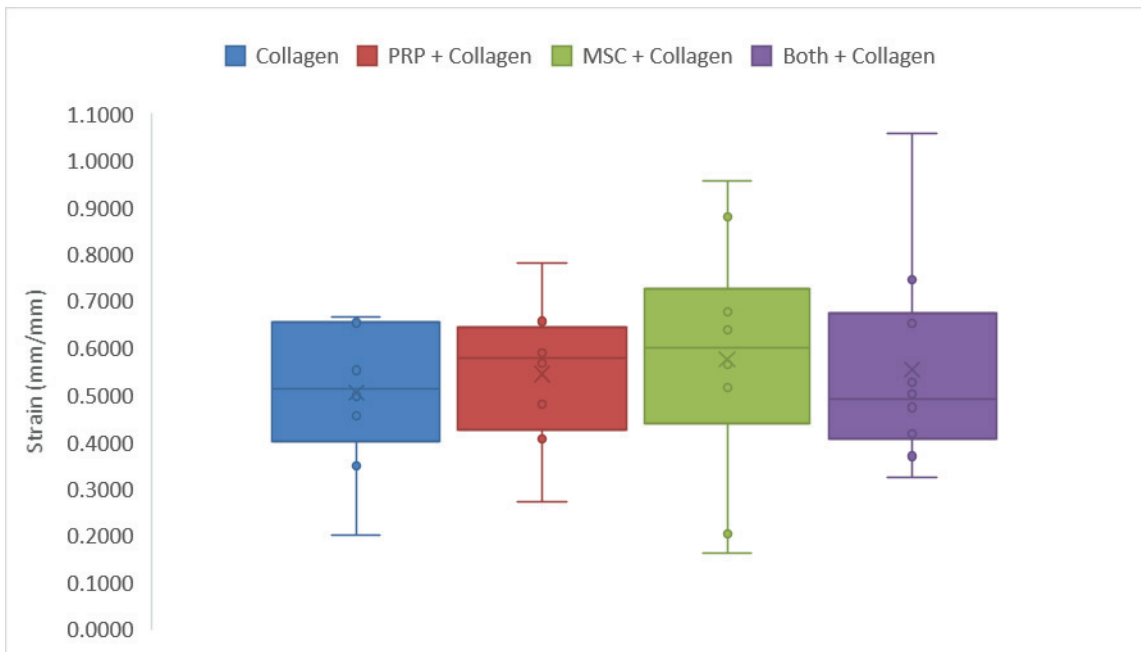


Figure D.14: Strain at Failure at 1 Week Recovery

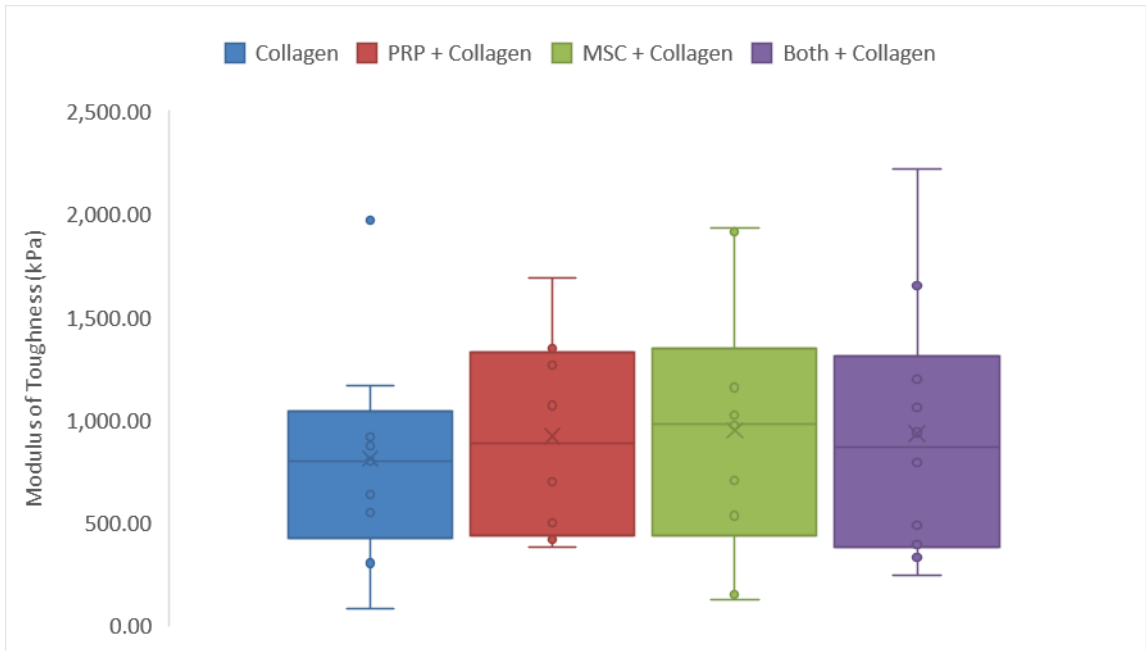


Figure D.15: Total Strain Energy at 1 Week Recovery

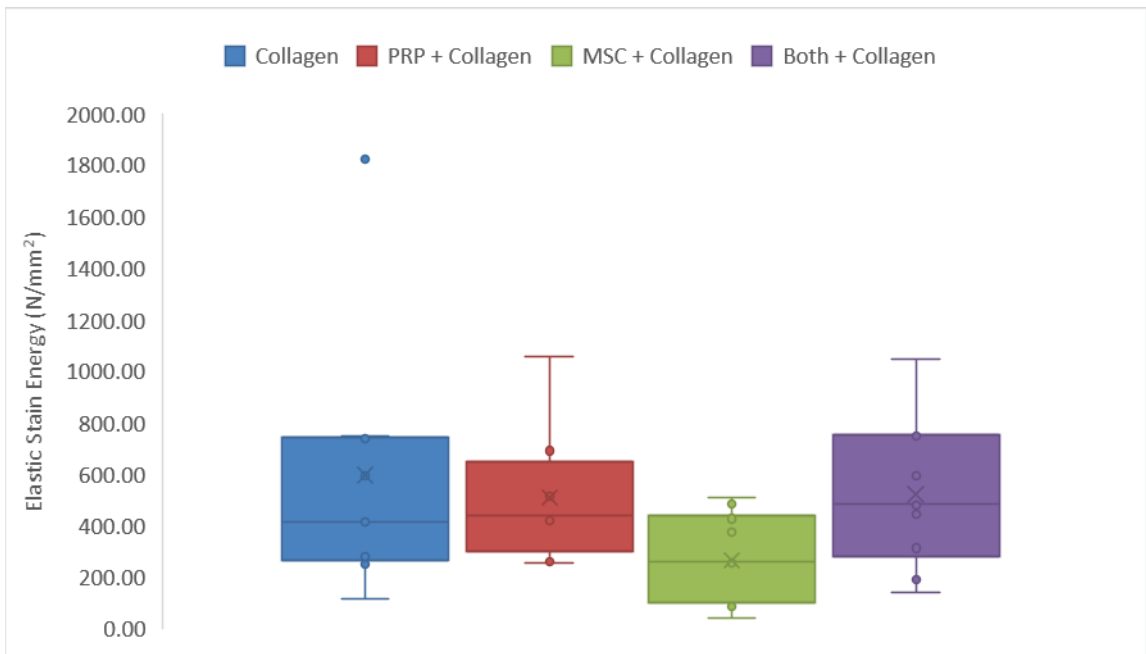


Figure D.16: Elastic Strain Energy at 1 Week Recovery

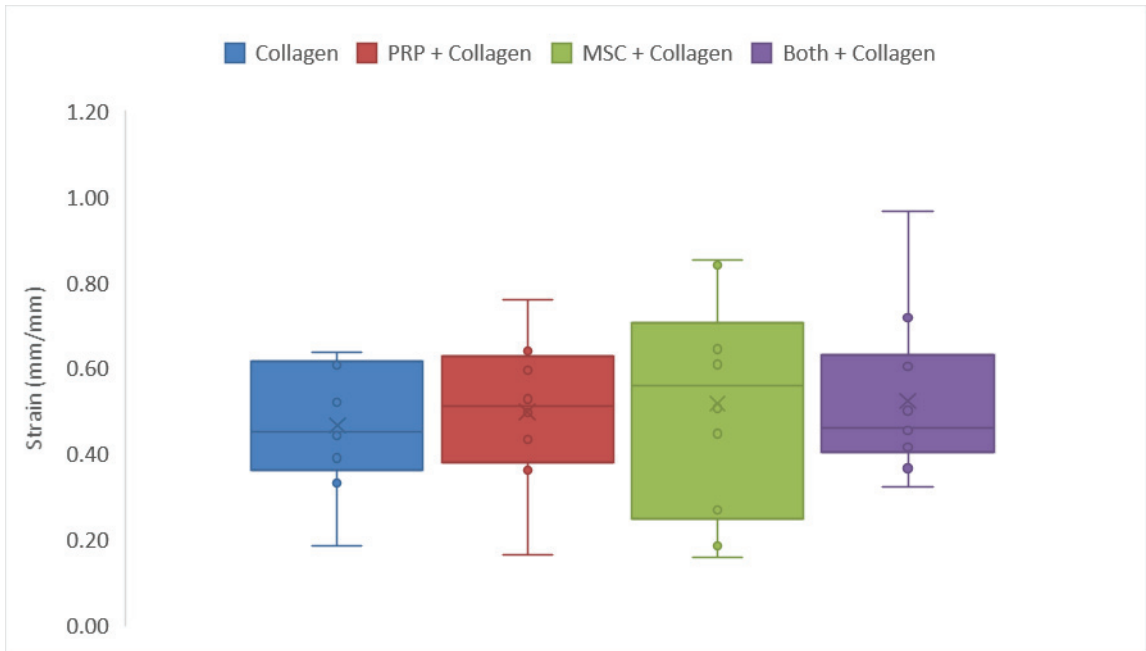


Figure D.17: Strain at UTS at 1 Week Recovery

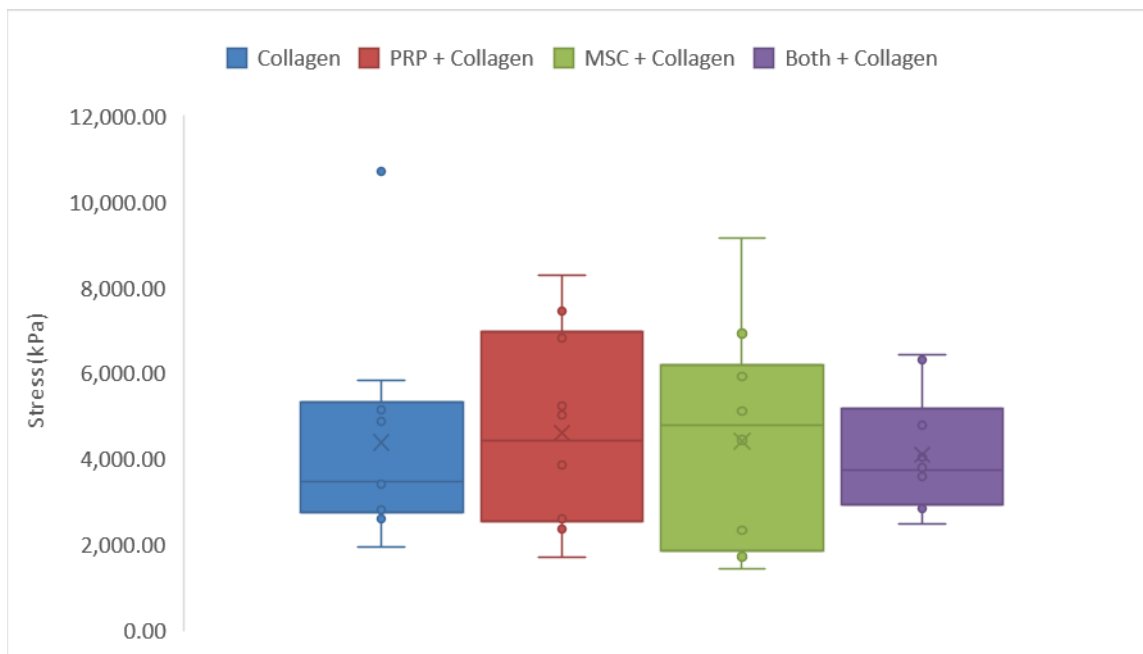


Figure D.18: Maximum Stress at 2 Week Recovery

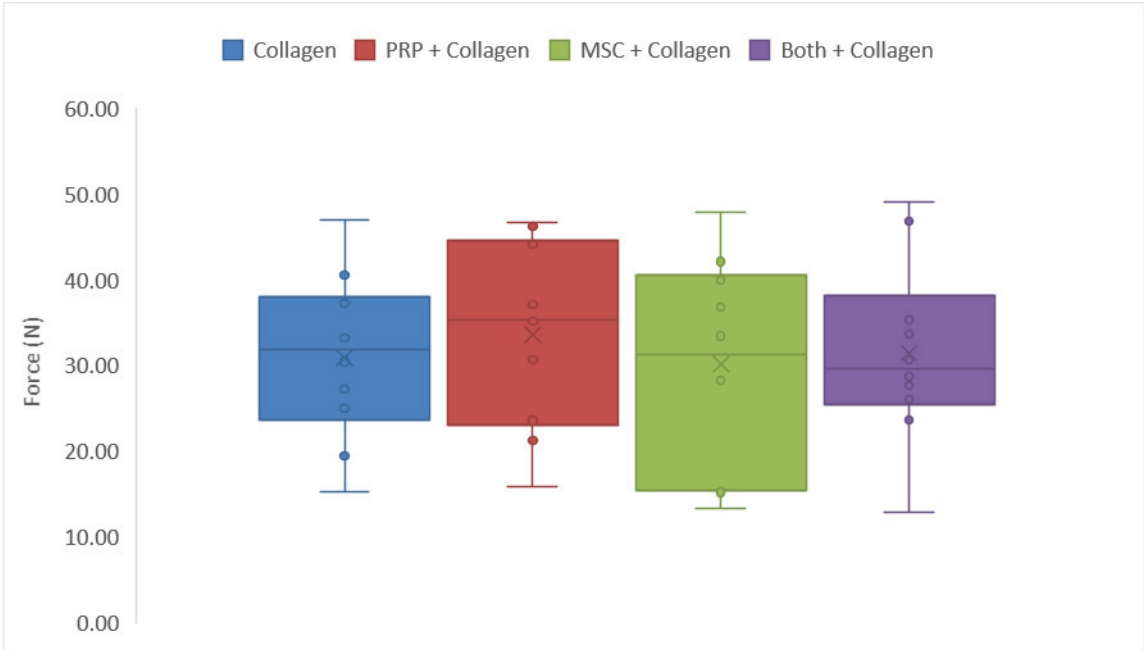


Figure D.19: Maximum Force at 2 Week Recovery

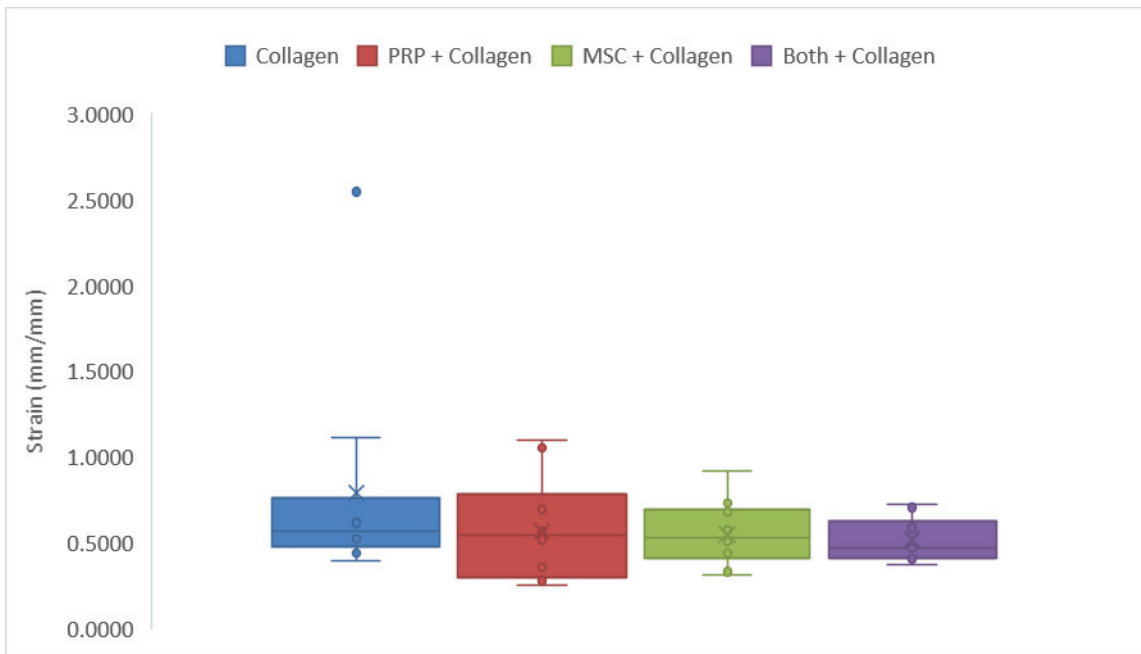


Figure D.20: Strain at Failure at 2 Week Recovery (with Outlier)

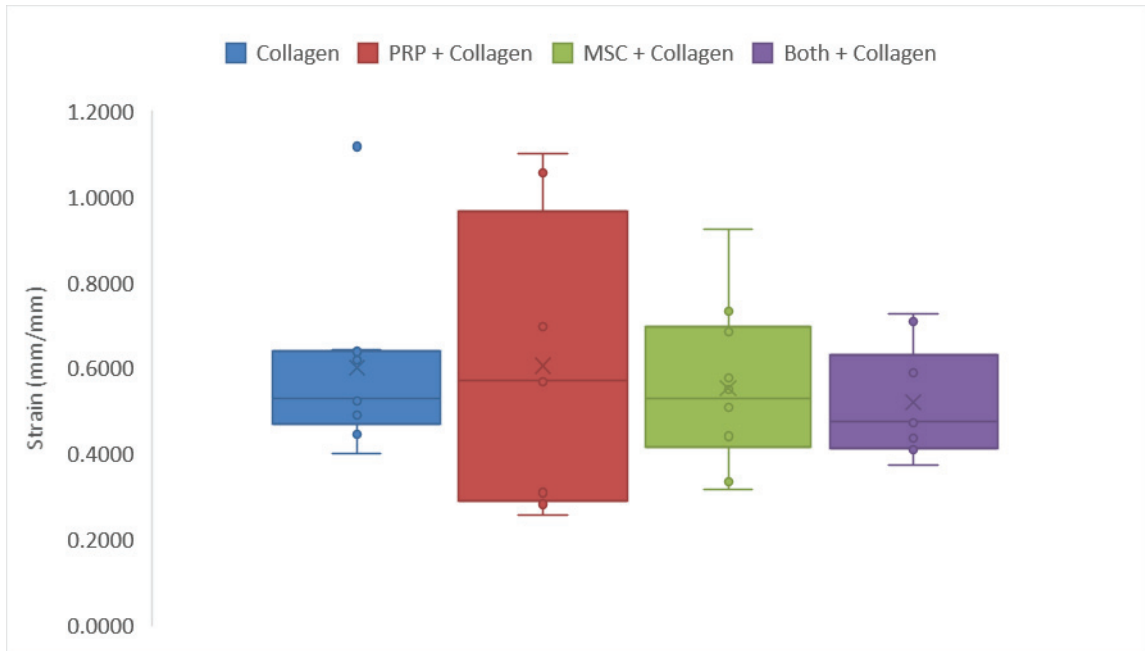


Figure D.21: Strain at Failure at 1 Week Recovery (without Outlier)

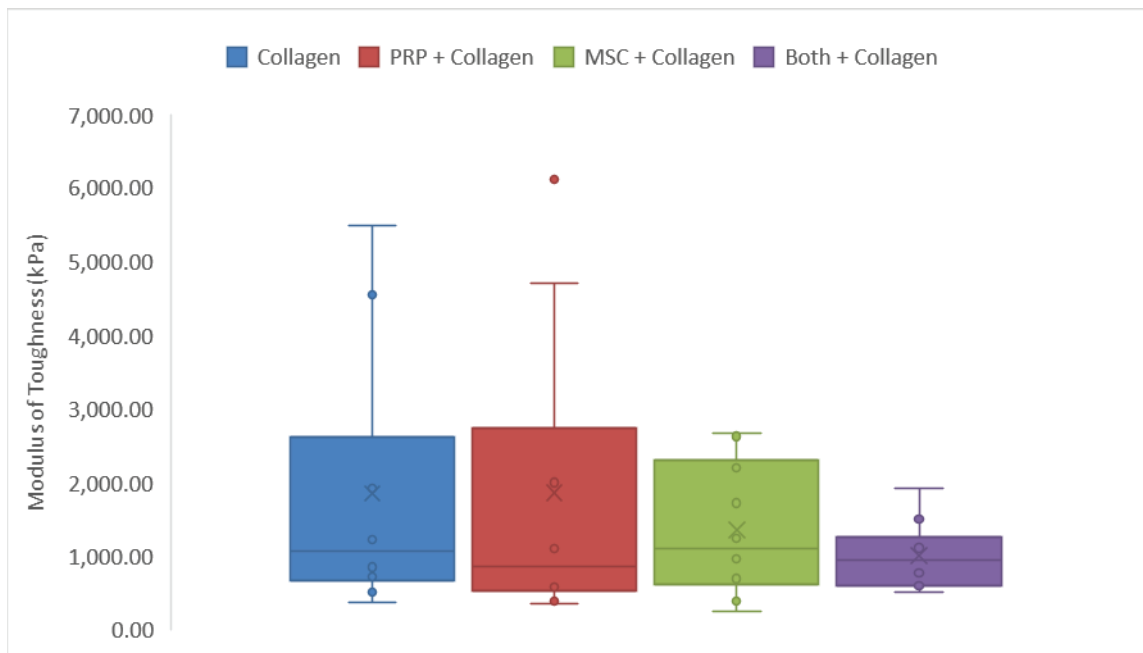


Figure D.22: Total Strain Energy at 2 Week Recovery

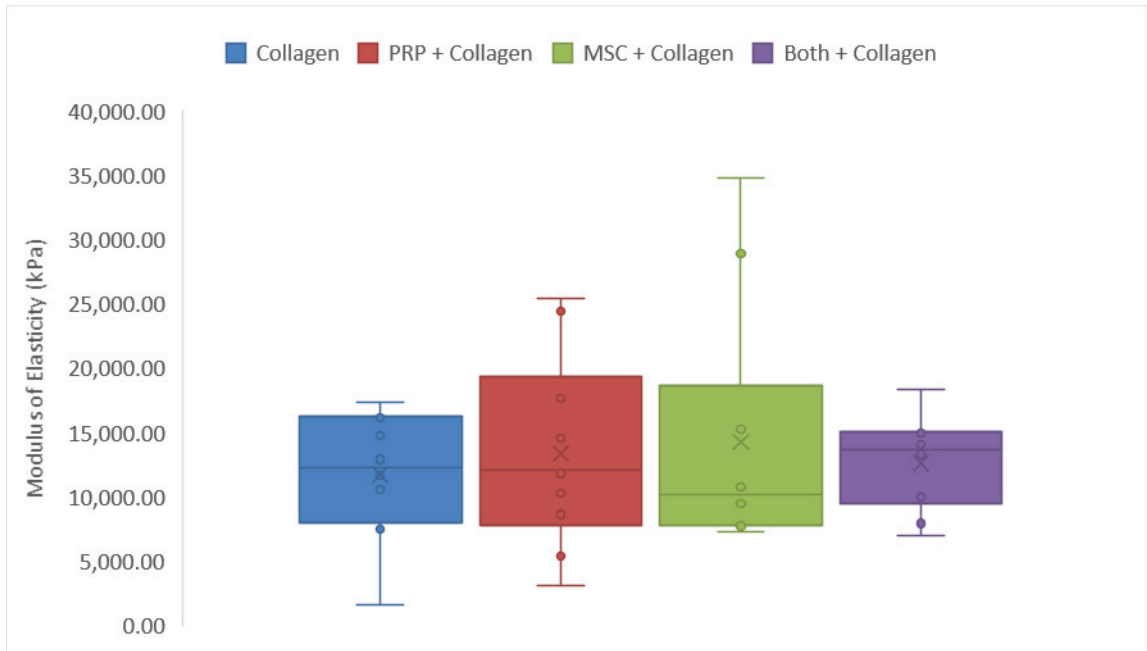


Figure D.23: Elastic Strain Energy at 1 Week Recovery

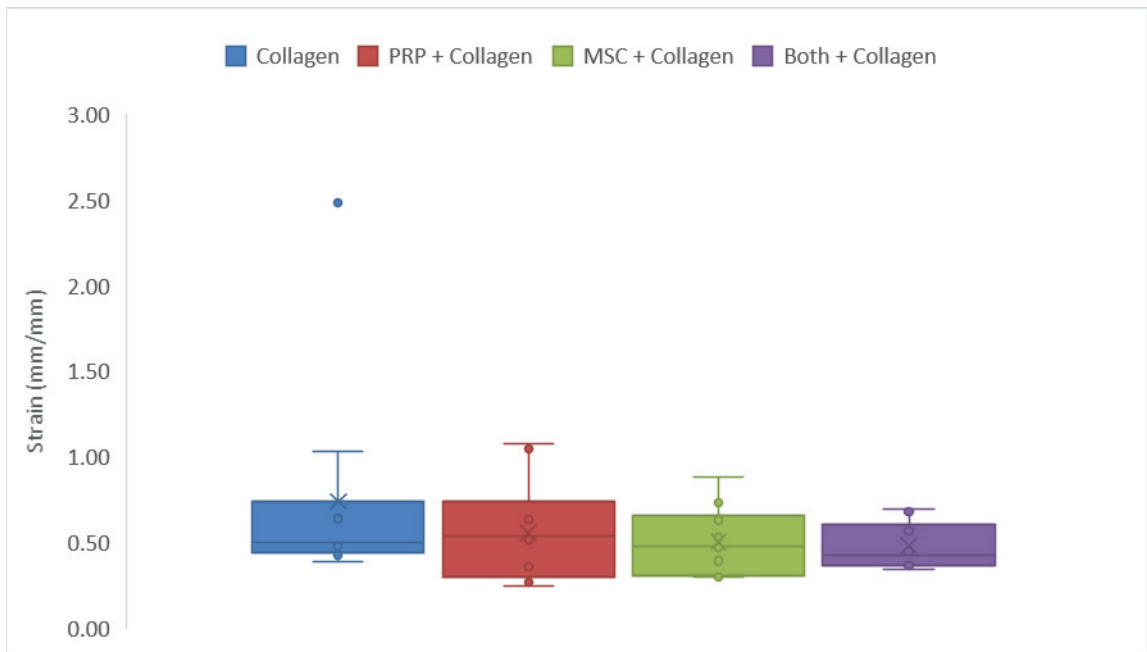


Figure D.24: Strain at UTS at 2 Week Recovery (with Outlier)

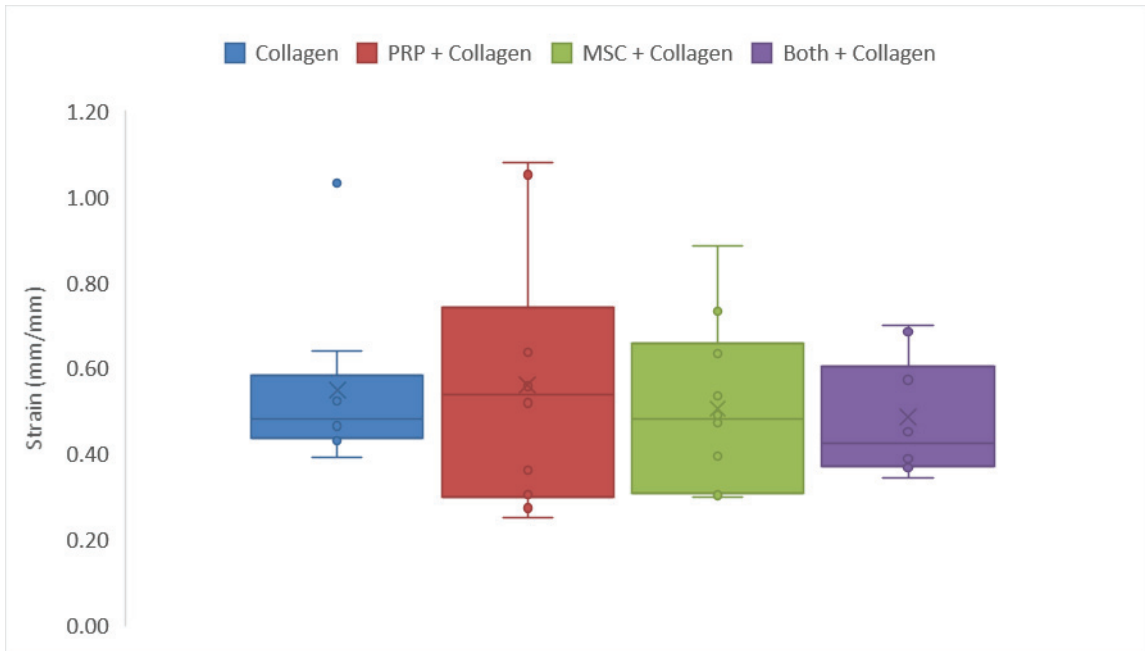


Figure D.25: Strain at UTS at 2 Week Recovery (without Outlier)

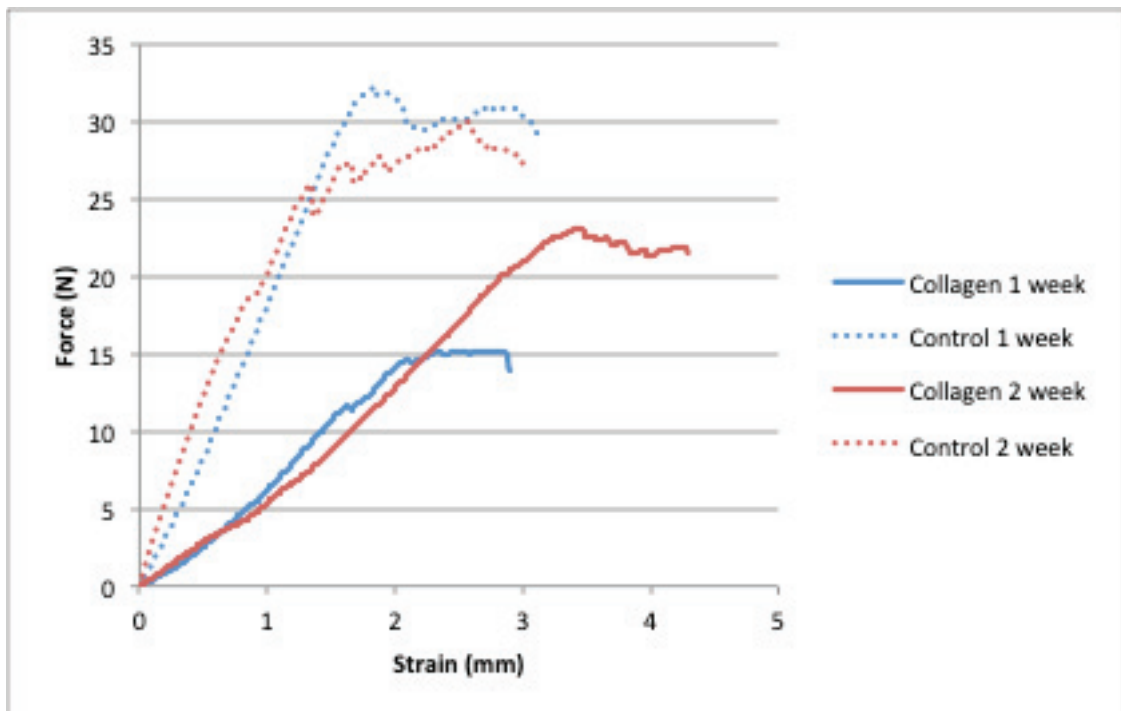


Figure D.26: Force-Extension 1 and 2 Week Recovery Collagen and Controls

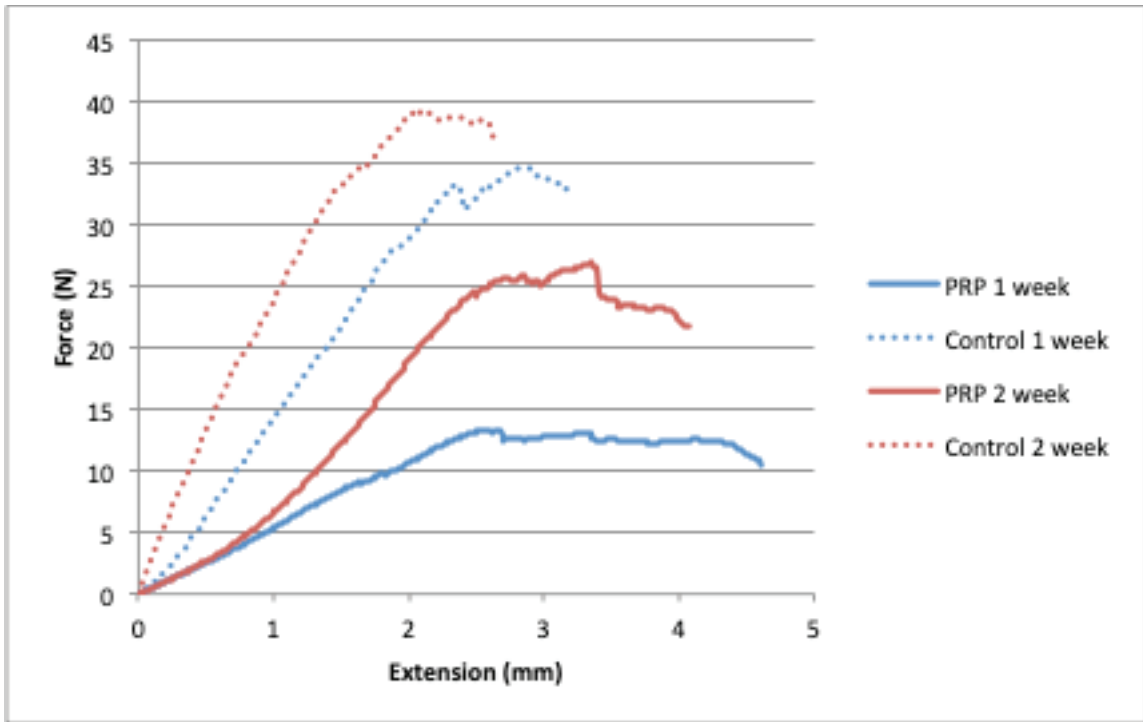


Figure D.27: Force-Extension 1 and 2 Week Recovery PRP and Controls

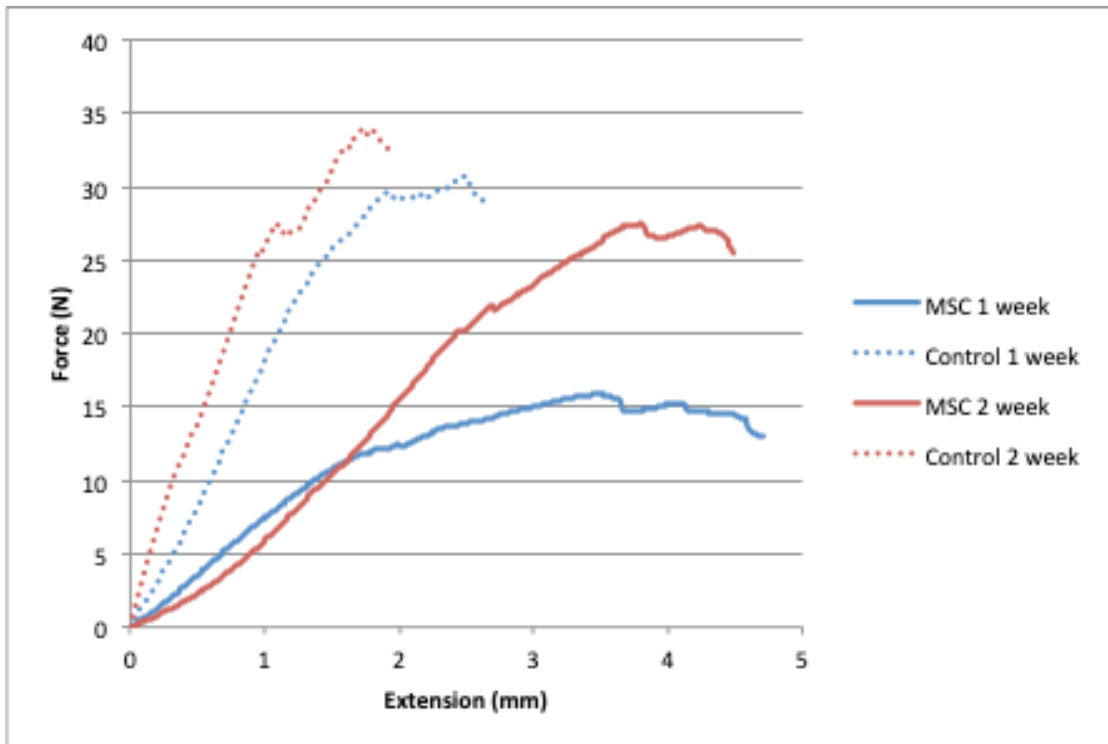


Figure D.28: Force-Extension of 1 and 2 Week Recovery of MSC and Controls

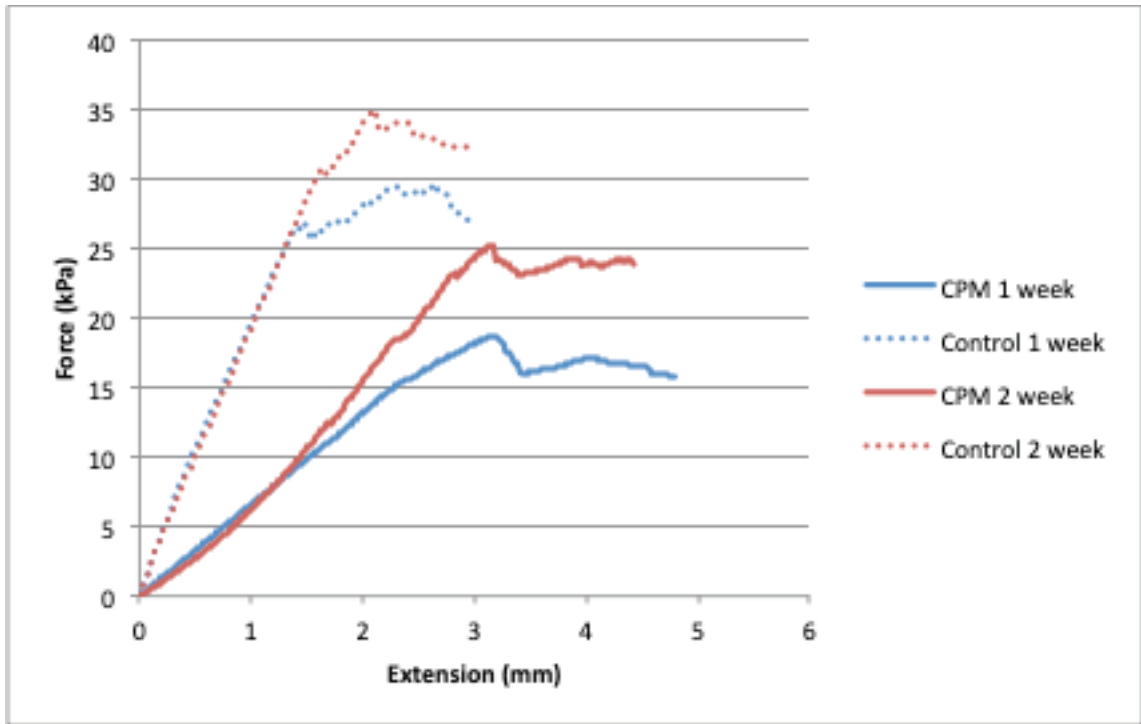


Figure D.29: Force-Extension of 1 and 2 Week Recovery of CPM and Control

REFERENCES

- American Academy of Orthopaedic Surgeons. (2011). *Platelet-Rich Plasma (PRP)*. Retrieved 7 2018, from OrthoInfo: <https://orthoinfo.aaos.org/en/treatment/platelet-rich-plasma-prp/>
- Aspenburg, P., & Virchenko, O. (2004). Platelet concentrate injection improves achilles tendon repair in rats. *Acta Orthopaedica Scandinavica* , 75 (1), 93-99.
- Bajuri, M., Isaksson, H., Eliasson, P., & Thompson, M. (2016). A hyperelastic fibre-reinforced continuum model of healing tendons with distributed collagen fibre orientations. *Biomechanics and Modeling in Mechanobiology* , 15, 1457-1466.
- Balaji, S., Keswani, S., & Crombleholme, T. (2012). The role of mesenchymal stem cells in the regenerative wound healing phenotype. *Advances in Wound Care* , 1 (4), 159-165.
- Butler, D., Grood, E., Noyes, F., & Zernicke, R. (1978). Biomechanics of Ligament and Tendons. *Exercise and Sports Science Review* , 6, 125-181.
- C, R. (2017, 9). *Difference Between Tendons and Ligaments*. Retrieved 12 2018, from biodifferences.com: <https://biodifferences.com/difference-between-tendons-and-ligaments.html>
- Cetti, R., Christensen, S.-E., Ejsted, R., Jensen, N., & Jorgensen, U. (1993). Operative versus nonoperative treatment of Achilles tendon rupture: A prospective randomized study and review of literature. *The American Journal of Sports Medicine* , 21 (6), 791-799.

- Chong, A., Ang, A., Goh, J., Hui, J., Lim, A., Lee, E., et al. (2007). Bone marrow-derived mesenchymal stem cells influence early tendon-healing in rabbit achilles tendon model. *The Journal of Bone & Joint Surgery* , 89-A (1), 74-81.
- Cleveland Clinic. (2017, 3 17). *Achilles Tendon Injury-Including Achilles Tendonitis and Achilles Tendon Rupture*. Retrieved 7 2018, from Cleveland Clinic:
<https://my.clevelandclinic.org/health/diseases/15225-achilles-tendon-injury---including-achilles-tendinitis-and-achilles-tendon-rupture>
- Cleveland Clinic. (2016). *Tendinitis or Teninosis? Why the Difference is Important, What Treatments Help*. Retrieved 7 2018, from Cleveland Clinic health essentials:
<https://health.clevelandclinic.org/tendinitis-tendinosis-difference-important-treatments-help/>
- Cretnik, A., Kosanovic, M., & Smrolj, V. (2004). Percutaneous suturing of the ruptured Achilles tendon under local anesthesia. *J Foot Ankle Surg.* , 43 (2), 72-81.
- Dai, W., Hale, S., Martin, B., Kuang, J.-Q., Dow, J., Wold, L., et al. (2005). Allogeneic mesenchymal stem cell transplantation in postinfarcted rat myocardium: Short- and long-term effects. *Circulation* , 112 (2), 214-223.
- Department of Health and Human Services. (2016). *Stem Cell Information*. Retrieved 7 2018, from National Institutes of Health:
<https://stemcells.nih.gov/info/basics/2.htm>
- Dhurat, R., & Sukesh, M. (2014). Principles and Methods of Preparation of Platelet-Rich Plasma: A Review and Author's Perspective. *J Cutan Aesthet Surg* , 7 (4), 189-197.

- Dowshen, S. (2015). *Your Bones*. Retrieved 7 2018, from Kids Health:
<https://kidshealth.org/en/kids/bones.html>
- Encyclopedia Britannica. (1998c). *Ligament*. Retrieved 7 2018, from Encyclopedia Britannica online: <https://www.britannica.com/science/ligament>
- Encyclopedia Britannica. (2009). *Adipose Tissue*. Retrieved 7 2018, from Encyclopedia Britannica online: <https://www.britannica.com/science/adipose-tissue>
- Encyclopedia Britannica. (1998a). *Ground Substance*. Retrieved 7 2018, from Encyclopedia Britannica online: <https://www.britannica.com/science/ground-substance>
- Encyclopedia Britannica. (2000). *Human body*. Retrieved 7 2018, from Encyclopedia Britannica online: <https://www.britannica.com/science/human-body>
- Encyclopedia Britannica. (1998b). *Tendon*. Retrieved 7 2018, from Encyclopedia Britannica online: <https://www.britannica.com/science/tendon>
- Fawcett, D. (1999). *Connective tissue*. Retrieved 7 2018, from Encyclopedia Britannica online: <https://www.britannica.com/science/connective-tissue>
- Gebauer, M., Beil, F., Beckmann, J., Savary, A., Ueblacker, P., Ruecker, A., et al. (2007). Mechanical evaluation of different techniques for Achilles tendon repair. *Arth Orthop Trauma Surg.* , 127 (9), 795-799.
- Gott, M., Ast, M., Lane, L., Schwartz, J., Catanzano, A., Razzano, P., et al. (2011). Tendon phenotype should dictate tissue engineering modality in tendon repair: a review. *Discovery Medicine* , 12 (62), 75-84.

- Health Communities. (1999b). *Anatomy of Foot and Ankle*. Retrieved 7 2018, from Health Communities: <http://www.healthcommunities.com/foot-anatomy/foot-anatomy-overview.shtml>
- Health Communities. (1999a). *Foot & Ankle Anatomy-Muscles, Tendons, and Ligaments*. Retrieved 7 2018, from Health Communities: <http://www.healthcommunities.com/foot-anatomy/muscles-tendons-ligaments.shtml>
- Heffner, J., Holmes, J., Ferrari, J., Krontiris-Litowitz, J., Marie, H., Fagan, D., et al. (2012). Bone marrow-derived mesenchymal stromal cells and platelet-rich plasma on a collagen matrix to improve fascial healing. *Hernia*, 16 (6), 677-687.
- Isakson, M., Blacam, C., Whelan, D., McArdle, A., & Clover, A. (2015). Mesenchymal Stem Cells and Cutaneous Wound Healing: Current Evidence and Future Potential. *Stem Cells International* (7).
- Jacobs, D., Martens, M., Audekercke, R., Mulier, J., & Mulier, F. (1978). Comparison of conservative and operative treatment of Achilles tendon rupture. *The American Journal of Sports Medicine*, 6 (3), 107-111.
- Javazon, E., Colter, D., Schwarz, E., & Prockop, D. (2001). Rat marrow stromal cells are more sensitive to plating density and expand more rapidly from single-cell-derived colonies than human marrow stromal cells. *Stem Cells*, 19 (3), 219-225.
- Khayyeri, H., Longo, G., Gustafsson, A., & Isaksson, H. (2016). Comparison of structural anisotropic soft tissue model for simulating Achilles tendon tensile behavior. *Mechanical Behavior of Biomedical Materials*, 61, 431-443.

- Kohen, R., Warren, R., & Rodeo, S. (2010). *Platelet-Rich Plasma (PRP) Treatment: An Overview*. Retrieved 7 2018, from HSS: https://www.hss.edu/conditions_platelet-rich-plasma-prp.asp
- Kvist, M. (1994). Achilles Tendon Injuries in Athletes. *Sports Medicine* , 18 (3), 173-201.
- Laerd Statistics. (n.d.). *Two-way ANOVA using Minitab*. Retrieved March 2019, from Laerd Statistics: <https://statistics.laerd.com/minitab-tutorials/two-way-anova-using-minitab.php>
- Leppilahti, J., Puranen, J., & Orava, S. (1996). Incidence of Achilles tendon rupture. *Acta Orthopaedica Scandinavica* , 67 (3), 277-279.
- Maekawa, Y., Yagi, K., Nonomura, A., Kuraoku, R., Nishiura, E., Uchibori, E., et al. (2003). A tetrazolium-based colorimetric assay for metabolic activity of stored blood platelets. *Thrombosis research* , 109, 307-314.
- Maganaris, C., & Narici, M. (2005). Mechanical Properties of Tendons. *Tendon Injuries* , 2, 14-21.
- Marie, H., Zhang, Y., Heffner, J., Dorion, H. A., & Diana, F. L. (2010). Biomechanical and Elastographic Analysis of Mesenchymal Stromal Cell Treated Tissue Following Surgery. *J Biomech Eng* , 132 (7).
- Mayo Clinic. (2017). *Achilles tendon rupture*. Retrieved 7 2018, from Mayo Clinic: <https://www.mayoclinic.org/diseases-conditions/achilles-tendon-rupture/diagnosis-treatment/drc-20353239>
- Mazzone, M., & McCue, T. (2002). Common Conditions of the Achilles Tendon. *Am Fam Physician* , 65 (9), 1850-1811.

- McDonald, J. H. (2014). *Handbook of Biological Statistics* (3rd Edition ed.). Baltimore, Maryland: Sparky House Publishing.
- Melina, R. (2010, 11 16). *Why do Medical Researchers use Mice?* Retrieved 7 2018, from Live Science: <https://www.livescience.com/32860-why-do-medical-researchers-use-mice.html>
- Metzl, J., Ahmad, C., & Levine, W. (2008). The ruptured achilles tendon: operative and non-operative treatment options. *Current Reviews of Musculoskeletal Medicine* , 1, 161-164.
- Min, Y., Seo, J., Kwon, Y.-B., & Lee, M.-H. (2013). Effect of the Position of Immobilization Upon the Tensile Properties in Injured Achilles Tendon of Rat. *Annals of Rehabilitation Medicine* , 37 (1), 1-9.
- Minitab. (n.d.). *Understanding test for equal variances*. Retrieved March 2019, from Minitab 18 Support: <https://support.minitab.com/en-us/minitab/18/help-and-how-to/modeling-statistics/anova/supporting-topics/basics/understanding-test-for-equal-variances/>
- National Association for Biomedical Research. (n.d.). *Mice and Rats*. Retrieved 6 2018, from National Association for Biomedical Research: <https://www.nabr.org/biomedical-research/laboratory-animals/species-in-research/mice-and-rats/>
- National Cancer Institute. (n.d.). *NCI Dictionary of Cancer Terms*. Retrieved 7 2018, from National Cancer Institute: <https://www.cancer.gov/publications/dictionaries/cancer-terms/def/hematopoietic-stem-cell>

National Cancer Institute. (n.d.). *Nervous Tissue*. Retrieved 7 2018, from National Cancer Institute SEER Training Modules:

https://training.seer.cancer.gov/anatomy/cells_tissues_membranes/tissues/nervous.html

New York State Stem Cell Science. (n.d.). *What is the difference between totipotent, pluripotent, and multipotent?* Retrieved 7 2018, from New York State Stem Cell Science: <https://stemcell.ny.gov/faqs/what-difference-between-totipotent-pluripotent-and-multipotent>

Ode, G. (2016). *What Is the Difference Between Tendonitis, Tendinosis, and Tendinopathy?* Retrieved 7 2018, from Sports-health: <https://www.sports-health.com/sports-injuries/general-injuries/what-difference-between-tendonitis-tendinosis-and-tendinopathy>

OpenStax College. (n.d.). *Epithelial Tissue*. Retrieved 7 2018, from Lumin: <https://courses.lumenlearning.com/nemcc-ap/chapter/epithelial-tissue/>

Rice University. (n.d.). *4.4 Muscle Tissue and Motion*. Retrieved 7 2018, from BC campus: <https://opentextbc.ca/anatomyandphysiology/chapter/4-4-muscle-tissue-and-motion/>

Shapiro, E., Grande, D., & Drakos, M. (2015). Biologics in achilles tendon healing and repair: a review. *Current Reviews in Musculoskeletal Medicine* , 8, 9-17.

Silverman, L. (2015). *Why Is It Called Your Achilles Tendon?* Retrieved 7 2018, from Silverman Ankle & Foot: <https://www.anklefootmd.com/why-is-it-called-your-achilles-tendon/>

- Southern Illinois University. (2015). *Connective Tissue Study Guide*. Retrieved 7 2018, from siumed.edu: <http://www.siumed.edu/~dking2/intro/ct.htm>
- Strauss, E., Ishak, C., Jazrawi, L., Sherman, O., & Rosen, J. (2007). Operative treatment of acute Achilles tendon ruptures: an institutional review of clinical outcomes. *Injury* , 38 (7), 832-838.
- Tang, C., Ng, G., Wang, Z., Tsui, C., & Zhang, G. (2011). Parameter optimization for the visco-hyperelastic constitutive model of tendon using FEM. *Bio-Medical Materials and Engineering* , 21, 9-24.
- Teng, C., Zhou, C., Xu, D., & Bi, F. (2016). Combination of platelet-rich plasma and bone marrow mesenchymal stem cells enhances tendon-bone healing in a rabbit model of anterior cruciate ligament reconstruction. *Journal of Orthopaedic Surgery and Research* , 11 (96).
- Vergari, C., Pourcelot, P., Holden, L., Ravary-Plumioen , B., Gerard, G., Laugier, P., et al. (2011). True stress and Poisson's ratio of tendons during loading. *Journal of Biomechanics* , 44, 719-724.
- Wang, J. (2006). Mechanobiology of tendon. *Journal of Biomechanics* , 39, 1563-1582.
- Young, R., Weber, W., Caplin, A., Gordon, S., & Fink, D. (1998). Use of mesenchymal stem cells in a collagen matrix for achilles tendon repair. *Journal of Orthopedic Research* , 16 (4), 406-413.
- Yuksel, S., Guleç, M., Gultekin, M., Adanır, O., Caglar, A., Beytemur, O., et al. (2016). Comparison of the early period effects of bone marrow-derived mesenchymal stem cells and platelet-rich plasma on the achilles tendon ruptures in rats. *Connective Tissue Reseach* , 57 (5), 360-373.

Zimmer Biomet. (n.d.). *Collagen Wound care*. Retrieved April 2019, from Zimmer

Biomet Dental:

[https://www.zimmerbiometdental.com/en/wps/portal/dental/site/dental/dental-professionals/regenerative-solutions/collagen-wound-care/zimmer-collagen-tape-](https://www.zimmerbiometdental.com/en/wps/portal/dental/site/dental/dental-professionals/regenerative-solutions/collagen-wound-care/zimmer-collagen-tape-patch-)

[patch-](https://www.zimmerbiometdental.com/en/wps/portal/dental/site/dental/dental-professionals/regenerative-solutions/collagen-wound-care/zimmer-collagen-tape-patch-)

[plug!/ut/p/z1/xVJNU4MwFPw1PcYXwFI8YnXqV3XGagtcOmn6WICS0BBa9df](https://www.zimmerbiometdental.com/en/wps/portal/dental/site/dental/dental-professionals/regenerative-solutions/collagen-wound-care/zimmer-collagen-tape-patch-)

[7UMepM6jjSSYHePvY3dksZJBAPSW2WAtXGC1K-k6zcH521Pe9S-](https://www.zimmerbiometdental.com/en/wps/portal/dental/site/dental/dental-professionals/regenerative-solutions/collagen-wound-care/zimmer-collagen-tape-patch-)

[5fRf7dkMfB-WQ6nk6uvdEAppBBJrWrXA6pW6J2omTSaEdvPZ4bhT3-](https://www.zimmerbiometdental.com/en/wps/portal/dental/site/dental/dental-professionals/regenerative-solutions/collagen-wound-care/zimmer-collagen-tape-patch-)

[Ma2sWWFdvxHXPW5xjRotKW2R1aZsWkmaS1OWgiC2M41eMiksUbwUSqFl](https://www.zimmerbiometdental.com/en/wps/portal/dental/site/dental/dental-professionals/regenerative-solutions/collagen-wound-care/zimmer-collagen-tape-patch-)

[n5gTFbJKOJmzqmzWrYIKFktlj_wgFDxYsjBaeOzQCwZs4UWcBYNoFXn9KIz](https://www.zimmerbiometdental.com/en/wps/portal/dental/site/dental/dental-professionals/regenerative-solutions/collagen-wound-care/zimmer-collagen-tape-patch-)

[62G7XKKzM55sG7TOkw5a35dyDRONyYwu9dqgqQhFSi7VprESY_RZLRjD_](https://www.zimmerbiometdental.com/en/wps/portal/dental/site/dental/dental-professionals/regenerative-solutions/collagen-wound-care/zimmer-collagen-tape-patch-)

[5ok5_Z91rMT8-NY_Djgf3fidC184UvIw-](https://www.zimmerbiometdental.com/en/wps/portal/dental/site/dental/dental-professionals/regenerative-solutions/collagen-wound-care/zimmer-collagen-tape-patch-)

[NbDTQizbYE7uNfGKrrJyd8z2kl18B7GwUdOotkLIId00-](https://www.zimmerbiometdental.com/en/wps/portal/dental/site/dental/dental-professionals/regenerative-solutions/collagen-wound-care/zimmer-collagen-tape-patch-)

[8mdcbh48_xDLFSn4mGzyWLqTNuRJwfJ_5WG3Ph2PBxTfWias0KvDCRdwp](https://www.zimmerbiometdental.com/en/wps/portal/dental/site/dental/dental-professionals/regenerative-solutions/collagen-wound-care/zimmer-collagen-tape-patch-)

[B0C0PSIQzJb8KVUIFA55k9rsangYrnJ1c4i-](https://www.zimmerbiometdental.com/en/wps/portal/dental/site/dental/dental-professionals/regenerative-solutions/collagen-wound-care/zimmer-collagen-tape-patch-)

[NXBjKJfw!!/dz/d5/L2dBISEvZ0FBIS9nQSEh/](https://www.zimmerbiometdental.com/en/wps/portal/dental/site/dental/dental-professionals/regenerative-solutions/collagen-wound-care/zimmer-collagen-tape-patch-)